

UNCLASSIFIED

LA-1025  
VOLUME 24  
UNCLASSIFIED  
LA75  
SECTION F

**DO NOT CIRCULATE**

DO NOT CIRCULATE

Retention Copy

**PERMANENT RETENTION**

**REQUIRED BY CONTRACT**

LOS ALAMOS NATIONAL LABORATORY



3 9338 00329 3239

UNCLASSIFIED

UNCLASSIFIED

UNCLASSIFIED

PUBLICLY RELEASABLE

Per *B. Palatino* 88-16 Date: *1-6-88*By *M. D. L. L. L.* CIC-14 Date: *9-6-96*

IA-1025

August 20, 1947

This document contains 141 pages

VOLUME 24

Trinity

Appendix

Appendix 49

Classification changed to UNCLASSIFIED  
by authority of the U. S. Atomic Energy Commission,Per *ACR(Tid 1299); dtd 4-30-64*By REPORT LIBRARY *Susan Paxton*  
*7-20-64*

SCANNED DEC 05 1996



UNCLASSIFIED

UNCLASSIFIED

UNCLASSIFIED

## Appendix 49

April 2, 1946

## JULY 16th NUCLEAR EXPLOSION:

## SPACE-TIME RELATIONSHIPS

WORK DONE BY:

B. C. Benjamin  
N. Bifano  
R. B. Bloom  
B. Brixner  
M. Caldes  
R. L. Conrad  
G. A. Econnomou  
F. E. Geiger  
W. L. Kudlaciak  
D. C. Livingston  
R. Loevinger  
J. E. Mack  
T. S. Needels  
E. S. Palsvsky  
J. A. Schwartz  
K. J. Shue  
G. W. Thompson  
J. P. Wahlen  
E. D. Wallis  
E. N. York

REPORT WRITTEN BY:

J. E. Mack

Notes:

This appendix was originally issued as IA-531

UNCLASSIFIED

000000  
000000

UNCLASSIFIED

Page

## TABLE OF CONTENTS INCLUDING PHOTOGRAPHIC PRINTS

	ABSTRACT	2
I	INTRODUCTION	3
	Purpose Photographs included in this report Equipment (refer to Table I, Appendix I) Coordinates and notation Measurement methods Recommendations for future tests	
II	GENERAL DESCRIPTION OF THE EXPLOSION Fig. 1	5
III	DEVELOPMENTS BEFORE THE GROUNDSTRIKE ( $6.5 \cdot 10^{-4}$ seconds)	7
	Radius proportional to the two-fifths power of the time Hot, pinched bottom - Figs. 2,3 Eqs. (1), (2) Blisters - (Table II) Spikes - (Table III) Time of groundstrike	
IV	DEVELOPMENTS APPARENTLY CONSEQUENT UPON THE GROUNDSTRIKE	14
	Skirt - Figs. 4,5,6,7 Curtain of light Hot V in the skirt Belt, or Mach front - (Table IV)	
V	OTHER DEVELOPMENTS BEFORE $10^{-2}$ SECONDS	16
	Irregular curvature Hot spots Area boundaries	
VI	DEVELOPMENTS BETWEEN $10^{-2}$ AND $10^{-1}$ SECONDS	18
	Separation of the shock front from the ball of fire Dark front - Fig. 8 Departure of the shock velocity from the two-fifths power law - Eqs. (3), (4)	
VII	REFRACTION BY THE SHOCK FRONT AT $10^{-1}$ SECONDS Fig. 9	21

000000  
000000

UNCLASSIFIED



DECLASSIFIED  
-11-

UNCLASSIFIED

VIII MASS MOTION OF THE AIR AT  $3 \times 10^{-1}$  SECONDS-FIG. 10 23

IX DEVELOPMENTS BETWEEN  $10^{-1}$  SECONDS AND 1 SECONDS 24

Partial envelopment of the ball by the skirt

X DEVELOPMENTS BETWEEN 1 and 10 SECONDS 25

Transition from the ball-of-fire stage to the smoke-cloud stage

Stoppage and resumption of the ascent of the top of the ball

Torus

Neck formation

Convection stem

Formation and rise of the smoke cloud - Fig. 11

Change of shape of the smoke cloud

Persistence of the torus in the smoke cloud

Expansion of the smoke cloud - (Table .)

XI DEVELOPMENTS BETWEEN  $10$  AND  $10^2$  SECONDS 31

Cloud ring formation - (Table V.)

Glow

Condensation

Stem twist

XII DEVELOPMENTS AFTER  $10^3$  SECONDS 34

Smoke pall

APPENDIX I EQUIPMENT - (Table I) 35

APPENDIX II MEASUREMENT METHODS 36

APPENDIX III RECOMMENDATIONS FOR FUTURE TESTS 39

Time of day

Following the shock wave further by cable motions

Improvements in time resolution during the early stages

More space reference marks

Increased number of motion picture cameras

Fixed position required for spectroscopy

LIST OF PHOTOGRAPHS (see page 111)

DECLASSIFIED  
-11-

UNCLASSIFIED

## Viewpoint Time Scale

Viewpoint	Time	Scale
1	10 <sup>4</sup> N time exposure	1: 4,400
2	800N W 0.10-0.21 ms	1: 2,000
3	800N W 1.03-1.93	1: 2,000
4	800N 2.18-4.38	1: 2,000
5	10 <sup>4</sup> N 6	1: 2,000
6	800N 5.69-8.66	1: 2,000
7	10 <sup>4</sup> N 16	1: 2,000
8	10 <sup>4</sup> N 15.1-26.0	1: 10,000
9	800N 18.1-21.1	1: 2,000
10	10 <sup>4</sup> N 25	1: 2,000
11	10 <sup>4</sup> N 34	1: 2,000
12	10 <sup>4</sup> N 44	1: 2,000
13	10 <sup>4</sup> N 53	1: 2,000
14	10 <sup>4</sup> N 62	1: 2,000
15	10 <sup>4</sup> N 72	1: 2,000
16	10 <sup>4</sup> N 81	1: 2,000
17	10 <sup>4</sup> N 90	1: 2,000
18	10 <sup>4</sup> N 100	1: 2,000
19 <sup>a</sup>	10 <sup>4</sup> N 100	1: 2,000
20	10 <sup>4</sup> N 109	1: 2,000
21	10 <sup>4</sup> N 116	1: 2,000
22	10 <sup>4</sup> N 127	1: 2,000
23	10 <sup>4</sup> N 0.2 sec	1: 2,000
24	10 <sup>4</sup> N 0.5	1: 2,000
25	10 <sup>4</sup> N 1.0	1: 2,000
26	10 <sup>4</sup> N 1.5	1: 2,000
27	10 <sup>4</sup> N 2.0	1: 2,000
28	110 <sup>4</sup> N 2.5	1: 2,000
29	10 <sup>4</sup> N 3.0	1: 2,000
30	10 <sup>4</sup> N 4.0	1: 2,000

31	10 <sup>4</sup> N 5.0 sec	1: 2,000
32	10 <sup>4</sup> N 10.0	1: 2,000
33	10 <sup>4</sup> N 0.118-0.214	1: 10,000
34	10 <sup>4</sup> N 0.01 - 0.50	1: 1,000
35	10 <sup>4</sup> N 0.21	1: 1,000
36	10 <sup>4</sup> N 0.34	1: 1,000
37	10 <sup>4</sup> N 5.00	1: 1,000
38 <sup>b</sup>	3.3-10 <sup>4</sup> NW 11.5	1: 100,000
39 <sup>b</sup>	3.3-10 <sup>4</sup> NW 14.5	1: 100,000
40 <sup>b</sup>	3.3-10 <sup>4</sup> NW 18.1	1: 100,000
41	3.3-10 <sup>4</sup> NW 8.1-18.1	1: 100,000
42	3.3-10 <sup>4</sup> NWL 8.1	1: 50,000
43	3.3-10 <sup>4</sup> NWL 11.5	1: 50,000
44	3.3-10 <sup>4</sup> NWL 14.8	1: 50,000
45	3.3-10 <sup>4</sup> NWL 18.1	1: 50,000
46	10 <sup>4</sup> N 1	1: 10,000
47	10 <sup>4</sup> N 2	1: 10,000
48	10 <sup>4</sup> N 3	1: 10,000
49	10 <sup>4</sup> N 4	1: 10,000
50	10 <sup>4</sup> N 5	1: 10,000
51	10 <sup>4</sup> N 6	1: 10,000
52	10 <sup>4</sup> N 7	1: 10,000
53	10 <sup>4</sup> N 8	1: 10,000
54	10 <sup>4</sup> N 9	1: 10,000
55	10 <sup>4</sup> N 10	1: 10,000
56	10 <sup>4</sup> N 11	1: 10,000
57	10 <sup>4</sup> N 12	1: 10,000
58	10 <sup>4</sup> N 13	1: 10,000
59	10 <sup>4</sup> N 14	1: 10,000
60	10 <sup>4</sup> N 15	1: 10,000

61	10 <sup>4</sup> N 16 sec	1: 10,000
62	10 <sup>4</sup> N 17	1: 20,000
63	10 <sup>4</sup> N 18	1: 10,000
64	10 <sup>4</sup> N 19	1: 10,000
65	10 <sup>4</sup> N 20	1: 10,000
66	10 <sup>4</sup> N 21	1: 10,000
67	10 <sup>4</sup> N 22	1: 10,000
68	10 <sup>4</sup> N 23	1: 10,000
69	10 <sup>4</sup> N 24	1: 10,000
70	10 <sup>4</sup> N 25	1: 10,000
71	10 <sup>4</sup> N 30	1: 10,000
72	10 <sup>4</sup> N 35	1: 10,000
73	10 <sup>4</sup> N 40	1: 10,000
74	10 <sup>4</sup> N 50	1: 10,000
75	10 <sup>4</sup> N 60	1: 10,000
76 <sup>c</sup>	4-10 <sup>4</sup> NW 30-40	~10 <sup>-4</sup>
77 <sup>c</sup>	4-10 <sup>4</sup> NW 50 - 60	~10 <sup>-4</sup>
78 <sup>c</sup>	4-10 <sup>4</sup> NW 80 - 90	~10 <sup>-4</sup>
79 <sup>c</sup>	4-10 <sup>4</sup> NW ~2 min	~10 <sup>-4</sup>
80	3.3-10 <sup>4</sup> NW ~5 min	~10 <sup>-4</sup>
81	3.3-10 <sup>4</sup> NW ~10	~10 <sup>-4</sup>
82 <sup>d</sup>	10 <sup>4</sup> N 40	~10 <sup>-4</sup>
83	vertical 28 hrs.	1: 10,400

<sup>a</sup> High contrast copy.<sup>b</sup> Vectograph (stereo print);  
use the viewer in pocket.<sup>c</sup> Courtesy of Stanley Frankel;  
the time and space scales of  
these pictures are not known.  
Color print.

U.S. AIR FORCE  
 OFFICE OF  
 THE SECRETARY

UNCLASSIFIED

-2-

Abstract

Fig. 1 is a compilation of almost all the data.

Except for the extra brightness and retardation of a part of the sphere near the bottom, a number of blisters, and several spikes that shot radially ahead of the ball below the equator, the expansion of the ball of fire before striking the ground was almost symmetric, following the relationship,  $R \propto t^{2/5}$ , where  $R$  is the radius and  $t$  is the time in seconds.

Contact with the ground was made at  $0.65 \pm 0.05$  milliseconds. Thereafter, the ball became rapidly smoother. From 1.5 to 32 milliseconds the time dependence of the radius followed closely the relationship,  $R \propto (t + 4 \cdot 10^{-4})^{2/5}$ . At 3 milliseconds there appeared at the bottom of the ball an irregular line of demarcation, below which the surface was appreciably brighter than above; this line rose like the top of a curtain until it disappeared near the top of the ball at about 11 milliseconds. Shortly after the spikes struck the ground there appeared on the ground ahead of the shock front a wide skirt of lumpy matter, and within and above the skirt a smooth belt (interpreted as the Mach wave), originally brighter than the main front but rapidly growing dimmer.

Two successive visible fronts dropped behind the well-defined shock front. The brighter but less sharply limited ball of fire fell behind it at about 0.016 seconds. At about 0.032 seconds there appeared immediately behind the shock front a dark front of absorbing matter, which traveled slowly out until it became invisible at 0.85 seconds. The shock

U.S. AIR FORCE  
 OFFICE OF  
 THE SECRETARY

UNCLASSIFIED

000000  
000000

UNCLASSIFIED

-2A-

front itself became invisible at about 0.10 seconds, but was followed until 0.39 seconds, first by its light-refracting property and later by the impulse it imparted to a balloon cable. The mass motion of the air could be determined from a study of the motion of the vapor of the balloon cable.

The ball of fire grew ever more slowly to a radius of about  $3 \cdot 10^2$  meters, until the dust cloud growing out of the skirt almost enveloped it. The top of the ball started to rise again at 2 seconds. At 3.5 seconds a minimum horizontal diameter, or neck, appeared one-third of the way up the skirt, and the portion of the skirt above the neck formed a vortex ring. The neck narrowed, <sup>and</sup> the ring and the fast-growing pile of matter above it rose as a new cloud of smoke, carrying a convection stem of dust up behind it. A boundary within the cloud, between the ring and the upper part, persisted for at least 22 seconds. The stem appeared twisted like a left-handed screw. The cloud of smoke, surrounded by a faint purple haze, rose with its top traveling at 57 meters per second, at least until the top reached 1.5 kilometers. The later history of the cloud was not quantitatively recorded.

UNCLASSIFIED

000000  
000000

000000  
000000JULY 16TH NUCLEAR EXPLOSION - SPACE-TIME RELATIONSHIPS

## 1. INTRODUCTION

Purpose

The purpose of this report is to make a detailed description of the events consequent upon the explosion, as determined by the analysis of photographs. Approximately  $10^5$  photographic exposures were made, almost all of them motion picture frames. The report does not include any spectrographic or radiometric results; these are in separate reports <sup>1,2</sup>. A great deal of the material contained here is presented less quantitatively but more graphically in a series of motion picture titles<sup>3</sup> and edited motion pictures<sup>4</sup>.

Photographs included in this report

Eighty-three prints are included at the end of this report. They are listed in the table of contents in tabular form, showing the viewpoint, the dimensional scale of the print, and the time, for each. Among the prints are several composites, four stereo prints (for which a stereo viewer is included), and one color print. There is some departure from chronological order for the sake of continuity of the sequences. In order to avoid a confusing array of references in almost every sentence, all reference to the prints is avoided in the body of the report.

<sup>1</sup> D. Williams and P. Yuster, LA - 353.

<sup>2</sup> F. E. Geiger, J. E. Mack, and S. Nicholson, LA - 589

<sup>3</sup> Cf. J. E. Mack, LAMS - 373

<sup>4</sup> On file in Group M - 8.

UNCLASSIFIED

000000  
000000

U U U U  
S I F I E D

-4-

Almost everything mentioned in the report is illustrated by at least one of the prints included here. The pertinent prints can usually be found easily by searching for prints belonging to the appropriate time.

#### Equipment

Appendix I contains, in Table I, a compilation of the principal equipment used for producing the pictures measured for this report, together with all the most important data regarding the equipment and the pictures.

UNCLASSIFIED

#### Coordinates and notation

Measurements were made in terms of a coordinate system whose cardinal directions are N, W, S, and E, where N is, according to an engineering survey,  $21^{\circ}56'$  west of north, and W, S, and E are successive intervals of  $90^{\circ}$  counterclockwise. When a point is referred to by latitude or azimuth, the origin is the explosion center, the latitude is an angle measured positive upward from the horizontal, and the azimuth is measured counterclockwise from the direction N. The four principal camera stations were all nearly (within 10 minutes of arc) in cardinal azimuthal directions from the origin, viz., at 800 and  $10^4$  yards N and W. The stations are usually designated by distance in yards and direction, e.g., 800 N is approximately 800 yards in the direction N from the gadget center. A station called  $3.3 \cdot 10^4$  N had two cameras at azimuths  $251\frac{1}{3}^{\circ}$  and  $262\frac{2}{3}^{\circ}$ , called  $3.3 \cdot 10^4$  NW<sub>L</sub> and  $3.3 \cdot 10^4$  NW<sub>R</sub>, respectively. Reference points for determining distance were the centers of four billboards ten feet square, centered 200 meters from the vertical line through the center of the gadget in the

U U U U  
S I F I E D





000000  
000000

-5-

directions N, W, S and E.<sup>5</sup> Time intervals were measured with reference to the period of a 1000-cycle tuning fork. The origin of the time scale was fixed at approximately the time of the nuclear explosion by extrapolating the radius of the ball of fire backward to zero (cf. Fig. 2 below). Numerical values appearing after the sign  $\pm$  in this paper are estimated probable errors.

UNCLASSIFIED

#### Measurement methods

The details of the methods used in determining the space-time relationships shown in the graphs are given in Appendix II.

#### Recommendations for future tests

Recommendations for future tests are given in Appendix III.

## II. GENERAL DESCRIPTION OF EXPLOSION

The significant space-time relationships that we have measured from the photographic records are shown in the graphs, Figs. 1 to 11. Fig. 1 is a compilation of almost all the data.

Except for the extra brightness and retardation of a part of the sphere near the bottom, a number of blisters, and several spikes that shot radially ahead of the ball below the equator, the expansion of the ball of fire before striking the ground was almost symmetric, following the relationship,  $R \propto t^{2/5}$ , where  $R$  is the radius in meters, and  $t$  is the time in seconds.

Contact with the ground was made at  $0.65 \pm 0.05$  milliseconds.

<sup>5</sup>Surveying details may be found on page 47 of LA notebook number 884.

000000  
000000



U.S. AIR FORCE  
 REPORT

-6-

UNCLASSIFIED

Thereafter the ball became rapidly smoother. From 1.5 to 32 milliseconds the time dependence of the radius followed closely the relationship  $R \propto (t - 4 \cdot 10^{-4})^{2/5}$ . At 3 milliseconds there appeared at the bottom of the ball an irregular line of demarcation, below which the surface was appreciably brighter than above; this line rose like the top of a curtain until it disappeared at the top of the ball at about 11 milliseconds. Shortly after the spikes struck the ground (about 2 milliseconds) there appeared on the ground ahead of the shock front a wide skirt of lumpy matter, and within and above the skirt a smooth belt (interpreted as the Mach wave), originally brighter than the main front but rapidly growing dimmer.

Two successive visible fronts dropped behind the well-defined shock front. The brighter but less sharply limited ball of fire fell behind it at about 0.016 seconds (105 meters). At about 0.032 seconds (150 meters) there appeared immediately behind the shock front a dark front of absorbing matter, which traveled slowly out until it became invisible at 0.85 seconds (375 meters). The shock front itself became invisible 0.10 seconds ( $2.4 \cdot 10^2$  meters), first by its light-refracting property and later by the impulse it imparted to a balloon cable. The mass motion of the air could be determined from a study of the motion of the vapor of the balloon cable.

The ball of fire grew ever more slowly to a radius of about  $3 \cdot 10^2$  meters, until the dust cloud growing out of the skirt almost enveloped it. At 2 seconds the top of the ball started to rise again. At 3.5 seconds a minimum horizontal diameter, or neck, appeared, one-third of

U.S. AIR FORCE  
 REPORT

DECLASSIFIED

-7-

UNCLASSIFIED

the way up the skirt, and the portion of the skirt above the neck formed a new vortex ring. The neck narrowed, and the ring and the fast-growing pile of matter above it rose as a new cloud of smoke, carrying a convection stem of dust up behind it. An approximately horizontal boundary within the cloud, between the ring and the upper part, persisted for at least 25 seconds. The stem appeared twisted like a left-handed screw. The cloud of smoke, surrounded by a faint purple haze, rose with its top traveling at 57 meters per second, at least until the cameras lost its relationship to the horizon at 1.5 kilometers.

### III. DEVELOPMENTS BEFORE THE GROUNDSTRIKE ( $6.5 \cdot 10^{-4}$ seconds)

Radius proportional to the two-fifths power of the time.

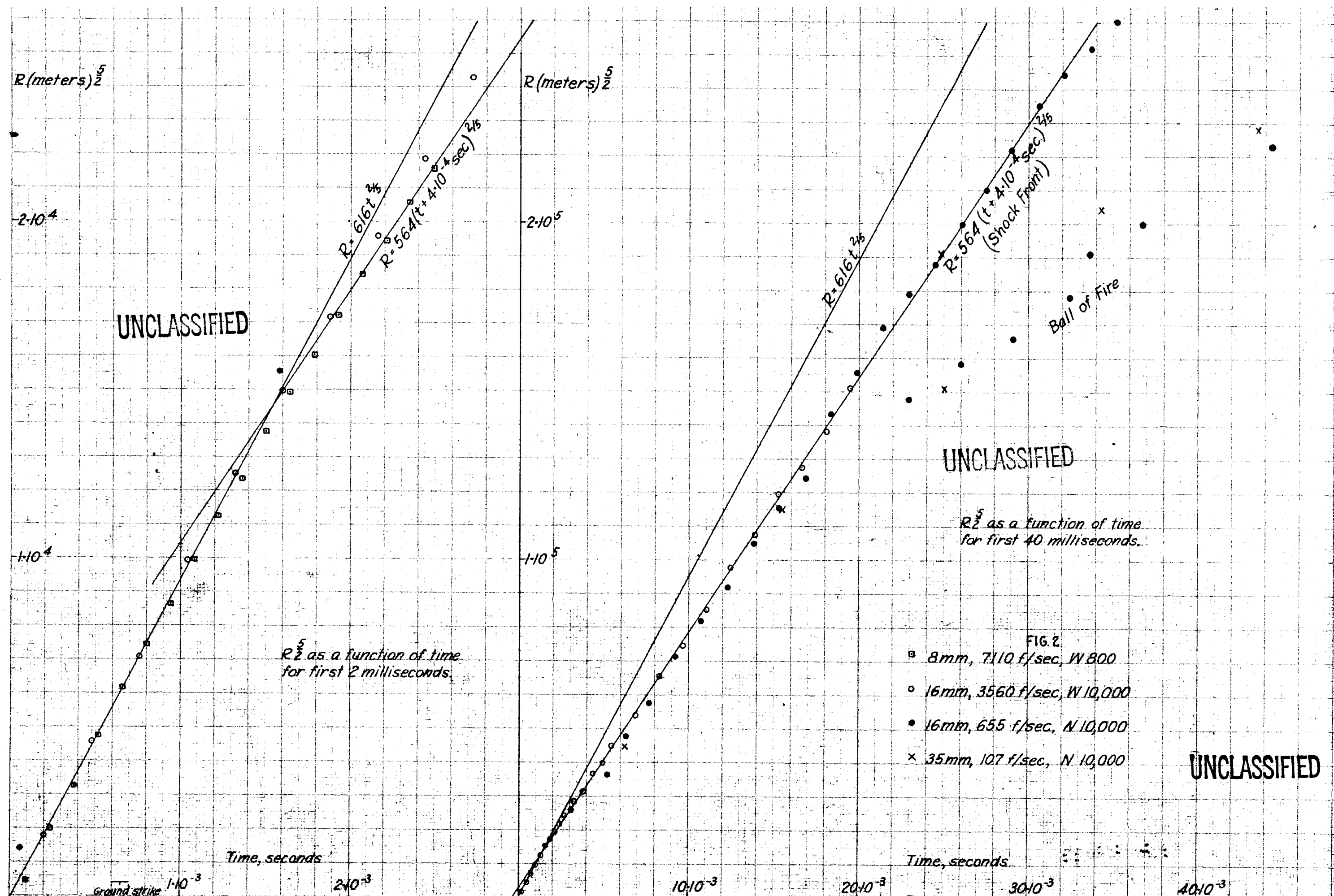
Within the limits imposed by our best resolving time of about 0.1 milliseconds, the observed value of the radius during the early expansion of the ball of fire (Figs. 1, 2, 3), was proportional to the  $0.404 \pm 0.008$  power of the elapsed time. The relationship can be expressed, within the accuracy of the observations, as:

$$R \approx 616 t^{2/5} \quad \text{Eq. (1)}$$

where  $R$  is the radius in meters, and  $t$  is the time in seconds. This agrees with Taylor's theoretical relation  $R \propto t^{2/5}$ . After 1.5 milliseconds the expansion was slightly slower, following a two-fifths power law with a shifted zero of time:

$$R = 564 (t + 4 \cdot 10^{-4})^{2/5} \quad \text{Eq. (2)}$$

Eq. (2) was followed from 1.5 to 32 milliseconds. Three weaknesses of the



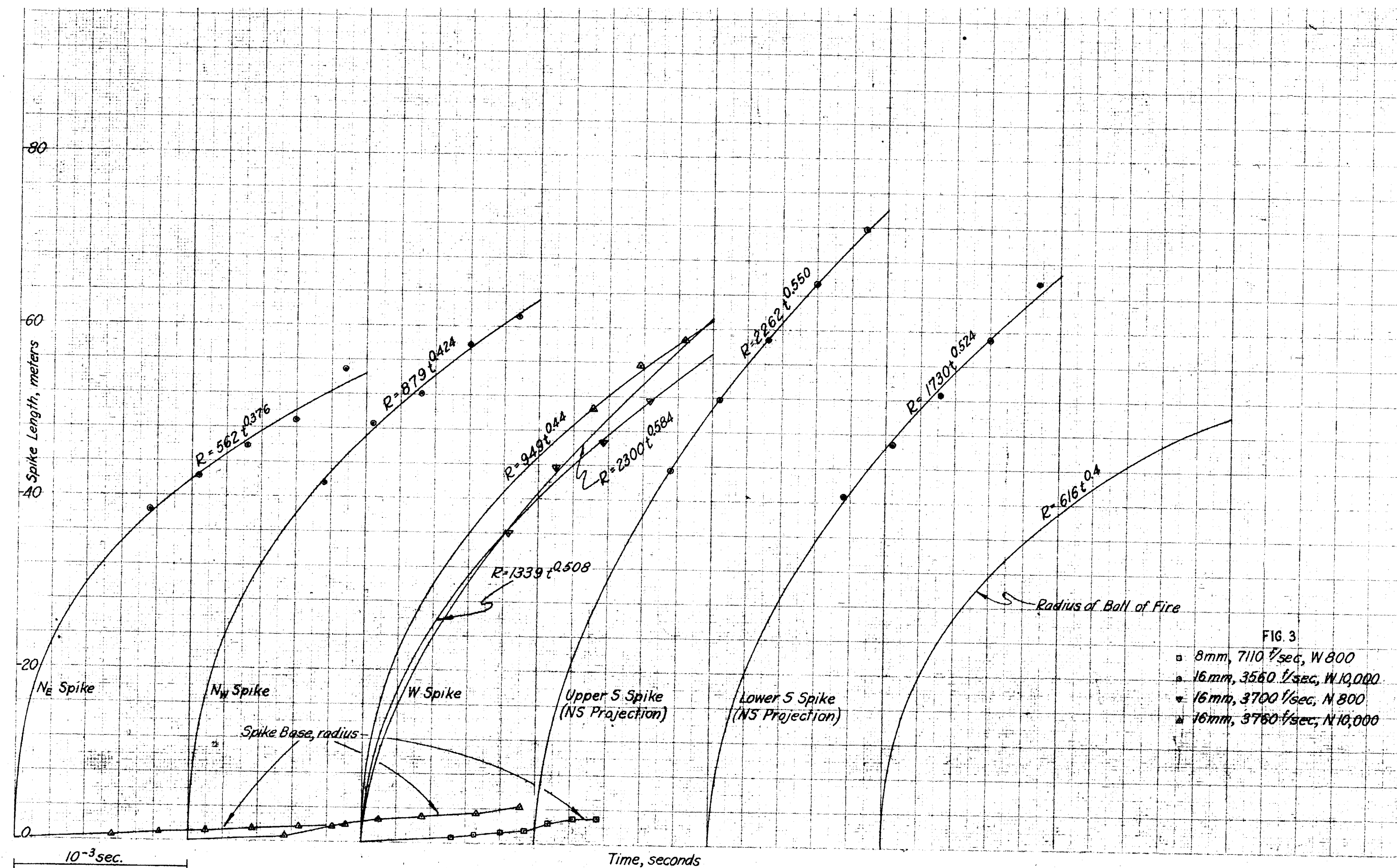
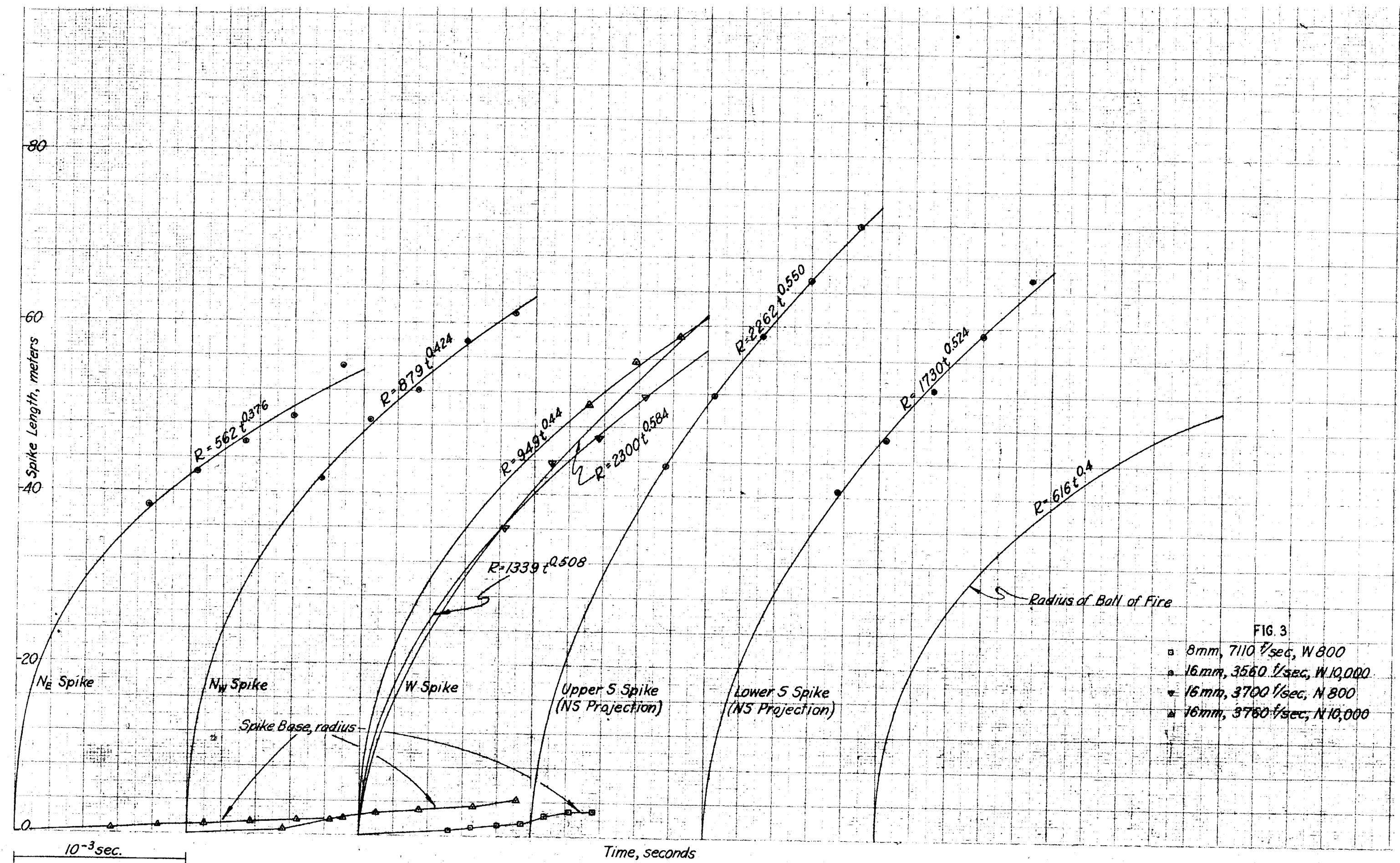


FIG 3

- 8mm, 7110 f/sec, W 800
- 16mm, 3560 f/sec, W 10,000
- ✦ 16mm, 3700 f/sec, N 800
- ▲ 16mm, 3760 f/sec, N 10,000

UNCLASSIFIED

UNCLASSIFIED



UNCLASSIFIED

UNCLASSIFIED

000000  
000000

UNCLASSIFIED

-8-

analysis ought to be pointed out: First, the time scale of all the other cameras is fitted to that of the slow 16mm Fastax at  $10^4$  N (#209), so the abscisses for all the points other than the solid discs are valuable only for their internal consistency. Second, the time is not independently known relative to the nuclear explosion; our zero was determined by extrapolation in Fig. 2. Third, with regard to the radius measurements, which for the 8 and 16mm cameras were all determined from horizontal diameters, it was necessary to decide what to interpret as the extent of the ball, in view of the blisters (cf. Blisters, below): the measurements were made to the extremes of the ball, except that the limit in the direction W was taken at the base rather than the outer surface of the compound blister, a policy that brought fair agreement between pictures from N and W.

Bethe has pointed out the usefulness of the early radius-time relationship in the determination of the total energy released in the explosion, and Fuchs<sup>6</sup> has given detailed consideration to this aspect of the data.

Hot, pinched bottom

The slight information that we have for the first 0.1 milliseconds indicates that at the end of that period there was a uniformly bright body, spherically symmetric except for an approximately uniform retardation

<sup>6</sup>K. Fuchs, IA - 516.

000000  
000000

000000  
000000

UNCLASSIFIED

of about 30 percent in radius within a zone extending about 50 degrees from a polar axis directed about 10 degrees W of the nadir. By 0.2 milliseconds the retarded portion was brighter than the rest, and surrounded by a sharp demarcation line<sup>7</sup>. At 0.5 milliseconds the zone boundary was still retarded about 20 percent, but the polar region had a radius indistinguishable in magnitude from the horizontal one. The strike occurred at (0.65 0.05) milliseconds. The bright zone persisted until it was covered by the skirt at about 2.0 milliseconds.

These phenomena have been attributed by Peierls to the steel-supported wooden platform on which the gadget cradle rested. The floor was 1.1 meters below the gadget center, and extended symmetrically in a 4.65 meter square. The platform consisted of a steel frame of mass  $1.48 \cdot 10^3$  kilograms and an oakwood floor of  $1.17 \cdot 10^3$  kilograms. Above the platform there were  $1.43 \cdot 10^3$  kilograms of steel, in addition to the sheet metal house of  $0.68 \cdot 10^3$  kilograms<sup>8</sup>.

<sup>7</sup>Possibly the absence of evidence of any earlier line arises from insufficient time resolution during the initial high-speed expansion, which was at the rate of about 62 km per sec. at 0.1 milliseconds and only 16 km per sec. at 1 millisecond. The period of the pertinent camera was  $1.4 \cdot 10^{-4}$  sec. Since more than half the field of an 8mm Fastax camera is exposed for 55 percent of the period (cf. record of experiments by T. J. Walker, in the files of the Optics group), the boundary line could have moved about 5 meters, or more than enough to hide it by blurring, during a single exposure at 0.1 milliseconds.

<sup>8</sup>The data on the tower components is based upon information supplied by P. W. Anderson.

000000  
000000

DECLASSIFIED

-10-

UNCLASSIFIED

Blisters

By about 0.2 milliseconds, between thirty and forty blisters (the numerical estimate is based on two views at right angles) had formed on the ball. They were approximately hemispherical and of roughly the same order in size, with radii of about 1 to 2 meters. By 0.5 milliseconds they covered surface regions with about two or three times their original diameters, but they protruded slightly less than originally. After that time they subsided rapidly, until at 1 millisecond most of the surface of the ball was exceedingly smooth. The only especially noticeable blisters remaining then were one compound one and four or five others, which will be described below.

Pointing slightly above the horizontal and almost straight W, there grew early an exceptionally prominent blister (latitude  $13^{\circ}$  azimuth  $88^{\circ}$ ) surmounted by a second one slightly below its center (latitude  $10^{\circ}$  azimuth  $93^{\circ}$ ) that from 1 to 4 milliseconds appears thermally isolated and considerably cooler than the main ball; almost diametrically opposite was a rather large blister that lasted until about 1 millisecond. The dimensions of the compound blister are given in Table II.

DECLASSIFIED



U.S. GOVERNMENT  
PRINTING OFFICE

-11-

TABLE II

UNCLASSIFIED

DIMENSIONS OF THE COMPOUND BLISTER AT LATITUDE  $10^{\circ}$ ,  $13^{\circ}$ , AZIMUTH  $88^{\circ}$ ,  $93^{\circ}$

All distances are given in meters

Time, milliseconds	0.2	0.5	1.0	5	8
Base blister, radius	4	8	11	30	(gone)*
Extent from spherical surface	3	7	4	4	0*
Superposed blister, radius	1	3	6	(gone)	
Total extent from spherical surface	5	10	8	4	0*

\* That is, the extent is too slight for accurate measurement in the small-scale Fastax images, ( $\sim 1$  meter). It is still noticeable at 10 milliseconds; cf. Sec. V, Irregular curvature.

Three rather prominent blisters (and possibly a fourth, to the S of E where it can be seen only from the cameras in direction N, and hardly from them) grew at latitude about  $60^{\circ}$ , at irregularly spaced azimuths. For the second quarter millisecond they made the ball appear flat-topped. One of them (at latitude  $70^{\circ}$ , azimuth  $6^{\circ}$ ) appears quite isolated, as though it were a completely separate oblate spheroid set into a dimple in the main ball. From the outset it was cooler than the sphere; the brightness contrast increased until about 1 millisecond. It grew in equatorial radius from 3 meters at 0.2 millisecond to 6 meters at 1 millisecond. Thereafter it flattened out, remaining distinctly indentifiable for almost  $10^{-1}$  seconds (cf. Sec. V, Hot spots, Area boundaries).

U.S. GOVERNMENT  
PRINTING OFFICE

000000  
-12-  
000000

UNCLASSIFIED

Spikes

Before 0.5 milliseconds, V-shaped spikes started to appear ahead of the expanding front. Whenever a spike appeared against the ball, it appeared very dark. Five spikes could be seen on the three-fourths of the sphere visible from the cameras. They struck the ground between 2.0 and 2.4 milliseconds. All occurred at nearly the same latitude, about  $-30^\circ$ , near the boundary of the pinched region. In azimuth, two projected almost straight N and one almost straight E; and although the other two could not be seen in stereo, they appeared to be nearly S. Fig. 3 shows the length and base radius, or projected length, of each spike. For these measurements, the base is taken as the intersection of the spike with the ball of fire, and the length is measured from the center of the sphere even though there is evidence that the spikes are not radial. Table III shows some of the other details for each of the spikes. It is clear from Table III that each of the three spikes that was observed in stereo originated near a vertical cardinal plane through the center of the gadget, and that it traveled in a direction better approximated by a line parallel to that plane than by a radius.

TABLE III

## SPIKES

"Early" and "late" refer to the times of the two entries in the azimuth columns.

Name of spike	Latitude	Azimuth at				Displacement of vertex from central vertical cardinal plane	
		0.52 ms	0.78 ms	1.2 ms	1.3 ms	early	late
N <sub>1</sub>	$-35^\circ$		344.6°		355.4°	3.6,	3.7 meters E of N
E <sub>1</sub>	$-24^\circ$		2.5°		2.0°	1.8,	1.8 meters E of N
S <sub>1</sub>	$-29^\circ$	84.5°		86.0°		2.9,	3.3 meters N of E
Upper S (MS projection only)	$-28^\circ$	(not determinable)				(Not determinable)	
Lower S (MS projection only)	$-36^\circ$	(not determinable)				(Not determinable)	

U.S. GOVERNMENT  
PRINTING OFFICE

-13-

UNCLASSIFIED

Six wires and two associated cables ran to the ground from points on the tower near the gadget. Two coaxial cables ran to the ground, one at approximately 200 feet N (latitude  $-32^{\circ}$ ), and the other just west of it at approximately 300 feet N (latitude  $-21^{\circ}$ ). One guy wire supported each of these cables, two guy wires extended approximately S, and one each extended approximately east and west<sup>9</sup>. The systematic arrangement of the spikes in both azimuth and latitude points to a probable relationship between them and the guy wires. The geometric relationship between the two N spikes, as seen from the N cameras, is in qualitative agreement with that between the two coaxial cables. The observed cone shape would be expected if the velocity of the shock front along the cable were several times the velocity of the consequent shock front in the surrounding air. The absence of any spike to the east, the orientation of one spike toward W instead of west, and the ball-like end of the N spike at late times in contrast with the pointed ends of the others, are not yet accounted for by the cable hypothesis of the spikes' origin.

#### Time of the groundstrike

By interpolation, the time of the groundstrike has been determined to be  $(6.5 \pm 0.5) \cdot 10^{-4}$  seconds.

<sup>9</sup>The information given here regarding the guy wires east, S, and west was reported orally several months after the explosion, from the memory of H. S. Allen, who was in charge of the rigging at the tower, and of one of the riggers. It absolutely verifies, in J. E. M.'s opinion, the existence of a guy wire running in the general direction of east or E, but does not absolutely exclude the possibility that the guy wire reported as running west actually ran W.

U.S. GOVERNMENT  
PRINTING OFFICE

### III. DEVELOPMENTS APPARENTLY CORRELATING WITH THE GROUNDSTRIKE

UNCLASSIFIED

#### Skirt

Shortly after the groundstrike there arose from the ground, and advanced ahead of the ball, a skirt or mass of matter that persisted until it turned into, or was succeeded by, the great cloud of dust that eventually almost enveloped the ball. Unlike all the other elements of the early post-explosive stages, the skirt presented a lumpy, rather than a smooth, surface. The hot lumps were brighter than the ball of fire itself during the first few milliseconds of its existence, and equal to it in brightness at 30-1 milliseconds, after which they cooled rapidly.

The extent of the skirt is shown in Figs. 1, 4, 6, and 7, and the velocity, in Fig. 5.

While the travel of the outer border of the skirt along the ground agrees qualitatively with that of the expected ground shock, the early vertical extent of the lumpy material is puzzling.

#### Curtain of light

Starting at 3 milliseconds, an irregular boundary line appeared above the skirt. Below the line the ball was considerably brighter than above it. The boundary rose at a rate that increased, then decreased, until the boundary disappeared near the top of the ball at about 11 milliseconds. The ball appeared to be enveloped in a rising curtain of light. No satisfactory explanation has been given for this phenomenon.

Fig. 4 shows the altitude of the curtain as a function of the time, and Fig. 5, the vertical velocity. Each vertical line in Fig. 4 extends from 1 meter above the maximum height to 1 meter below the mean height, as measured in a frame. The dashed line at 10.8 milliseconds indicates that the curtain was indistinguishable from this point on, but undoubtedly reached the top of the ball.

UNCLASSIFIED

250

200

150

100

50

0

Distance, meters

FIG. 4

- 8mm, 710 f/sec, W 800
- 16mm, 3560 f/sec, W 10,000
- 16mm, 655 f/sec, N 10,000
- x 35mm, 107 f/sec, N 10,000

UNCLASSIFIED

Skirt, radius

Shock Front, radius

Ball of Fire, radius  
(edge indefinite)

Curtain, altitude

Mach Y, maximum altitude

Mach Y, minimum altitude

Skirt, maximum altitude

Skirt, minimum altitude

UNCLASSIFIED

APPROVED FOR PUBLIC RELEASE

Time, minutes

DATA SHEETS

CHARLES BRUNING COMPANY, INC. NO. 760-M

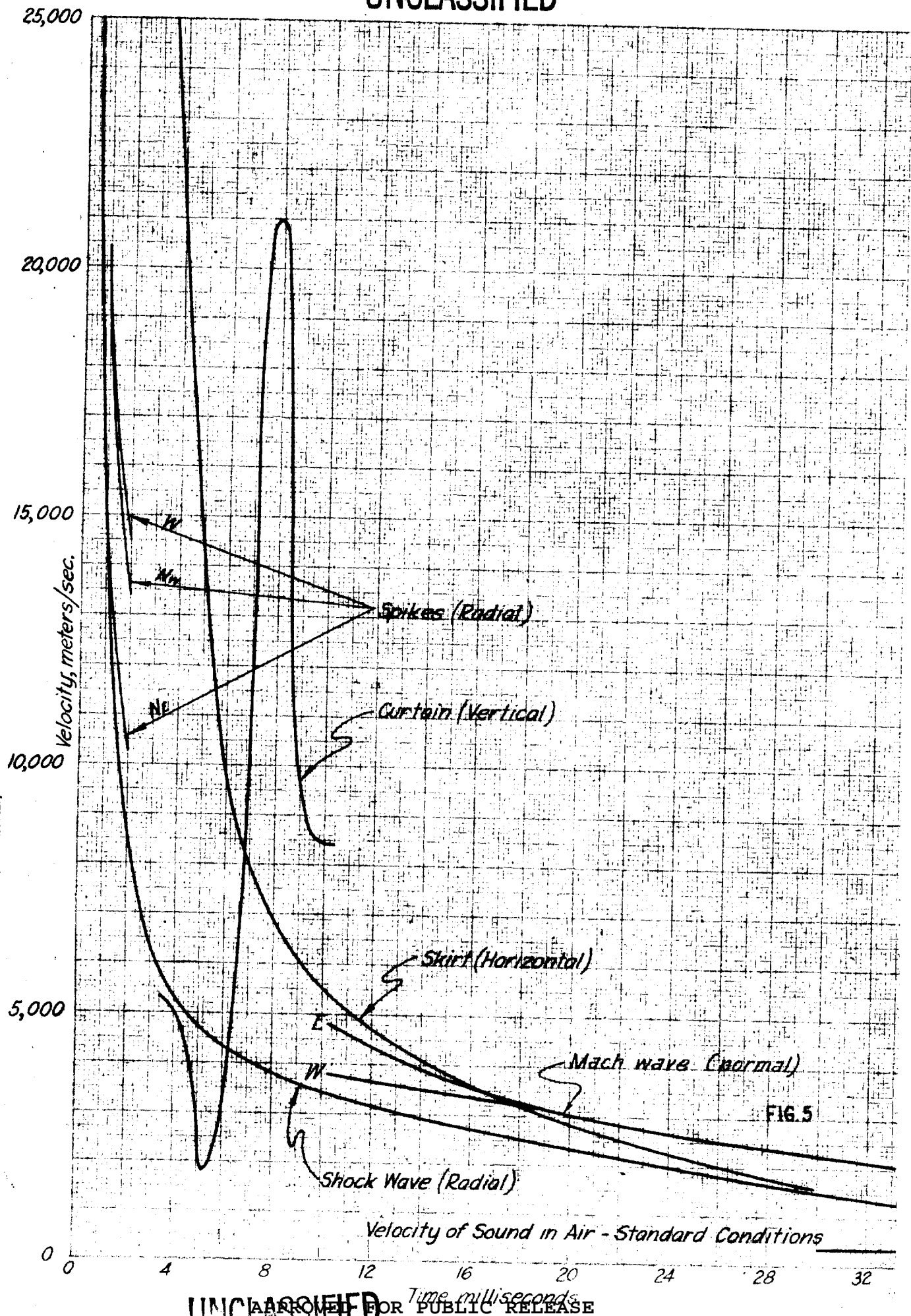
Millimeters, both horizontal and vertical

PRINTED

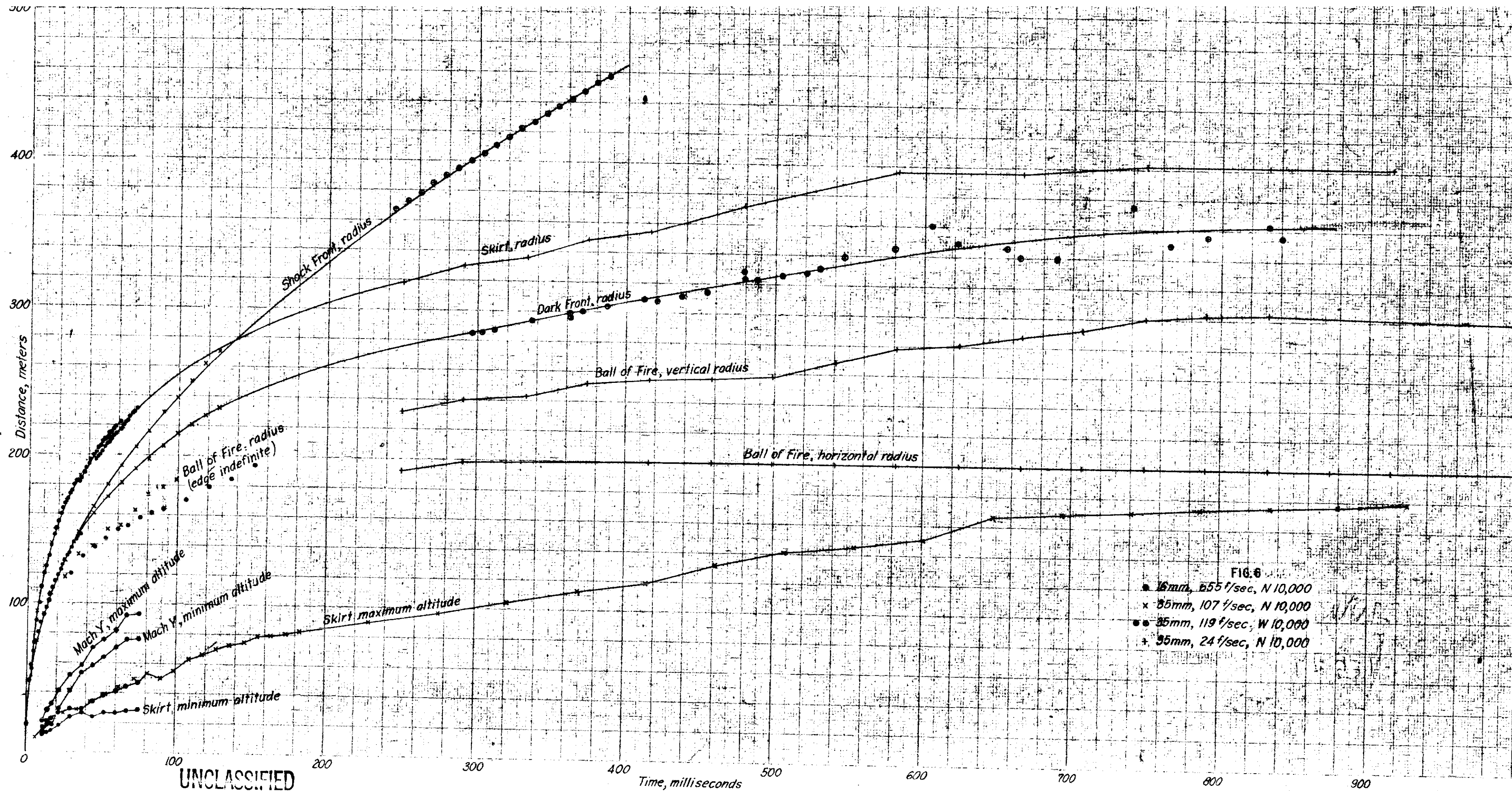
UNCLASSIFIED

DATA SHEETS

CHARLES BRUNING COMPANY, INC. NO. 700-2  
1000 Industrial Blvd. Long Beach, Calif. 90801



UNCLASSIFIED APPROVED FOR PUBLIC RELEASE

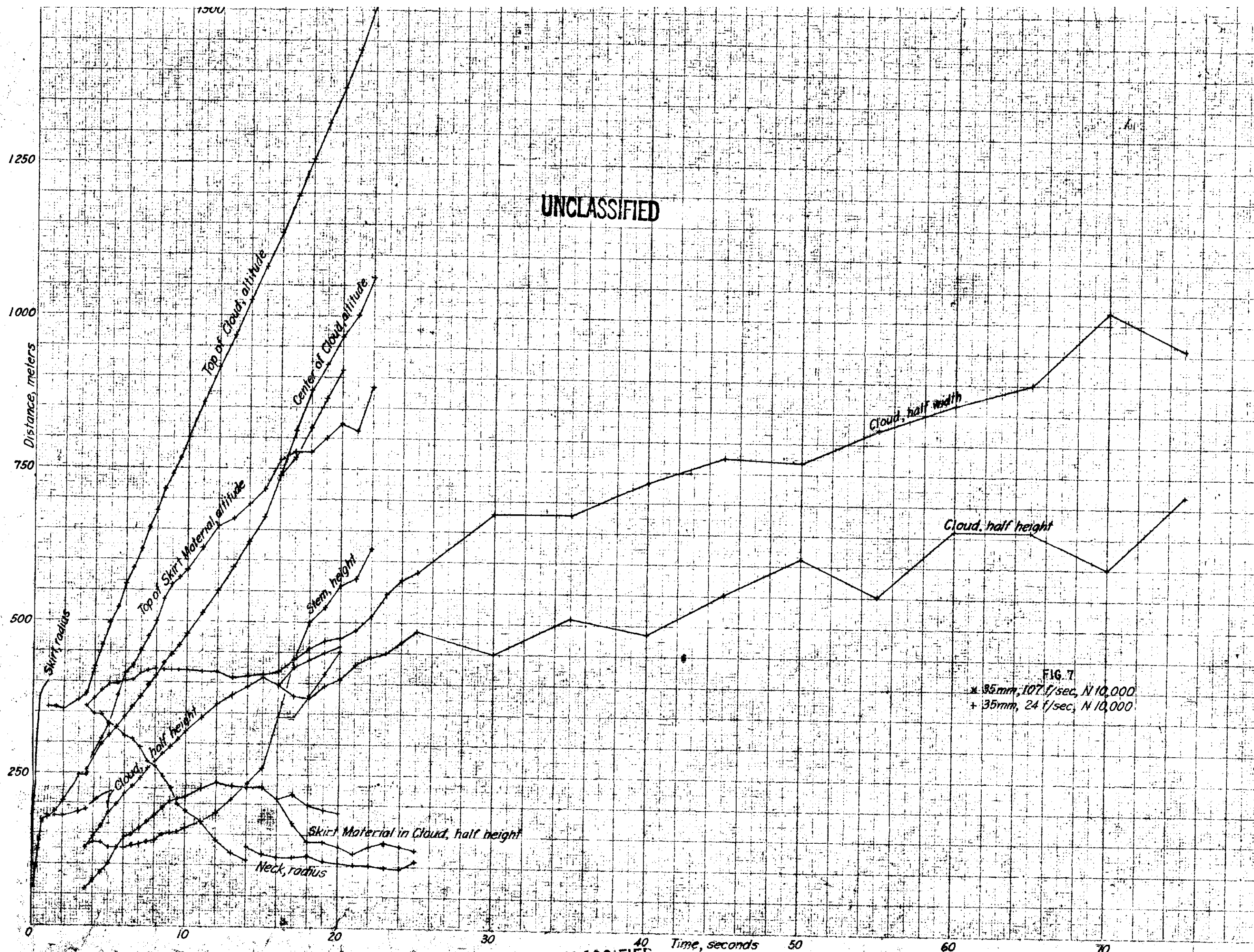


UNCLASSIFIED

UNCLASSIFIED



SCHEMATIC CROSS SECTION  
OF HEAVY 100 MILLIMETER





DECLASSIFIED

-15-

UNCLASSIFIED

Hot V in the skirt

In very nearly the direction N, where two coaxial cables extended obliquely from the gadget to the ground and where two spikes struck the ground at about 2 milliseconds, a V-shaped portion appeared at the birth of the skirt. Its apex rose from the ground to an altitude of about 10 meters in 40 milliseconds. During the early history of the skirt it was much hotter than the rest of the skirt; the difference became noticeable at 5 milliseconds and was very prominent in some lumps between 25 and 65 milliseconds, after which the V cooled rapidly. At about 30 milliseconds an indefinitely defined dark spot, evidently consisting of smoke, appeared immediately above it, and after 40 milliseconds, more of the V itself than of its surroundings was hidden by smoke. After the V cooled, there appeared, where the V had been, a relatively clear radial path in the smoky skirt region, that persisted for several seconds as though the combustible material near the spikes had been completely exhausted by burning while the V was especially hot.

Belt, or Mach front

At 3.6 milliseconds there appeared above the skirt a discontinuity in the orientation of the shock front. The belt below the break appeared to be a segment of a new, smooth, near-spherical surface with its center slightly below the ground, intersecting the old, spherical shock front. All the observations upon this belt are consistent with its being interpreted as the Mach front, and hereafter, it will be assumed that the belt was the Mach

DECLASSIFIED

U.S. GOVERNMENT  
PRINTING OFFICE

UNCLASSIFIED

-16-

wave front and that the break was the Mach "Y". The altitude of the Y was a slightly variable function of the azimuth. Previous to the separation of the shock wave from the ball of fire, the Mach front was considerably brighter throughout than the spherical shock front. After 19 milliseconds the part seen against the ball of fire appeared relatively dark until the boundary disappeared entirely at about 0.1 seconds, but even after 19 milliseconds the part that was viewed almost tangentially appeared bright in contrast with the spherical shock front. These observations indicate that the Mach front was more opaque, and hotter, than the spherical shock front. At about 0.04 seconds several approximately horizontal lines appeared within the region occupied by the Mach front. No explanation has been given for these lines. Table IV gives certain other details of the Mach front. Figures 4 and 6 show the time dependence of the altitude of the Y, and Fig. 5 shows its velocity during part of its history.

#### V. OTHER DEVELOPMENTS BEFORE $10^{-2}$ SECONDS.

##### Irregular curvature

The ball continuously approached sphericity in shape as long as its surface remained distinct. While at 1 millisecond the view from N showed concavities, especially near the compound blister and its opposite point, at 10 milliseconds the most prominent formerly concave segments were almost flat, and at 20 milliseconds, the surface was convex throughout, above the belt. At 10 milliseconds the contour of the ball appeared more like a

U.S. GOVERNMENT  
PRINTING OFFICE

000110

011110

TABLE IV

MACH FRONT

UNCLASSIFIED

All readings were taken on the original tracings, below.

Angles are measured with respect to the horizontal.

Positive angle means, velocity has an upward component.

Angular tolerances, unless specified: Fastax film #209,  $\pm 2^\circ$ .  
18" Mitchell film,  $\pm 1^\circ$ .

Frame no. 18" #209	Time, ms	Radius, meters	Angle, main wave normal		Angle, Mach wave normal		Angle, trajectory of Mach "Y"	
			E	W	E	W	E	W
1	6.3	74	-13.4°	-14.0°	+12° ± 3°	+14° ± 2°	+16°	+22°
	9	99	-4	-3	20	21	23	35
	10	103	-2	-1	19	23	23	33
2	15	109	-1.1	0.0	15 ± 1	24 ± 2	29	30
	11	107	-1	0	19	18	31	25
	12	111	+1	+1	19	18	35	22
	13	115	3	2	19	21	28	25
	14	119	3	3	22	24	29	44
	15	123	5	5	24	25	37	48
	16	127	6	7	23	25	41	45
3	25	130	6.0	5.0	25	26	46	36
	17	131	8	8	17	21	36	50
	18	134	9	8	22	21	35	22
	19	138	9	9	22	20	33	13
4	34	148	12.0	11.3	34	23	58	51

Fastax film #209

19

horizontal

gadget  
center

19

ground

18" Mitchell film

4

horizontal

gadget  
center

3

ground

DECLASSIFIED

-17-

UNCLASSIFIED

polygon than like a circle, with several edges about two-fifths as long as the radius.

#### Hot spots

From about 5 to 40 milliseconds many bright spots appeared on the surface of the ball. About 200 could be seen in one view. Almost all were from 1 to 3 meters in radius, but two were outstandingly large. A spot at latitude  $+20^{\circ}$ , azimuth  $19^{\circ}$ , was 8 meters in radius when it faded into the background at about 30 milliseconds. Another hot spot is discussed under "Area boundaries", below.

#### Area boundaries

Mild differences in brightness between different parts of the surface became evident at about 1 millisecond, and persisted until the shock wave became dark. The boundary lines were sharp and smooth. A little while after the separation of the shock wave from the ball of fire, the contrast between areas became unnoticeable, but the lines became darker than the areas they bounded and appeared to be in or close to the shock wave.

A hot spot at latitude  $+62^{\circ}$ , azimuth  $8^{\circ}$ , evidently related to a blister previously described (Sec. III Blisters), grew in radius from 4 meters at 16 milliseconds to 12 meters before it faded out of sight at about 100 milliseconds. It went from noticeably cooler to noticeably brighter than its background at about 5 milliseconds, and dimmer again at about 50 milliseconds. It was surrounded by an area that was somewhat brighter than

DECLASSIFIED

000000  
000000  
000000

UNCLASSIFIED

its surroundings until about 30 milliseconds. This roughly circular area grew in radius from 20 to about 40 meters between 16 and 100 milliseconds. It was not possible to trace the hot spot and boundary surely between 5 and 15 milliseconds, but from the fact that at 2 milliseconds the blister was 8 meters in radius and growing at the rate of 2 meters per millisecond, it appears that the boundary of the blister became the area boundary, and the hot spot was a sort of nucleus.

The boundaries mentioned here, which were relatively static in azimuth and latitude, are not to be confused with the pre-groundstrike boundary of the hot bottom, the boundary of the curtain, or the boundary between the Mach front and the spherical shock front.

#### VI. DEVELOPMENTS BETWEEN $10^{-2}$ AND $10^{-1}$ SECONDS

The interval from  $10^{-2}$  and  $10^{-1}$  seconds was characterized by the breaking up of the heretofore single front into three fronts.

##### Separation of the shock front from the ball of fire

Before 16 milliseconds only one front was discernible on the photographs. With the exception of the local irregularities listed above, the image of the shock front appeared as a uniformly bright disc. After (16 ± 1) milliseconds a slight darkening of the limb was noticeable and thereafter the relatively faint but sharp outer surface of the sphere, which we shall identify hereafter as the shock front, continued to expand according to Eq. (2), while the bright center region fell farther and farther behind it (Figs. 1, 4, 6). At any fixed time thereafter while it was measureable, the bright central region, which we shall identify as the

000000  
000000  
000000

DECLASSIFIED

UNCLASSIFIED

-19-

ball of fire, decreased gradually in brightness with increasing radius. As a consequence the ball of fire, unlike the shock front, was not susceptible to unique measurement. The disagreements among the values of the radius of the ball of fire in the figures are to be attributed not to disagreements in measurements, but to differences in exposure conditions among the several cameras, with consequent differences in the region of greatest contrast, (i.e., density gradient), which was arbitrarily taken to measure the approximate extent of the ball.

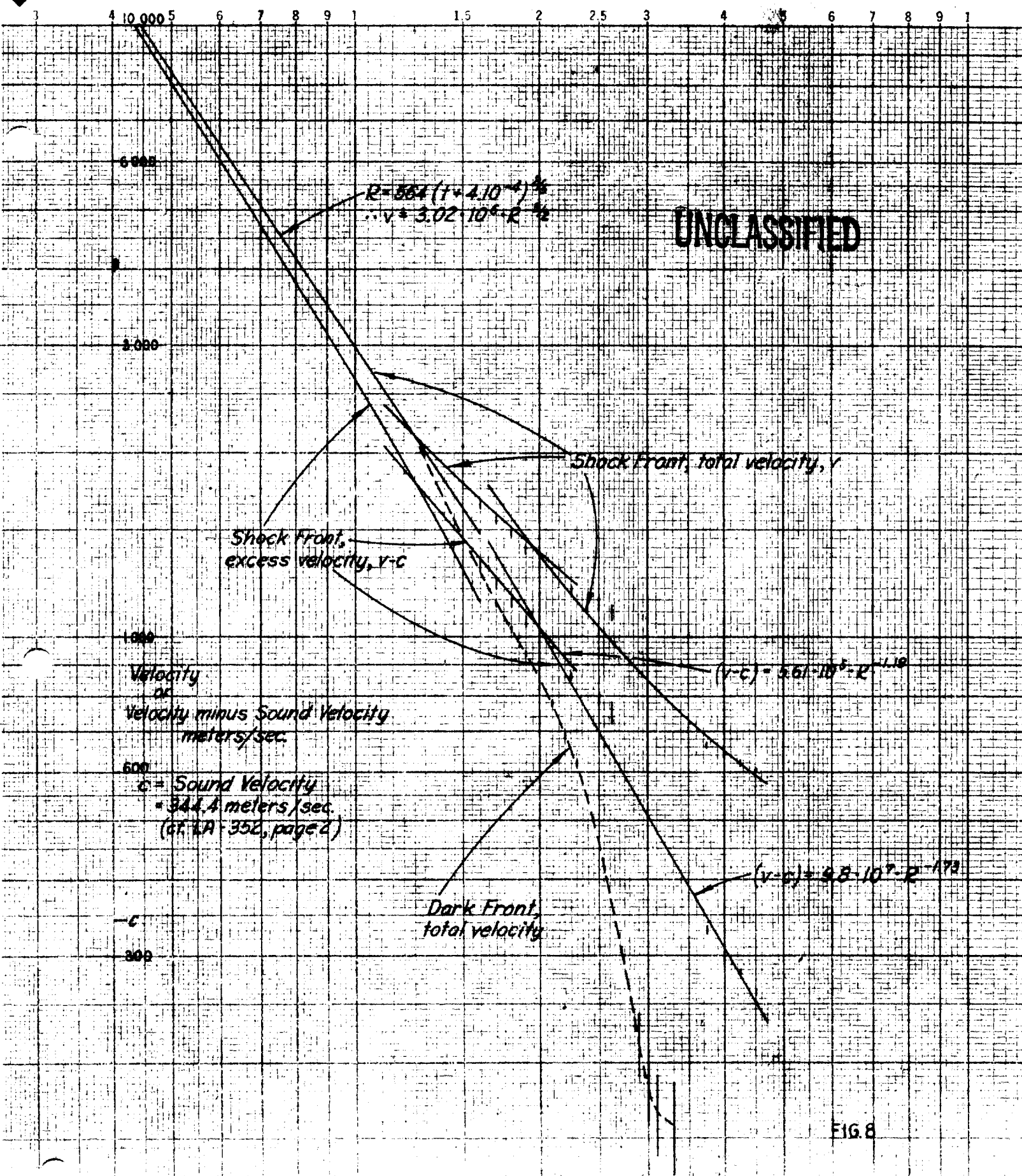
The ball of fire expanded with decreasing velocity to a radius between  $2 \cdot 10^2$  and  $3 \cdot 10^2$  meters (cf. Sec. IX, Partial envelopment of the ball by the skirt).

#### Dark front

At  $(32 \pm 3)$  milliseconds there split off behind the shock front a dark front, which progressed thereafter more slowly than the shock front (Figs. 1, 6, 8). The contrast at the dark front was originally almost the same as that at the shock front, but decreased more slowly than the contrast at the shock front, so that while the shock front became invisible at  $10^{-1}$  seconds, the dark front offered strong contrast at  $10^{-1}$  seconds and was noticeable until almost 1 second.

The dark front evidently consisted of absorbing matter. Probably it was a compound from the material of the damp air, produced by the thermodynamic conditions within the shock wave. It is evident that the formation

DECLASSIFIED



DECLASSIFIED

-20-

UNCLASSIFIED

of the compound required an increasing amount of time as the pressure and temperature within the shock wave decreased. A more detailed hypothesis of the dark wave is in preparation <sup>10</sup>.

Departure of the shock velocity from the two-fifths power law

Whereas the shock front followed the two-fifths power law up to the point of departure of the dark front from it (32-3 milliseconds, 143-6 meters), both fronts departed from the two-fifths power curve near the point of separation: the shock front traveled ahead of it and the dark front behind it (Figs. 1, 6, 8).

Very soon after the separation, the excess velocity, i.e., the shock front velocity  $v$  minus the sound velocity  $c$  (where  $c = 344.4$  meters per second<sup>11</sup>) followed the law:

$$v-c = 5.61 \cdot 10^5 R^{-1.19} \quad \text{Eq. (3)}$$

where the exponent -1.19 is accurate to about  $\pm 0.05$ . Near 0.07 seconds ( $2.0 \cdot 10^2$  meters) there appears to be another change in the velocity, to

$$v-c = 9.8 \cdot 10^7 R^{-1.73} \quad \text{Eq. (4)}$$

with an accuracy of about  $\pm 0.1$  in the exponent. The data for this last break, and Eq. (4), are less reliable than our information on the earlier stages. In fact, our points in the neighborhood of the break indicate

<sup>10</sup>A. L. Turkevitch, LA report in preparation.

<sup>11</sup>H. H. Barschall, R. W. Davis, W. C. Elmore, G. E. Kappelman, and G. Martin, LA - 352, Table II.



U.S. GOVERNMENT  
PRINTING OFFICE

-21-

UNCLASSIFIED

that Eq. 3 is followed to 0.11 seconds ( $2.6 \cdot 10^8$  meters), after which there is a gap extending to 0.25 seconds ( $3.7 \cdot 10^2$  meters); the value  $R = 2.0 \cdot 10^2$  meters for the break is used principally to avoid the necessity of postulating a more complicated law for the interval after the break.

The two-fifths power law, in the region where one may neglect the small additive time constant of Eq. (2), implies a velocity proportional to  $R^{-3/2}$ . The apparent simultaneity of the shock wave's marked departure from that law with the separation of the shock wave from the slower dark front points to a causal relationship between the two phenomena. It has been suggested by McGee that the unexpected high velocity of the shock wave in this region may arise from the absorption by the shock wave of radiant energy that originated in the ball of fire and was transformed in the dark front from the ultraviolet or visible into the infra-red; the coincidence of the split-off point between the two fronts with the point of departure of the shock front from two-fifths power dependence lends weight to McGee's suggestion.

The phenomena of the formation of the dark front and the enhancement of the velocity of the shock front deserve intensive further study.

#### VII. RETRACTION BY THE SHOCK FRONT AT $10^{-1}$ SECONDS.

All the space-time phenomena discussed in this report other than the one described in this section are believed to be real, i.e.,

REF ID: A66375

-22-


UNCLASSIFIED

the light is believed to have traveled in a substantially rectilinear path from the object to the camera, so that measurements on the film, with the application of proper geometric factors, can be considered tantamount to measurements on the objects. On the other hand, the apparent cable breaks referred to in this section are a pure optical phenomenon, arising from the refraction of light at and within the shock front on its way from the object to the camera.

One of the balloon cables extended upward, leaning slightly toward the tower from a point of attachment on the ground displaced 213.2 meters W, 216 meters S from the point directly under the gadget. Light traveling from the cable to the cameras in the direction N, after the shock wave had expanded  $2.0 \cdot 10^2$  meters, traversed the shock front. Points seen through the wave appeared farther from the center than they actually were, and points that in the absence of refraction would have appeared within about 2 meters of the edge, were not seen; instead, the image of the cable appeared hooked, with points between 2 and 4 meters from the edge appearing twice. Incidentally, since the shock front in this region was invisible the cutoff point made the only convenient point for the measurement of the radius.

Evidently in the earliest Mitchell camera picture of the refraction hook (0.072 seconds), the refraction took place in the Mach front, and in all the later pictures, in the spherical shock front; for a circle with its center at the image point corresponding to the original gadget center, and radius equal to the distance of the cutoff point, lies tangent to the extreme part

REF ID: A66375

  
SECRET

part of the hook in all pictures except the first. In the first picture, the circle intersects the hook.


UNCLASSIFIED

Fig. 9 shows the displacement as a function of distance within the shock wave for each of the eight Mitchell frames in which the phenomenon appears. From these data an attempt will be made in a later report to deduce the density as a function of distance within the shock wave.

#### VIII. MASS MOTION OF THE AIR AT $3 \cdot 10^{-1}$ SECONDS

The pictures in which the balloon cable is shown being pushed aside by the shock front yielded an opportunity for a determination, not only of the shock front velocity, but of the actual motion of the matter displaced in the shock wave. The motion of the vapor can be considered to be the same as that of the air if the cable is assumed to have been vaporized before the arrival of the shock front, and if one neglects the density difference between the air and the least dense particles of the visible remains of the balloon cable, as well as any inhomogeneity arising from the presence of the high-temperature vapor.

Fig. 10 shows the motion of the vapor front subsequent to the arrival of the shock wave, in the cases of several elements of volume originating at different distances from the center of the explosion. Since measurements were made only on the front, the velocity values given are those of the fastest accelerated particles only. In every case there is an almost continuous stream of particles behind the front and in a few instances there are streams back to almost undisplaced particles evidently much more dense than the surrounding air. The apexes, which are our extrapolated

  
SECRET

UNCLASSIFIED

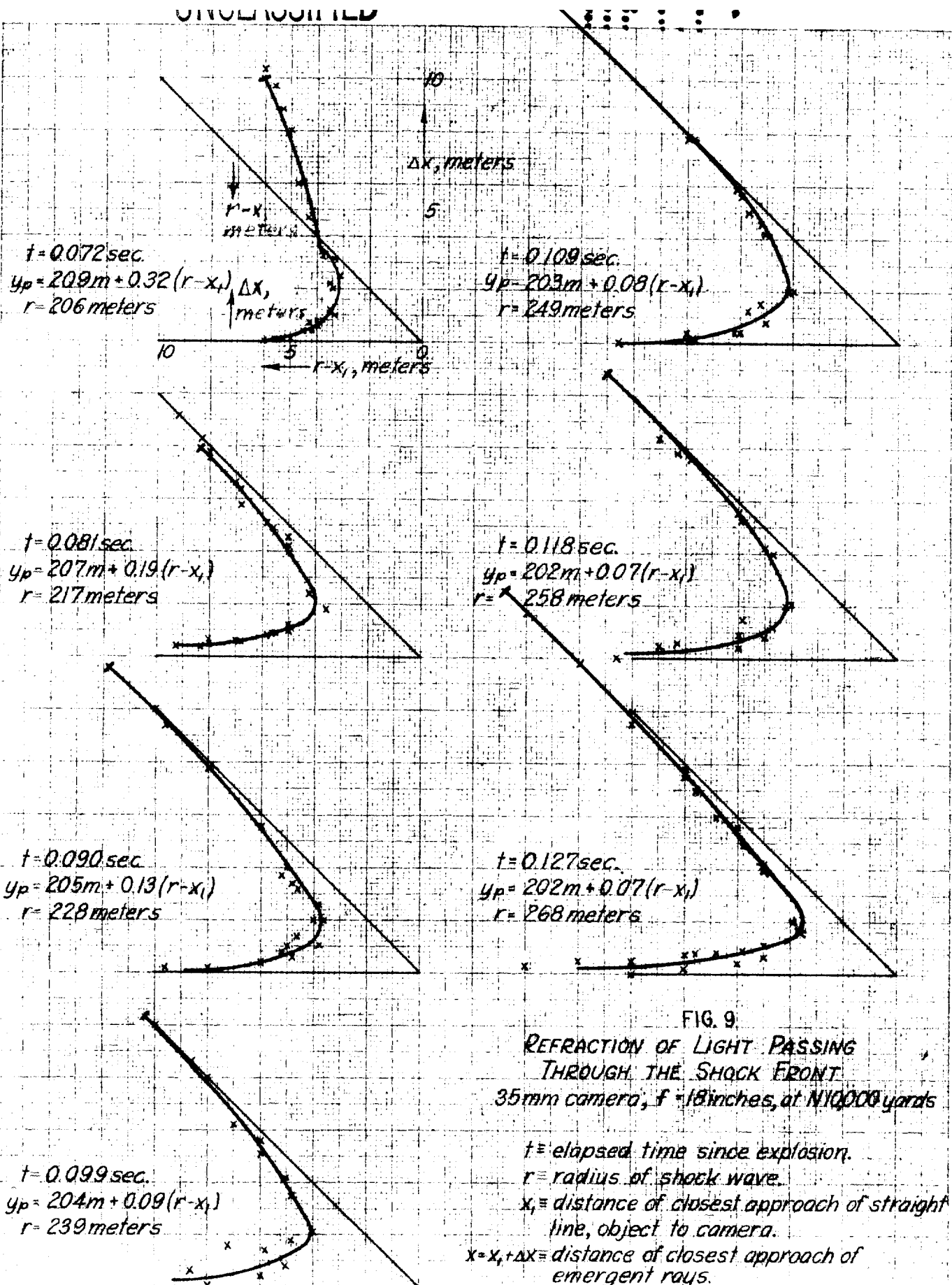


FIG. 9  
 REFRACTION OF LIGHT PASSING  
 THROUGH THE SHOCK FRONT  
 35mm camera,  $f = 18 \text{ inches}$ , at  $110000 \text{ yards}$

$t$  = elapsed time since explosion.

$r$  = radius of shock wave.

$x_i$  = distance of closest approach of straight line, object to camera.

$x = x_i + \Delta x$  = distance of closest approach of emergent rays.

$y_p$  = object distance minus gadget distance, from the camera.

Each hook ends at

UNCLASSIFIED

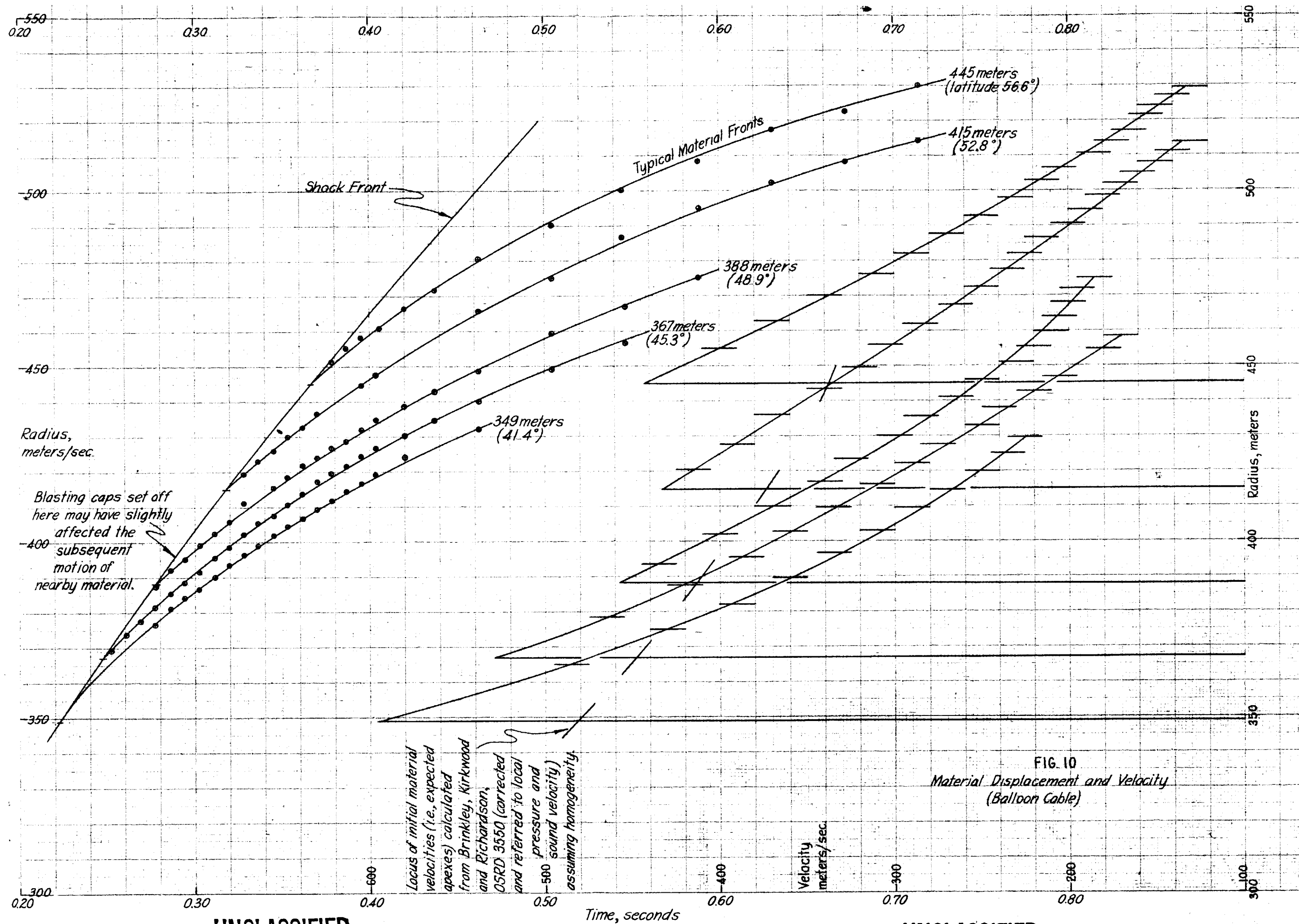


FIG. 10  
Material Displacement and Velocity  
(Balloon Cable)

UNCLASSIFIED

UNCLASSIFIED

-24-

values of the material velocity in the shock front itself, are from 10 to 30 per cent greater than the calculated values<sup>12</sup>. The spread probably represents a random error of about 10 per cent in our velocity values, which depend sensitively upon the choice of curves through our experimental space-time points. The average excess of 20 per cent in our values over the calculated values may arise, at least in part, from the inhomogeneity of the atmosphere consisting of hot cable vapors and hot air.

UNCLASSIFIED

#### IX. DEVELOPMENTS BETWEEN 10<sup>-1</sup> SECONDS AND 1 SECOND.

##### Partial envelopment of the ball by the skirt

Between one-tenth second and one second the dust skirt grew in height until it hid most of the ball of fire, and there occurred the preliminaries to the great convection movement by which the original ball of fire and the upper part of the dust skirt coalesced into a body that eventually became the new cloud of smoke.

The horizontal radius of the ball of fire itself reached a practically constant value of  $(2.0 \pm 0.2) \cdot 10^2$  meters at about 0.15 seconds, while the upper radius, probably on account of the incipient convection movement, continuously increased throughout the first second until the end of that period, when it was  $3.2 \cdot 10^2$  meters. The indefiniteness of the edge of the ball of fire continued to make a unique measurement of the radius impossible until the indefinite ball began to be replaced by definitely outlined flames

<sup>12</sup> Brinkley, Kirkwood, and Richardson, OSRD-1550, corrected and referred to the Trinity sound velocity (cf. ref. 11.).

000000  
000000  
000000

-25-

that allowed quantitative consideration of size again, after approximately one second.

UNCLASSIFIED

X. DEVELOPMENTS BETWEEN 3 AND 10 SECONDS.

Transition from the ball-of-fire stage to the smoke-cloud stage

At 1 second the character of the material left by the explosion was changing rapidly. At this instant the material consisted primarily of two portions; a ball of fire, which had become somewhat elongated vertically, and only the upper part of which could be seen from our ground positions; and a skirt of dust, which had grown vertically until it almost hid the ball of fire. In the interval between 1 and 3.5 seconds a new cloud of smoke formed from the ball of fire and the upper part of the skirt, and gradually changed shape until by about 2 seconds it had become almost a sphere, a shape it retained for several minutes. The necking of the dust skirt with the formation of a torus and a stem, and the variations in upward motion, described in this section, are all minor phases of the formation and rise of the cloud of smoke.

Stoppage and resumption of the ascent of the top of the ball

After rising steadily throughout the first second, the top of the ball of fire, i.e., the highest point on the whole ensemble, remained at a substantially constant altitude of (358 ± 1) meters from 1.0 to 2.0 seconds. It then acquired an upward velocity, almost all of it between 3.5 and 4.0 seconds (cf. Formation and rise of the cloud of smoke, below).

000000  
000000  
000000

0000000000  
0000000000  
0000000000

Torus

The top of the skirt material had suddenly slowed down at 0.7 seconds from a vertical velocity of about  $2 \cdot 10^2$  meters per second to one of about one-fifth of that value. During the pause in the rise of the top of the ball of fire, the skirt material continued its rise, gathering about the material of the ball of fire until the top of it formed an almost plane surface, much wider than the ball of fire and almost high enough to hide it. From two to four seconds the shape of the upper part of the skirt rapidly became that of a torus or vortex ring, presumably on account of the incipient strong upward convection at its axis. The outer radius of the skirt remained approximately constant, and the top of the skirt continued its slow rise.

Neck formation

UNCLASSIFIED

As the top of the ball or cloud resumed its rise, the sides of the flat-topped portion of the skirt material became steeper, and at  $(3.5 \pm 0.5)$  seconds, when the top of the skirt material was at 390 meters, an actual minimum or neck formed in the skirt material at an altitude of  $(128 \pm 3)$  meters. Thenceforward, the radius of the neck steadily decreased, going from 360 meters at 3.5 seconds to 99 meters at 23 seconds. The altitude of the neck, after remaining within 10 meters of its original value until 7 seconds, began an increase that attained a maximum rate of about 90 meters per second at 16 seconds. Thereafter, at least until its contact with the ground was lost at 22 seconds (620 meters, the neck rose at a lower rate, averaging about 30 meters per second.

Convection stem

The neck was followed in its rise by a great stem, apparently of solid matter, caught up by convection. The stem was narrowest at the neck.

0000000000  
0000000000  
0000000000



ALL INFORMATION CONTAINED  
HEREIN IS UNCLASSIFIED

Its sides were concave upward, reaching the ground tangentially. While this tangential structure prevented an accurate measurement of the bottom radius after 1.8 seconds, it can be stated that the radius of the stem at the ground was of the same order of magnitude as the radius of the cloud. Turbulence near the neck gave rise to a minor branch in the upper part of the stem, leading to ambiguities in the measurement of the height of the stem and related quantities, between 14 and 20 seconds.

Formation and rise of the smoke cloud

While these changes were going at the periphery of the skirt, a considerably more violent process was starting inside it. Matter from within and below the torus spilled over the top of the torus, and a new ball or cloud of smoke, consisting of the torus and the superposed matter, began to rise. The second, convective rise of the top of the ball, beginning at 2.0 seconds, was quite different in character from the first rise, which was part of the original symmetric expansion. This time the boundary was evidently that of a body of incandescent material, or later, of smoke, carried in a convective movement. In the half second between 1.5 and 2.0 seconds the measured displacement of the top was 1 meter downward, and in the half second between 3.5 and 4.0 seconds it was 43 meters upward: thus the average upward acceleration during this two-second interval was  $4.5g$ . Thereafter, the rate of rise decreased somewhat, and after 5 seconds it was nearly constant at 57 meters per second, at least until the camera lost its relation to the ground at 1500 meters (fig. 11).

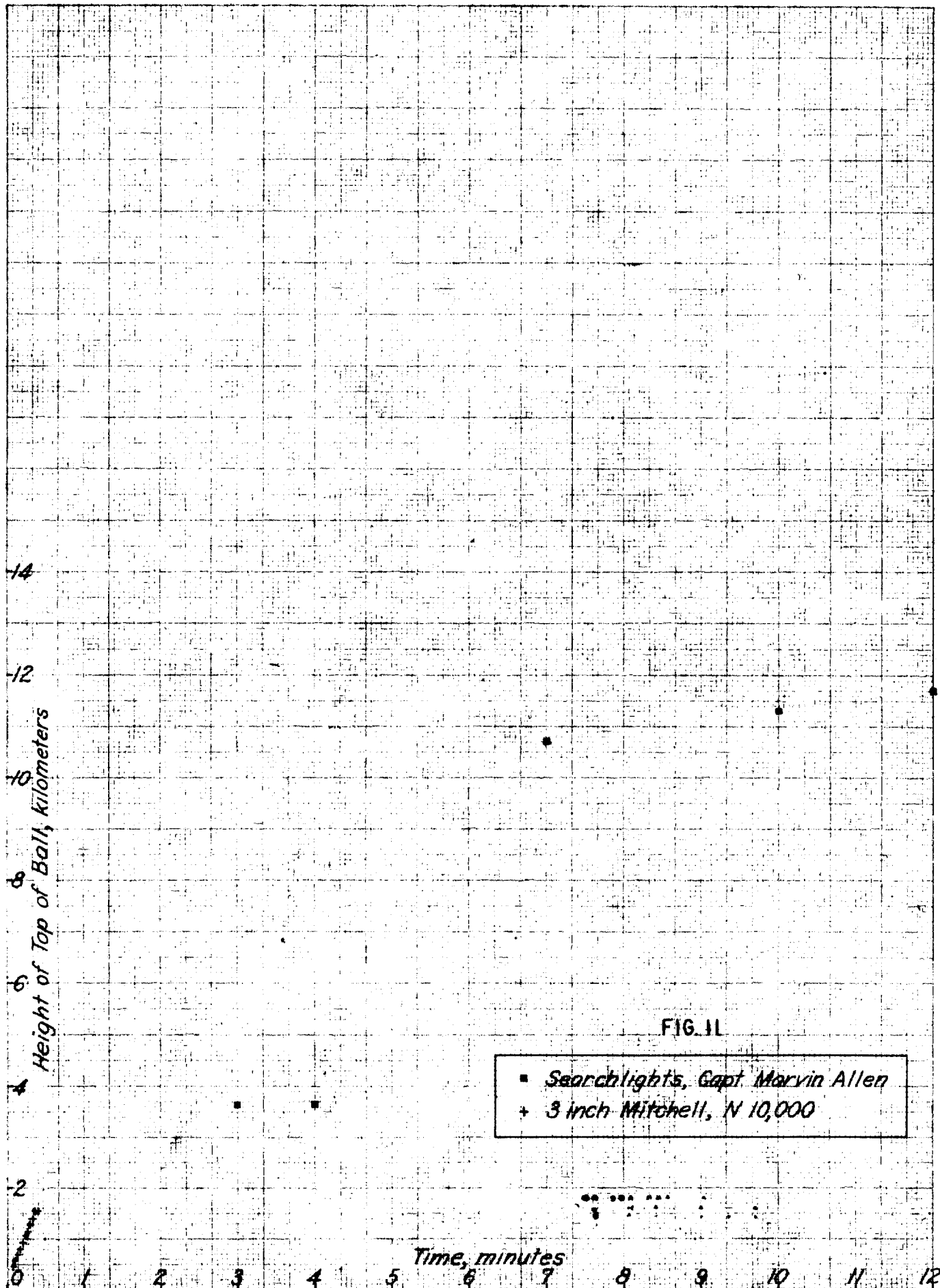
ALL INFORMATION CONTAINED  
HEREIN IS UNCLASSIFIED

UNCLASSIFIED

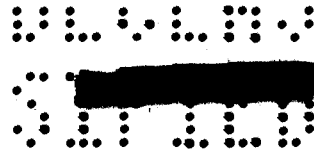
•••••

DATA SHEETS

CHARLES BRIDGES COMPANY INC. NO. 100-M  
MILWAUKEE, WIS. 53211



UNCLASSIFIED

Change in shape of the smoke cloud

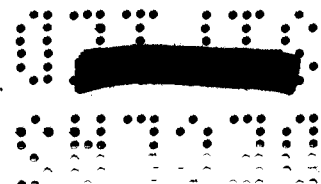
UNCLASSIFIED

At the time of formation of the smoke cloud, it consisted of the torus of skirt material with a relatively small volume of matter piled over its center. For a few seconds this pile grew without greatly affecting the torus, although the half-height of the torus increased considerable. By 8 seconds the portion above the torus was shaped something like a thimble, with sloping sides. From 10 to 15 seconds the whole gradually changed shape to very nearly a sphere. After 15 seconds the shape was approximately that of an increasingly oblate spheroid, with its axis vertical at 60 seconds the ratio of horizontal to vertical diameters was approximately 4 to 3. The near-spherical shape persisted for many minutes.

Persistence of the torus in the smoke cloud

During the early part of the rise of the smoke cloud, the torus, which, constituted the lower part of the cloud, maintained its identity within the cloud. The boundary of the torus was definite as an approximately horizontal circle until about 22 seconds, after which it gradually became harder to distinguish.

The vertical half-height of the torus itself, after increasing rapidly from 60 meters at 3.5 seconds to 210 meters at 10 seconds, remained approximately constant until 15 seconds and then decreased to a nearly constant value of about 130 meters at 18 seconds, which it maintained as long as it was distinguishable, although the cloud itself continued to grow in height.



000000  
000000

-29-

UNCLASSIFIED

Expansion of the smoke cloud

The approximate volumes of the torus and the whole cloud are given in Table V. No attempt is made here to calculate the actual accretion of material in the cloud, which would have to take into account not only the nature and temperature of the matter in the cloud but also the meteorological conditions encountered during its rise<sup>13</sup>.

Matter began streaming upward along the axis of the vortex ring at 2.0 seconds. Evidently the first material in this convective stream, which was exceedingly hot, originated near the center of the explosion. A consideration of the volume of the cloud shows that most of the matter in it must have originated a considerable distance from the center and have been swept near the center on its way to the cloud in the convection stream.

<sup>13</sup>J. M. Hubbard et al, LA - 357, p. 10.

000000  
000000

UNCLASSIFIED

-30-

UNCLASSIFIED

TABLE V

## VOLUME OF THE SMOKE CLOUD

(The values given are crude estimates from the vertical and horizontal extent: the shape of the torus, or the cloud, is taken as an ellipsoid of revolution except that for 4.5 and 5.0 seconds the non-skirt material is treated as a spherical segment bounded by a plane.)

Time, seconds	Volume of torus, cubic kilometers	Volume of cloud including torus, cubic kilometers
3.5	0.033	0.051
5.0	0.068	0.102
10	0.15	0.23
15	0.16	0.30
20	0.17	0.37
30		0.87
40		1.1
60		2.0
75		2.8

UNCLASSIFIED

SECRET

-51-

XI. DEVELOPMENTS BETWEEN 10 and 10<sup>2</sup> SECONDS

UNCLASSIFIED

Cloud ring formation

Meteorological observations showed that while the humidity was 77 per cent at the surface, it decreased with increasing altitude to a constant value of about 50 per cent, until at more than 2500 meters it increased to saturation value<sup>13</sup>.

Photographs taken at 3.3 second intervals show that as the rarefaction following the shock wave passed through layers at 3.3, 4.2, 4.4 and 5.2 kilometers, it produced clouds at these altitudes. Details are given in Table VI. A discussion of this phenomenon has been given by Reines<sup>14</sup>.

Glow

The average brightness of the cloud gradually decreased as the cloud rose. After 15 seconds most of the light from the cloud itself was from localized flames that progressed through the cloud as one would expect in a cloud which had gathered up a great deal of finely divided, incompletely burned material. At about 20 seconds the light from the flames had died down to such an extent that a dim glow beyond the surface of the cloud showed relatively prominently. This glow was brightest at the surface of the cloud itself and decreased in brightness with increasing distance from the cloud,

<sup>14</sup>F. Reines, LA - 448.

SECRET

U.S. AIR FORCE  
 AIR FORCE  
 AIR FORCE

-32-

TABLE VI.

UNCLASSIFIED

## CLOUD RINGS

Distances are given in kilometers,  $\pm 0.1$  kilometer unless specified.

Times are given in seconds,  $\pm 0.3$  seconds.

Angles are azimuth, measured counterclockwise, and are given in degrees,  $\pm 2^\circ$ .

Numbers in the body of the table are maximum radii.

Altitude at maximum radius	Maximum vertical extent	Time	8.1	11.4	14.7	18.1
3.3 $\pm$ 0.1	0.3		m	1.7*	4.0 $\phi_1$	5.0 $\phi_2$
4.2 $\pm$ 0.2	0.6		m		2.4 $\phi_1$	3.9 $\phi_2$
4.4 $\pm$ 0.3	0.2				1.1*	3 $\phi$
5.2 $\pm$ 0.3	1.0					2.8*

m Noticeable trace of scattering from mist at approximately this altitude.

\* Probably a cap or disc; possibly a ring with its aperture invisible from the camera positions.

$\phi_1$  Incomplete ring, with scattered wisps extending in azimuth from  $164^\circ$  to  $209^\circ$ , and solid cloud from  $209^\circ$  to  $49^\circ$ .

$\phi_2$  Incomplete ring, with solid cloud extending in azimuth from  $219^\circ$  to  $352^\circ$ , and scattered wisps from  $352^\circ$  to  $20^\circ$ .

$\phi_1$  Symmetric, complete ring.

$\phi_2$  Complete ring, heaviest toward S, and weakest toward NE and W.

$\phi$  Incomplete ring, without strongly predominant azimuth, but with incomplete portions; partly hidden by lower clouds.

000000  
000000

-50-

UNCLASSIFIED

until at about 100 meters from the surface it became invisible. In our slowest motion picture camera record, which could be expected to record brightness down to about 35 candles per square meter, the glow was noticeable for (75 ± 5) seconds. In a snapshot taken by Stanley Frankel, the glow appears to be several times as bright as the light from the cloud itself. From its position in a sequence of pictures, this picture appears to have been exposed for a few seconds during the time interval between 60 and 90 seconds.

#### Condensation

At 60 seconds, where an extrapolation of the cloud-top altitude curve (Fig. 11) indicates that the cloud was at an altitude of about 3.7 kilometers, there is evidence of a halo of cloud or condensation in a thin ring about the main cloud near its top. It will be noticed that the altitude of the cloud was approximately that in which the 8.1-second aero camera picture showed a faint mist. The halo formed in the presence of the cloud had approximately the extent of the glow and can be presumed to have been caused by ionization.

#### Stem twist

The convection stem at 60 seconds appeared as though it had been twisted into the form of a left-handed screw with  $3 \cdot 10^2$  meters pitch.

000000  
000000



DECLASSIFIED

-34-

XII. DEVELOPMENTS AFTER  $10^2$  SECONDS.

UNCLASSIFIED

Before the explosion, after the explosion time schedule had been adjusted from 4:00 a.m. to 5:30 a.m., the cameras were readjusted for daylight operation and, unfortunately, the daylight was slightly too faint for following the cloud after losing its self-luminosity until about 15 minutes after the explosion. Even after it was light enough to see the cloud ball, an overcast sky prevented the following of anything except the stem. Therefore we have no quantitative data on occurrences after  $10^2$  seconds.

Smoke pall

For more than an hour after the explosion, the neighborhood was covered with a pall of smoke. A color picture which was taken at 40 minutes shows this pall.

DECLASSIFIED

DECLASSIFIED

-35-

## APPENDIX I

UNCLASSIFIED

EQUIPMENT

Table I is a complete list of the cameras and auxiliary equipment used for producing the pictures upon which this report is based, together with all the pertinent photographic, geometrical, electrical, and timing data, and the file numbers under which the original negatives will be kept with the archives of Group G-11 (now M-8).

[REDACTED]

DECLASSIFIED

Exposure/Interval	Type of Camera	Local Number	Location	Object Distance	Lens Focal Length	Magnification	Width of Negative	Height of Negative	Object Field Width	Object Field Height	Estimated Space Resol.	Object Field Area	f-number of Lens	Neutral Density Filter	Effective f-number	Frame Speed	Shutter Setting	Exposure Time	Estimated Time Resol.	Timing Signals	Starting Signal	Stopping Signal	Amount of Film Run	Power Required	Type of Film	Negative File Number	REMARKS
			Yds Meters mm		mm		mm	mm	METERS		Horiz. vert.					F/sec	Days	Sec	Sec	Sec	Sec	Sec	Feet				
22 FASTAX C	8mm	B	800N 731 None																								Lens mount wrong type. Camera was not loaded. Ran O.K. Film badly fogged.
		B	800N 731 50	49.10 <sup>5</sup>	6.4	3.3	94	48.5	1.5				16	3	504												Film badly fogged. Camera may have run too soon.
		C	800W 731 50	49.10 <sup>5</sup>	6.4	3.3	94	48.5	1.5																		Ran O.K. Film Used For Measuring.
		B	800W 731 50	49.10 <sup>5</sup>	6.4	3.3	94	48.5	1.5				11	0	11	7110											Ran O.K. Film Used For Measuring.
FASTAX	16mm	D	800N 731 50	6.910 <sup>5</sup>	9.6	7.2	140	105	1.5				16	0	16	3700											Ran O.K. Film Used For Measuring.
		D	800W 731 35	4.810 <sup>5</sup>	9.6	7.2	900	150	0.1				0														Ran O.K. Film Badly Fogged.
			10°N 9140 25H	1.710 <sup>5</sup>	9.6	7.2	343	257	3.6				22	1	69	3760											Ran O.K. Film Used For Measuring.
			10°W 9140 15D	1.710 <sup>5</sup>	9.6	7.2	565	424	5.9				22	0	320	3560											Ran O.K. Film Used For Measuring.
3 SLOW EASTAX	16mm		10°N 9140 15D	1.710 <sup>5</sup>	9.6	7.2	565	424	5.9				22	2	320	651											Ran O.K. Film Used For Measuring.
			10°W 9140 15D	1.710 <sup>5</sup>	9.6	7.2	565	424	5.9				22	1	101	660											Ran O.K. Film Used For Measuring.
4N FASTAX	Primacord 16mm	A	800N 731 15D	2.010 <sup>5</sup>	9.6	7.2	43	34	0.5				3.5	0	3.5	1000											Ran O.K. Film too fogged to read.
		A	800W 731 25H	3.510 <sup>5</sup>	9.6	7.2	27	21	0.3				3.5	0	3.5	1000											Ran O.K. Film too fogged to read.
8 MITCHELL	35mm		10°N 9140 45D	5.010 <sup>5</sup>	24.0	18.0	480	360	3.6				16	0	16	1071	15°										Ran O.K. (The three Mitchells that ran were used for news-reel release from Washington (red) 25th baggage hallways. Line: U.S. Army.)
			10°N 9140 75	8.410 <sup>5</sup>	24.0	18.0	2860	2150	12				2.3	0	2.3	24	180°										Ran O.K.
			10°W 9140 610	7.210 <sup>5</sup>	24.0	18.0	343	257	1.4				3.6	0	3.6	119	180°										Ran O.K. Center Washington (red) 25th baggage hallways. Line: U.S. Army.)
			10°W 9140 75																								Variac burned out. Camera motor failed to start.
91 CINE E	16mm		10°N 9140 25	2.710 <sup>5</sup>	9.6	7.2	3500	2620	136				16	0	16	10	027	1.0									Operated Satisfactorily. Barrels.
			10°N 9140 25	2.710 <sup>5</sup>	9.6	7.2	3500	2620	36				9	0	9	10	025	1.0									
			10°N 9140 25	2.710 <sup>5</sup>	9.6	7.2	3500	2620	36				1.5	0	1.5	10	025	1.0									
			10°N 9140 25	2.710 <sup>5</sup>	9.6	7.2	3500	2620	36				1.5	0	1.5	0.25	180	2.0	4.0								
			10°N 9140 15	1.710 <sup>5</sup>	9.6	7.2	5650	4250	60				2.7	0	2.7	64	10	0003	0.16								
			10°N 9140 15	1.710 <sup>5</sup>	9.6	7.2	5650	4250	60				2.7	0	2.7	16	70	0016	0.16								
			10°N 9140 15	1.710 <sup>5</sup>	9.6	7.2	5650	4250	60				2.7	0	2.7	1	90	025	1.0								
			10°N 9140 15	1.710 <sup>5</sup>	9.6	7.2	5650	4250	60				2.7	0	2.7	0.24	180	2.0	4.0								
			10°N 9140 15	1.710 <sup>5</sup>	9.6	7.2	5650	4250	60				150	0	150	64	2	0016	0.16								
			10°N 9140 15	1.710 <sup>5</sup>	9.6	7.2	5650	4250	60				150	0	150	64	2	0016	0.16								
			10°N 9140 15	1.710 <sup>5</sup>	9.6	7.2	5650	4250	60				150	0	150	64	2	0016	0.16								
			10°N 9140 15	1.710 <sup>5</sup>	9.6	7.2	5650	4250	60				150	0	150	64	2	0016	0.16								
			10°N 9140 15	1.710 <sup>5</sup>	9.6	7.2	5650	4250	60				150	0	150	64	2	0016	0.16								
			10°N 9140 15	1.710 <sup>5</sup>	9.6	7.2	5650	4250	60				150	0	150	64	2	0016	0.16								
			10°N 9140 15	1.710 <sup>5</sup>	9.6	7.2	5650	4250	60				150	0	150	64	2	0016	0.16								
			10°N 9140 15	1.710 <sup>5</sup>	9.6	7.2	5650	4250	60				150	0	150	64	2	0016	0.16								
			10°N 9140 15	1.710 <sup>5</sup>	9.6	7.2	5650	4250	60				150	0	150	64	2	0016	0.16								
			10°N 9140 15	1.710 <sup>5</sup>	9.6	7.2	5650	4250	60				150	0	150	64	2	0016	0.16								
			10°N 9140 15	1.710 <sup>5</sup>	9.6	7.2	5650	4250	60				150	0	150	64	2	0016	0.16								
			10°N 9140 15	1.710 <sup>5</sup>	9.6	7.2	5650	4250	60				150	0	150	64	2	0016	0.16								
			10°N 9140 15	1.710 <sup>5</sup>	9.6	7.2	5650	4250	60				150	0	150	64	2	0016	0.16								
			10°N 9140 15	1.710 <sup>5</sup>	9.6	7.2	5650	4250	60				150	0	150	64	2	0016	0.16								
			10°N 9140 15	1.710 <sup>5</sup>	9.6	7.2	5650	4250	60				150	0	150	64	2	0016	0.16								
			10°N 9140 15	1.710 <sup>5</sup>	9.6	7.2	5650	4250	60				150	0	150	64	2	0016	0.16								
			10°N 9140 15	1.710 <sup>5</sup>	9.6	7.2	5650	4250	60				150	0	150	64	2	0016	0.16								
			10°N 9140 15	1.710 <sup>5</sup>	9.6	7.2	5650	4250	60				150	0	150	64	2	0016	0.16								
			10°N 9140 15	1.710 <sup>5</sup>	9.6	7.2	5650	4250	60				150	0	150	64	2	0016	0.16								
			10°N 9140 15	1.710 <sup>5</sup>	9.6	7.2	5650	4250	60				150	0	150	64	2	0016	0.16								
			10°N 9140 15	1.710 <sup>5</sup>	9.6	7.2	5650	4250	60				150	0	150	64	2	0016	0.16								
			10°N 9140 15	1.710 <sup>5</sup>	9.6	7.2	5650	4250	60				150	0	150	64	2	0016	0.16								
			10°N 9140 15	1.710 <sup>5</sup>	9.6	7.2	5650	4250	60				150	0	150	64	2	0016	0.16								
			10°N 9140 15	1.710 <sup>5</sup>	9.6	7.2	5650	4250	60				150	0	150	64	2	0016	0.16								
			10°N 9140 15	1.710 <sup>5</sup>	9.6	7.2	5650	4250	60				150	0	150	64	2	0016	0.16								
			10°N 9140 15	1.710 <sup>5</sup>	9.6	7.2	5650	4250	60				150	0	150	64	2	0016	0.16								
			10°N 9140 15	1.710 <sup>5</sup>	9.6	7.2	5650	4250	60				150	0	150	64	2	0016	0.16								
			10°N 9140 15	1.710 <sup>5</sup>	9.6	7.2	5650	4250	60				150	0	150	64	2	0016	0.16								
			10°N 9140 15	1.710 <sup>5</sup>	9.6	7.2	5650	4250	60				150	0	150	64	2	0016	0.16								
			10°N 9140 15	1.710 <sup>5</sup>	9.6	7.2	5650	4250	60				150	0	150	64	2	0016	0.16								
			10°N 9140 15	1.710 <sup>5</sup>	9.6	7.2	5650	4250	60				150	0	150	64	2	0016	0.16								
			10°N 9140 15	1.710 <sup>5</sup>	9.6	7.2	5650	4250	60				150	0	150	64	2	0016	0.16								
			10°N 9140 15	1.710 <sup>5</sup>	9.6	7.2	5650	4250	60				150	0	150	64	2	0016	0.16								
			10°N 9140 15	1.710 <sup>5</sup>	9.6	7.2	5650	4250	60				150	0	150	64	2	0016	0.16								
			10°N 9140 15	1.710 <sup>5</sup>	9.6	7.2	5650	4250	60				150	0	150	64	2	0016	0.16								
			10°N 9140 15	1.710 <sup>5</sup>	9.6	7.2	5650	4250	60				150	0	150	64	2	0016	0.16								
			10°N 9140 15	1.710 <sup>5</sup>	9.6	7.2	5650	4250	60				150	0	150	64	2	0016	0.16								
			10°N 9140 15	1.710 <sup>5</sup>	9.6	7.2	5650	4250	60				150	0	150	64	2	0016	0.16								
			10°N 9140 15	1.710 <sup>5</sup>	9.6	7.2	5650	4250	60				150	0	150	64	2	0016	0.16								
			10°N 9140 15	1.710 <sup>5</sup>	9.6	7.2	5																				

SECRET

## APPENDIX II

MEASUREMENT METHODS

With the exceptions listed here, all measurements for this report were made by direct readings upon negatives. The usual procedure with motion picture frames was to place directly upon the emulsion a scale which could be read directly to  $10^{-1}$  millimeters and easily interpolated to  $10^{-2}$  millimeters, a distance that in most cases corresponded to a distance of the order of decimeters in object space. The magnification was determined in almost every case by direct measurement of the distance in the image between the centers of the billboards, 400.0 meters apart in object space.

UNCLASSIFIED

For the measurement of the refraction by the shock front, measurement upon prints turned out to be more practical rather than measurement upon the original, because of the desirability of using construction lines that would have spoiled the original and would have had to be drawn with the impractically close spacing of several lines per millimeter.

In the measurement of the shock front radius and dark front radius after their separation, it was not practical to use the originals because of the lack of contrast as well as the necessity of determining the image point corresponding to the gadget center for diagonal measurements.

For these two kinds of measurements, prints were made that enhanced the contrast of the features to be measured, and the measurements were made upon these prints. For each frame several prints were made on double weight paper, and air-cooled along with pieces of the same kind of paper that had

SECRET

SECRET  
TOP SECRET

-37-

UNCLASSIFIED

been treated similarly, except that several circles accurately drawn on various parts of the surface by a compass replaced the photographic image. Measurements upon the circles indicated that the stretch or shrinkage in these prints was well within one per cent and that the inhomogeneities in the dimensional changes were considerably less than this. On each print the distance between billboard centers was measured, and the resulting correction factor applied to all measurements made on that print.

The measurements of the shock wave and dark wave radii and the mass motion of the air between 280 and 530 meters were made from the 24" Mitchell camera record. The absence of any scale marks on any frames of this camera made the direct measurement of distances impossible. Two almost wholly independent and indirect but rigorous methods for distance measurement were worked out: one graphical method and one analytical method. The final result of these two methods on the shock wave points agreed, on the average, within about one meter; for the dark wave, only the analytical method was used. The basis of both methods was the determination of the positions of certain points on the balloon cable, e.g. the bottoms of the balloons themselves, a bright spot corresponding to the explosion that was to release the balloons, and an aluminum cylinder attached to the cable, with the aid of the time exposures from the 2-meter cameras, each of which showed at least some of these points as well as the pair of billboards. After the determination

SECRET  
TOP SECRET

SECRET

of the scale with the aid of these time exposures, the graphical method made use only of the standard methods of descriptive geometry, and the analytical method made use only of the methods of solid analytical geometry plus the approximation of the portion of the cable under consideration by a straight line.

The points finally used for the shock wave were the result of the analytical determination.

UNCLASSIFIED

The dark wave in the region beyond 280 meters offered so little contrast that it was difficult to detect, except upon a moving image. The position of the dark wave was determined by running a positive film in a "Moviola" projection machine with its shutter removed, and tracing the position of the wave after watching the image move into place. Several runs were made and averaged. The two kinds of symbols representing the dark points represent two independent sets of runs.

For convenience, the image positions for the shock front and mass motion data from the 24" camera were determined also with the aid of a "Moviola" projector.

In the measurements upon the curtain, successive outlines of the ball of fire and the curtain were traced upon a single sheet of tracing paper with the aid of the "Moviola" projector, and subsequently measured. Two runs were made by different observers.

The measurements upon the shock front recorded in Table IV were made by tracing boundaries from film #209 by projection and from the 18" Mitchell from 1:2000 scale prints, upon the tracing paper reproduced in Table IV.

SECRET

010000  
010000  
[REDACTED]

-39-

UNCLASSIFIED

## APPENDIX III

RECOMMENDATIONS FOR FUTURE TESTSTime of day

Whatever the circumstances under which future tests are made, photographic work of great importance will clearly have to be done over an object distance of the order of 10 to 100 kilometers. The two principal optical hazards of long distance photography are haze and irregular refraction ripples. Experiences at the Trinity test showed that conditions for photography were the most important factor in the choice of time of day for the explosion. It is important that the time of day for any future explosion be chosen only after a study of contrast and resolution at the expected object distance, as functions of the time of day, preferably during the season of the year in which the test is to be made, so that the time may be chosen for optimum conditions. The success of the photography of the July 16th explosion was due in no small measure to our selection of the time of day. Fortunately, the delay of an hour and a half did no harm.

Following the shock wave further by cable motion

The accidental photography of the balloon cable allowed us to follow the shock front and the mass motion of the air behind the shock front past 450 meters. The means with which we had intended to follow the shock front photographically, v.z., the photography of explosions set off by shock switches, failed completely on account of fogging from the main flash and

[REDACTED]  
010000  
010000

SECRET

-10-

UNCLASSIFIED

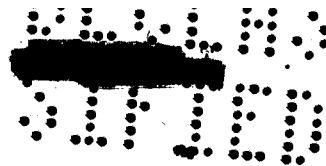
possibly also, in some instances, on account of disturbances of the arming circuit and melting of the shock switch apparatus, if we can judge by the experiences of others with apparatus within one kilometer of the explosion center. It is recommended, therefore, that the photography<sup>of</sup> cables or other objects with ordinary cameras be used hereafter to replace the more elaborate shock switch signals planned for the July 16th explosion.

Improvement in time resolution during the early stages

Theoretical interest in the early stages of the expansion has been greatly enhanced since the July 16th explosion. An increase in the order of magnitude of the frame frequency for a short interval during the early stages would require some development but is a problem already solved for somewhat different experimental conditions. The Marley camera exposures that we originally planned, but abandoned, would have yielded  $10^5$  frames per second for 50 frames. The fixed short focus and low quality of the lenses would probably have made the Marley camera pictures useless. The rotating mirror, Kerr-cell apparatus that has taken a series of about 60 exposures at  $10^{-6}$  second intervals would be difficult to control remotely, but it has the advantage of free choice of lens. There are other possible schemes, for which the development would be confined essentially to the problems of remote control and instrument protection. All the setups with higher frame frequency than the Fastax appear to require a considerable amount of development and ought to be considered only if their use is strongly encouraged by the theorists.

SECRET



More space reference marks

Several unexpected opportunities for measurements emphasize the paucity of our reference points and the great importance of the reliable ones that we had. Our inner stations at 50 meters turned out to be useless, possibly because of the difficulty of the erection and checking in the field of surface with the proper space orientation. A series of sets of surface at fixed distances from  $10^2$  to  $10^3$  meters would be relatively cheap insurance against loss of distance standards. The photography of a drop over water introduces new difficulties that need study.

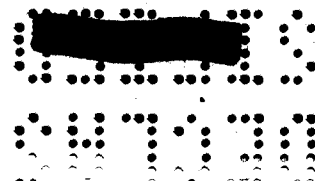
UNCLASSIFIED

Increased number of motion picture cameras

It was as much by good fortune as by foresight that a fairly complete record of the first minute after the explosion was obtained with the aid of only 12 Eastar and 4 Mitchell cameras. Several important phenomena, such as the dark wave, the cable refraction and the shock velocity and mass velocity from the balloon cables, were properly photographed only through sheer good luck. Increasing the number of stations and using several times as many high speed and 35mm motion picture cameras as we used would require no development work and would greatly enhance the probability of complete successful coverage.

Fixed position required for spectroscopy

It is clear that much further spectroscopic study will be required. The exceedingly narrow field of a slit spectrograph demands that, for any direct spectrographic study of the object itself, the position of the



04145  
071031

-42-

object be well known. Therefore, it is to be hoped that at least some future tests will be made with fixed-position bombs and that full advantage will be taken of the opportunities offered for spectroscopy at any such fixed-position test. One of the fields in which further spectroscopic study is urgently needed is that of the dark wave. It is possible that significant information as to the nature of the dark wave can be obtained by aiming a sufficiently large number of spectrographs (perhaps one will be sufficient) in the neighborhood of an approximately predicted drop location.

UNCLASSIFIED

04145  
071031

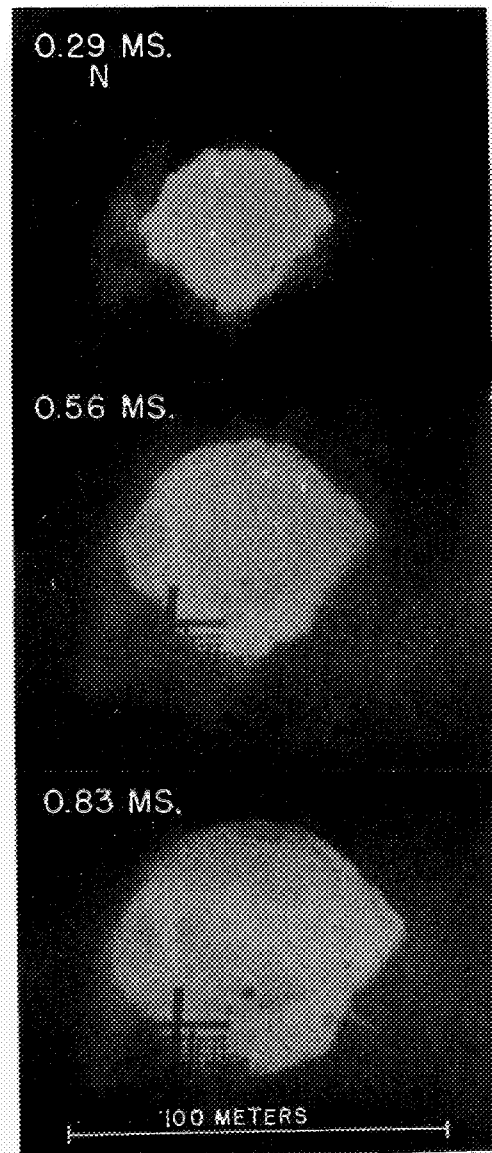
UNCLASSIFIED

UNCLASSIFIED

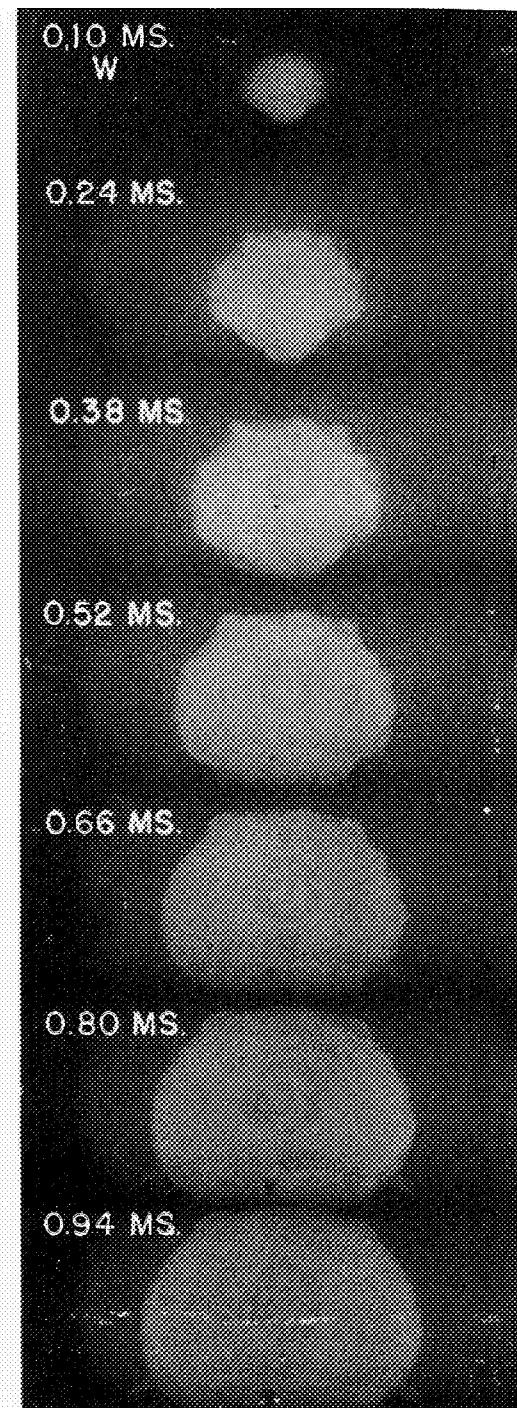
UNCLASSIFIED

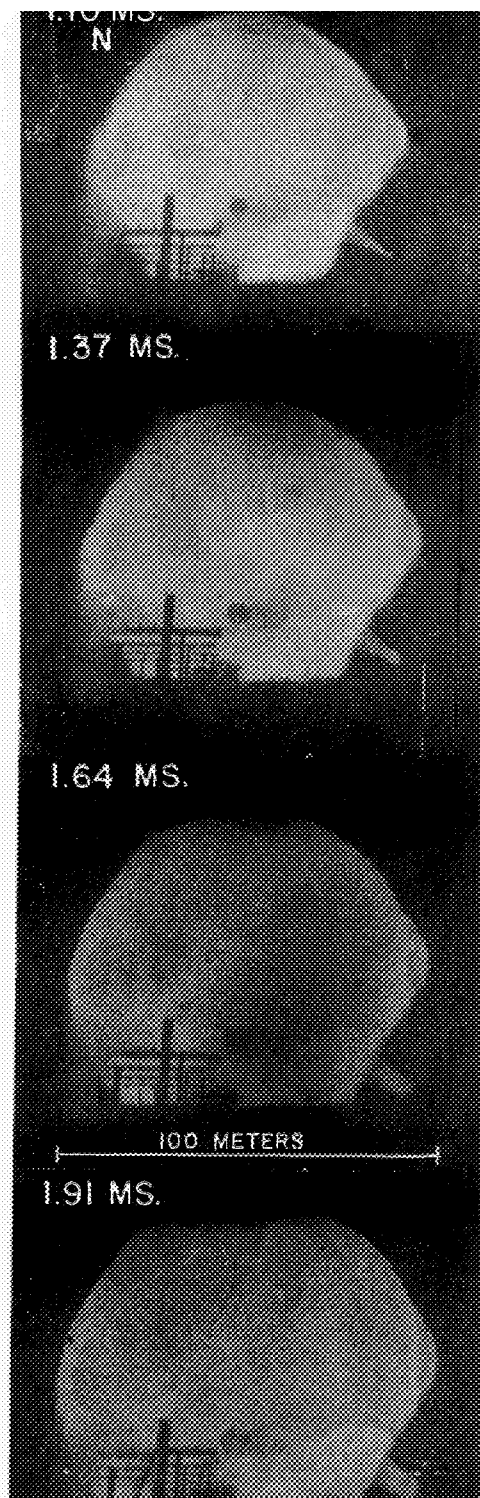
TIME EXPOSURE  
0 TO 5 SEC.  
N

100 METERS  
—

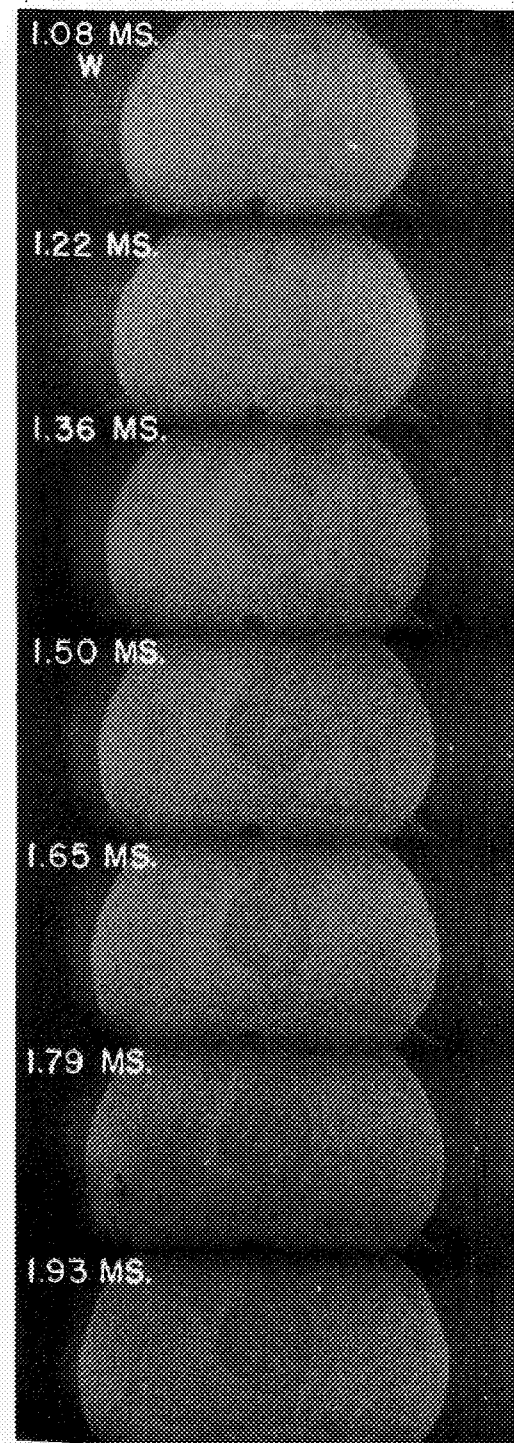


UNCLASSIFIED

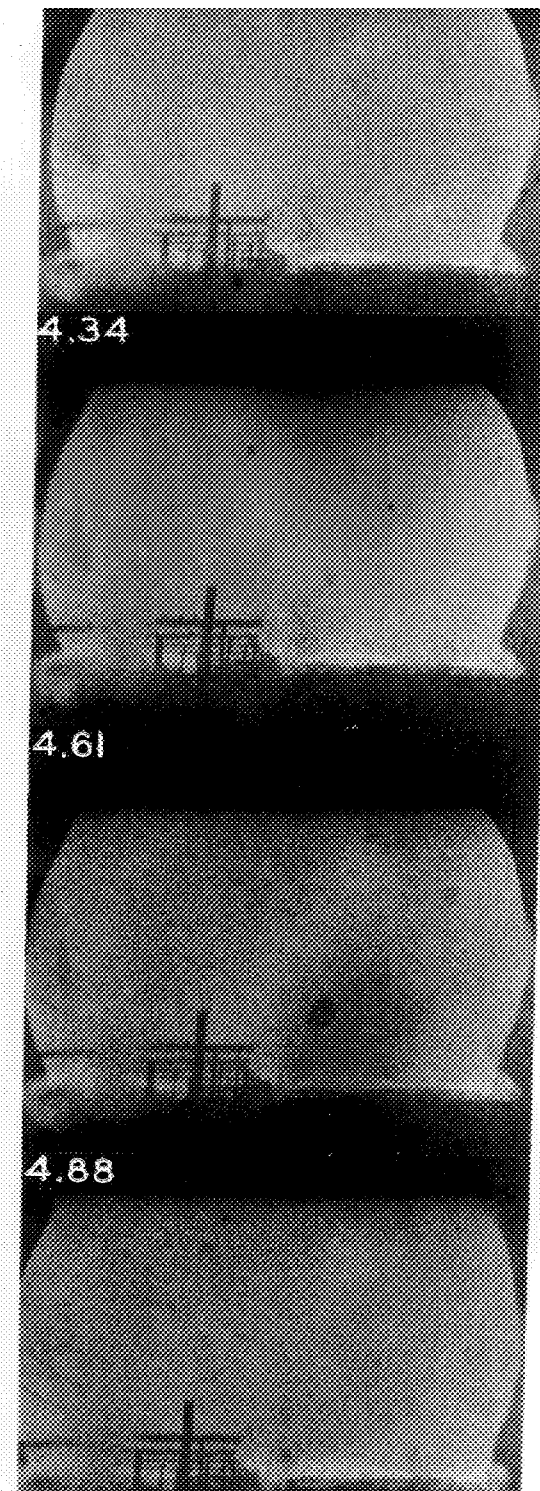
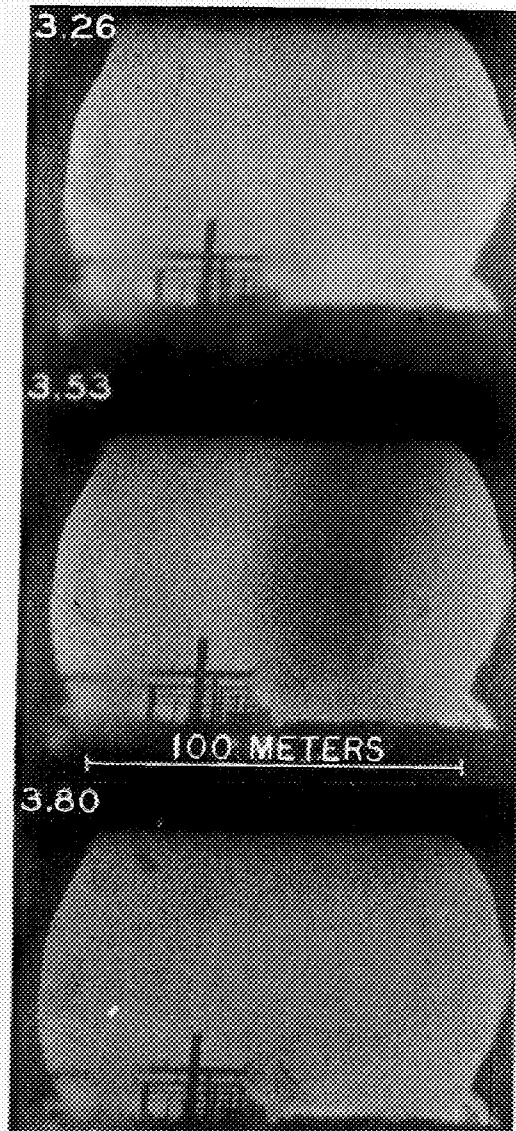
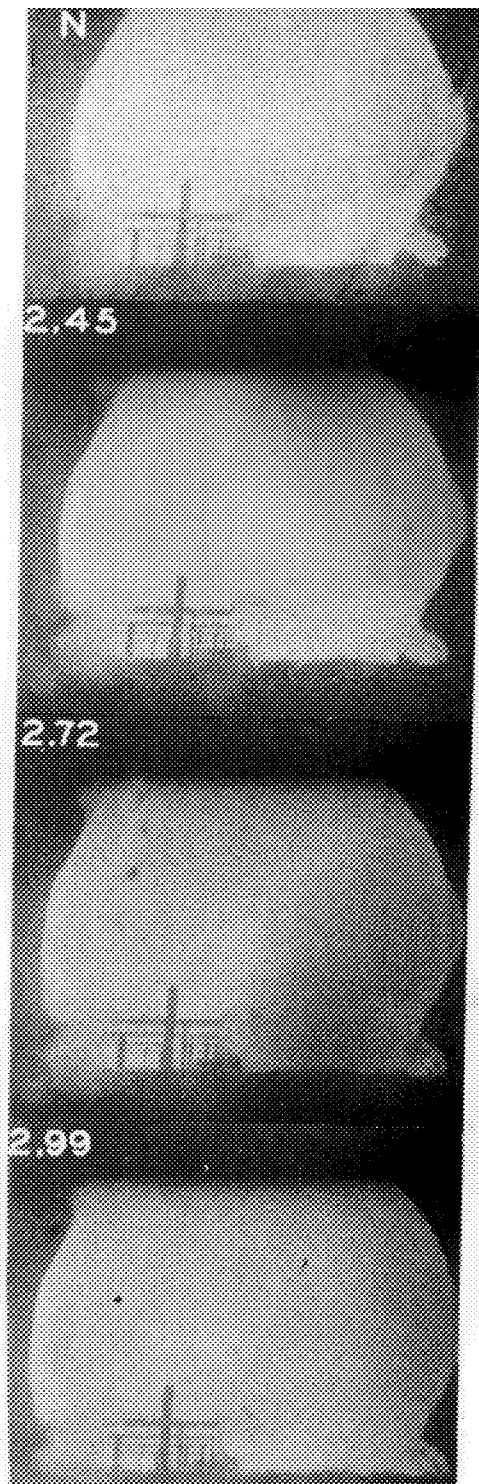




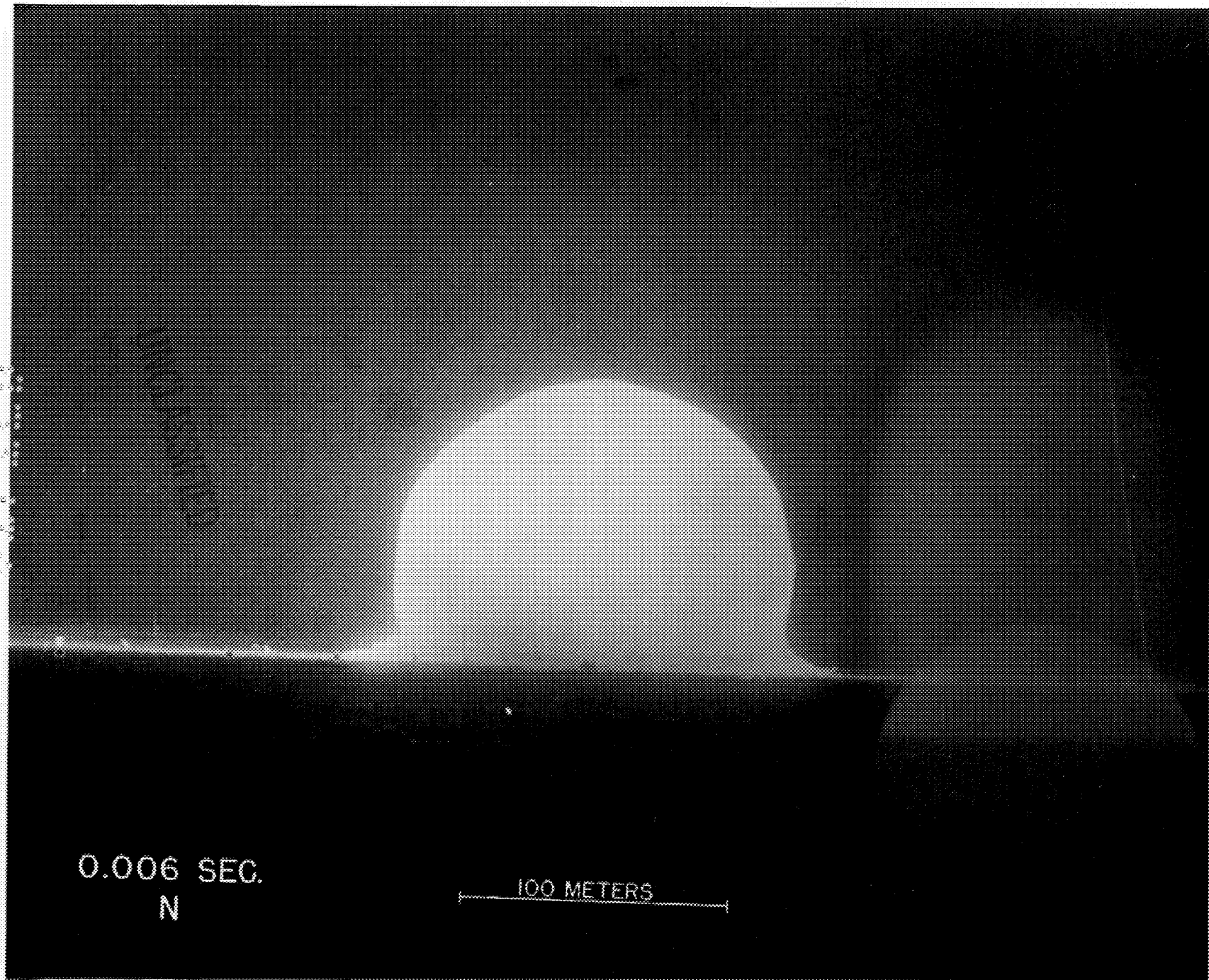
UNCLASSIFIED

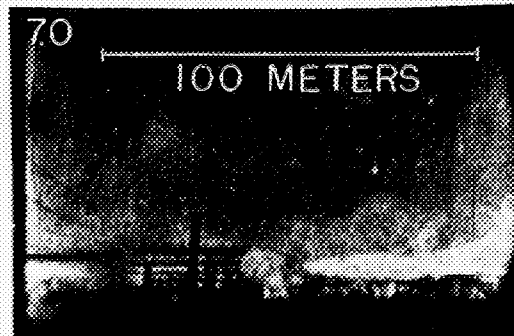
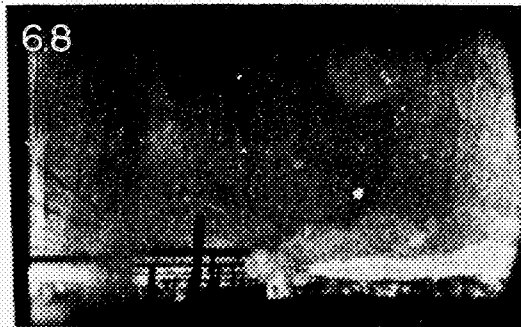
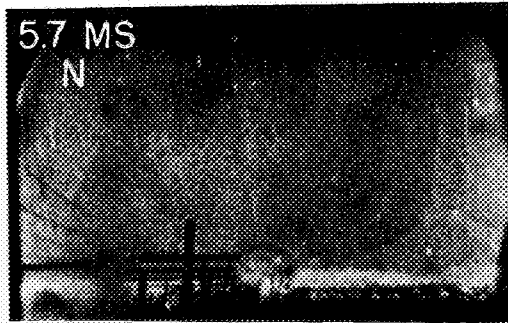






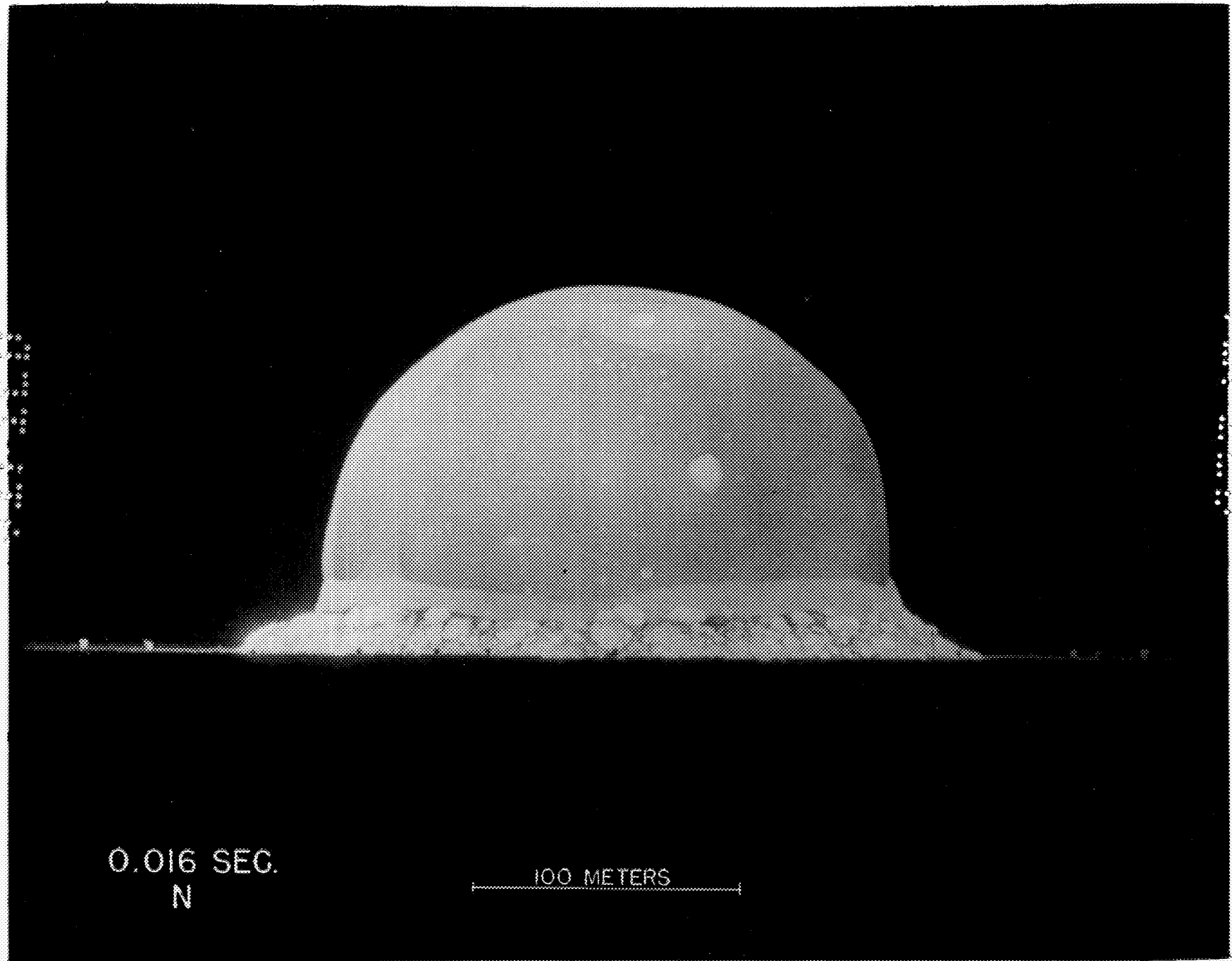
UNCLASSIFIED

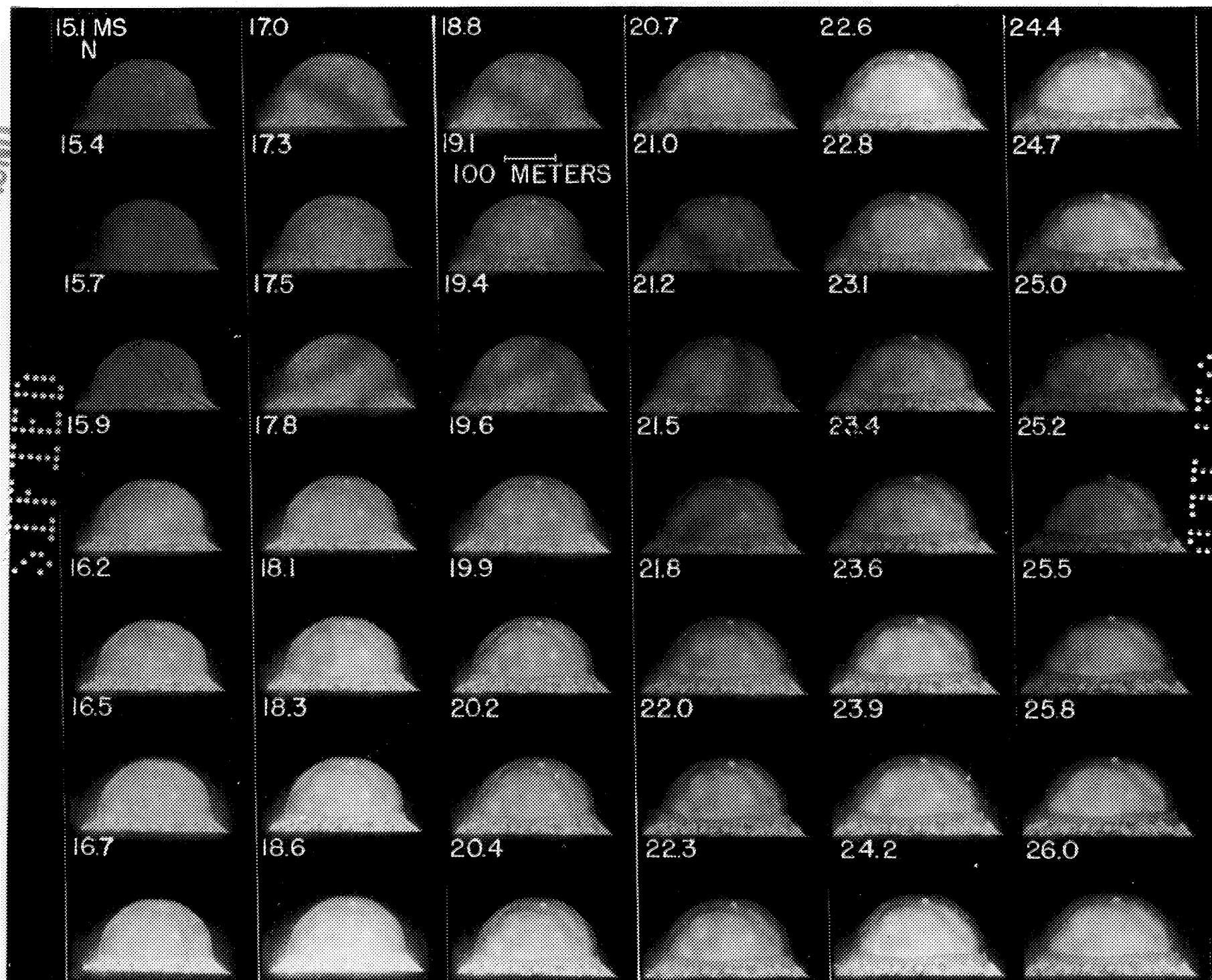


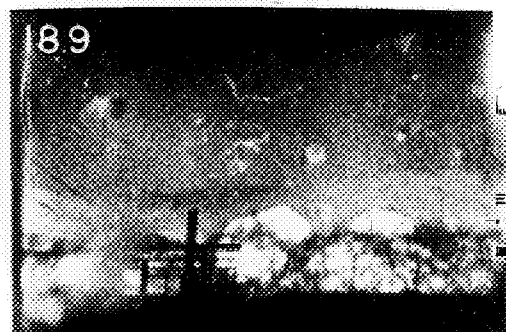
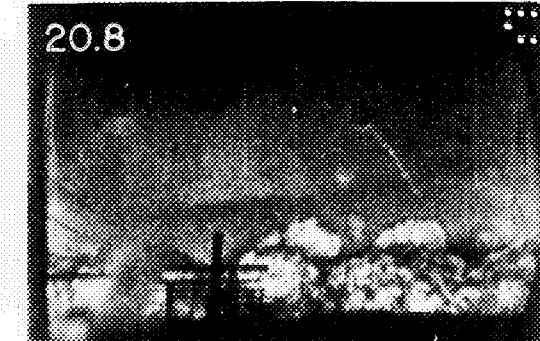
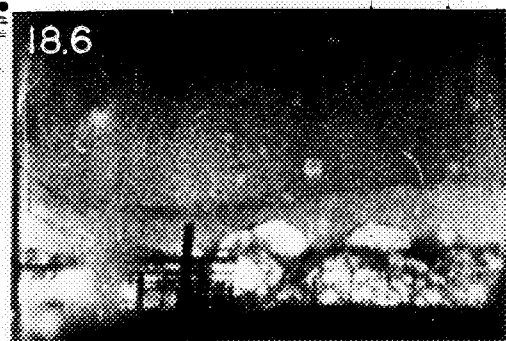
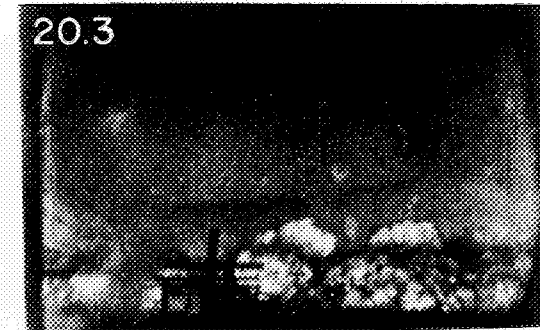
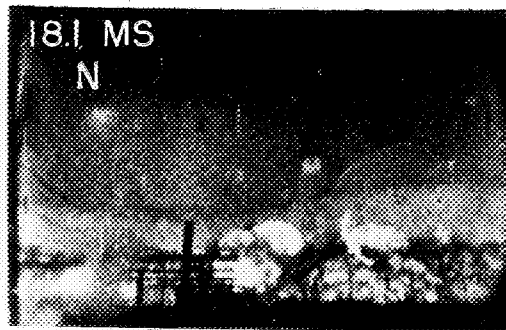


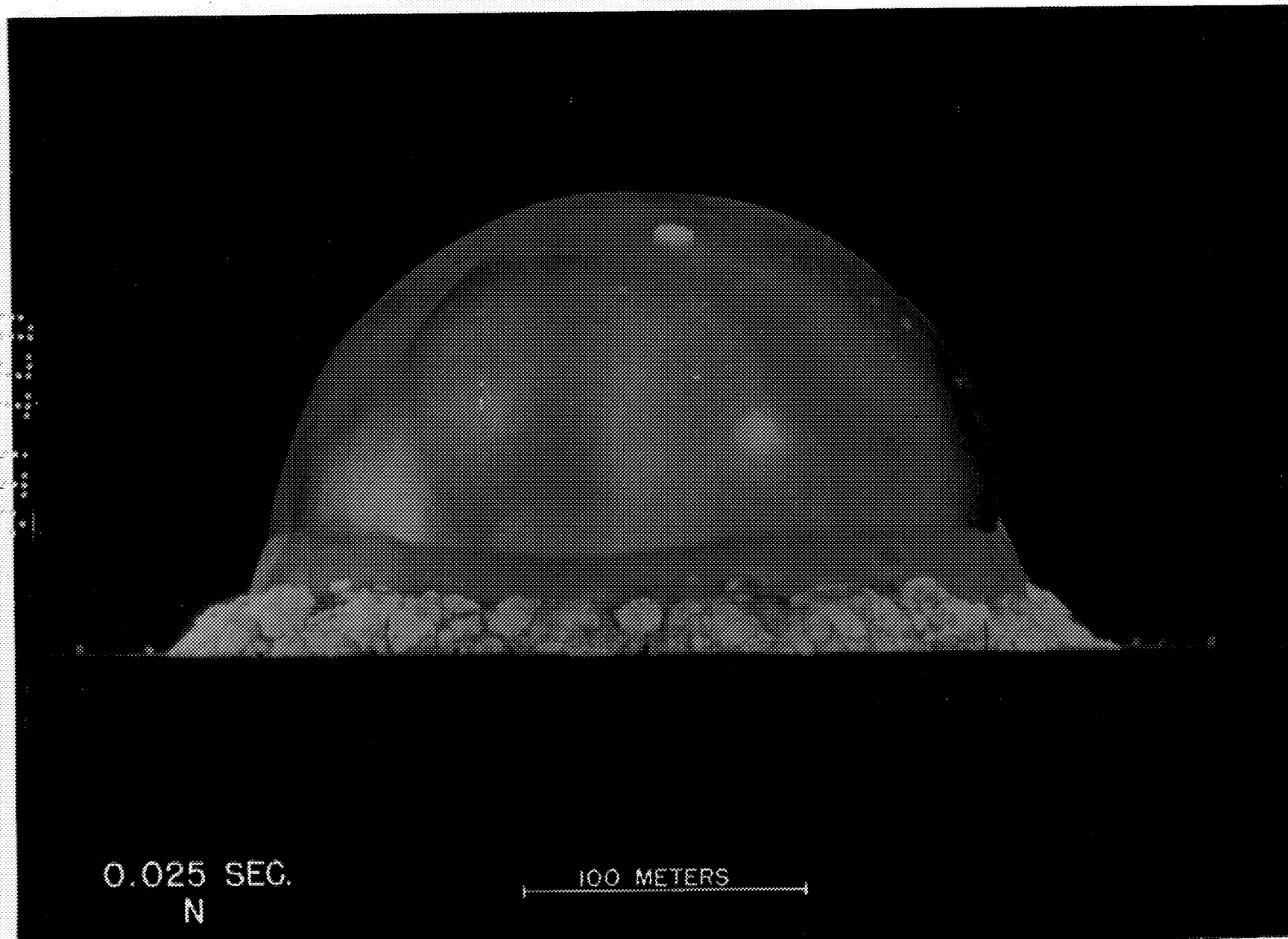
UNCLASSIFIED



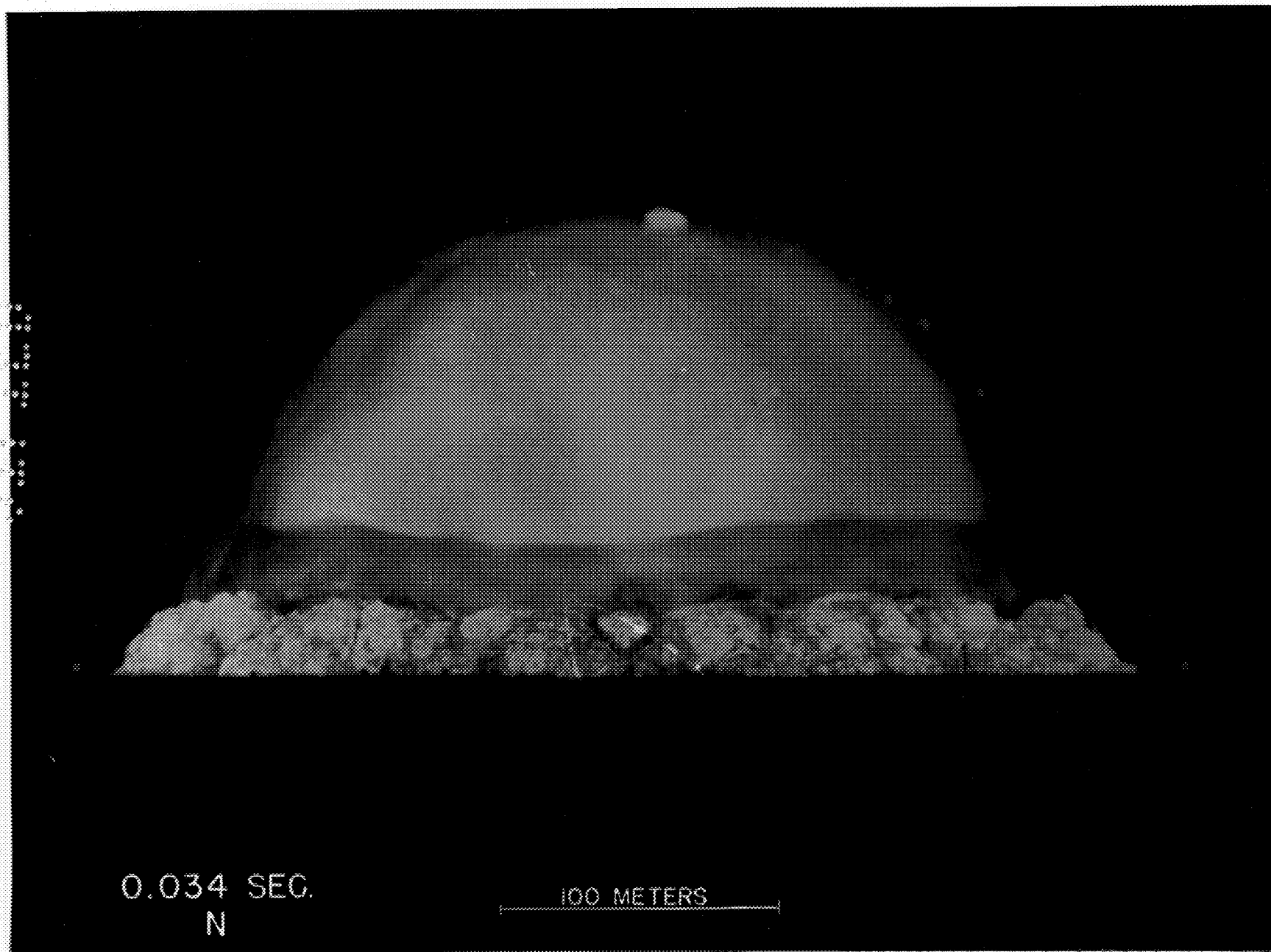








UNCLASSIFIED



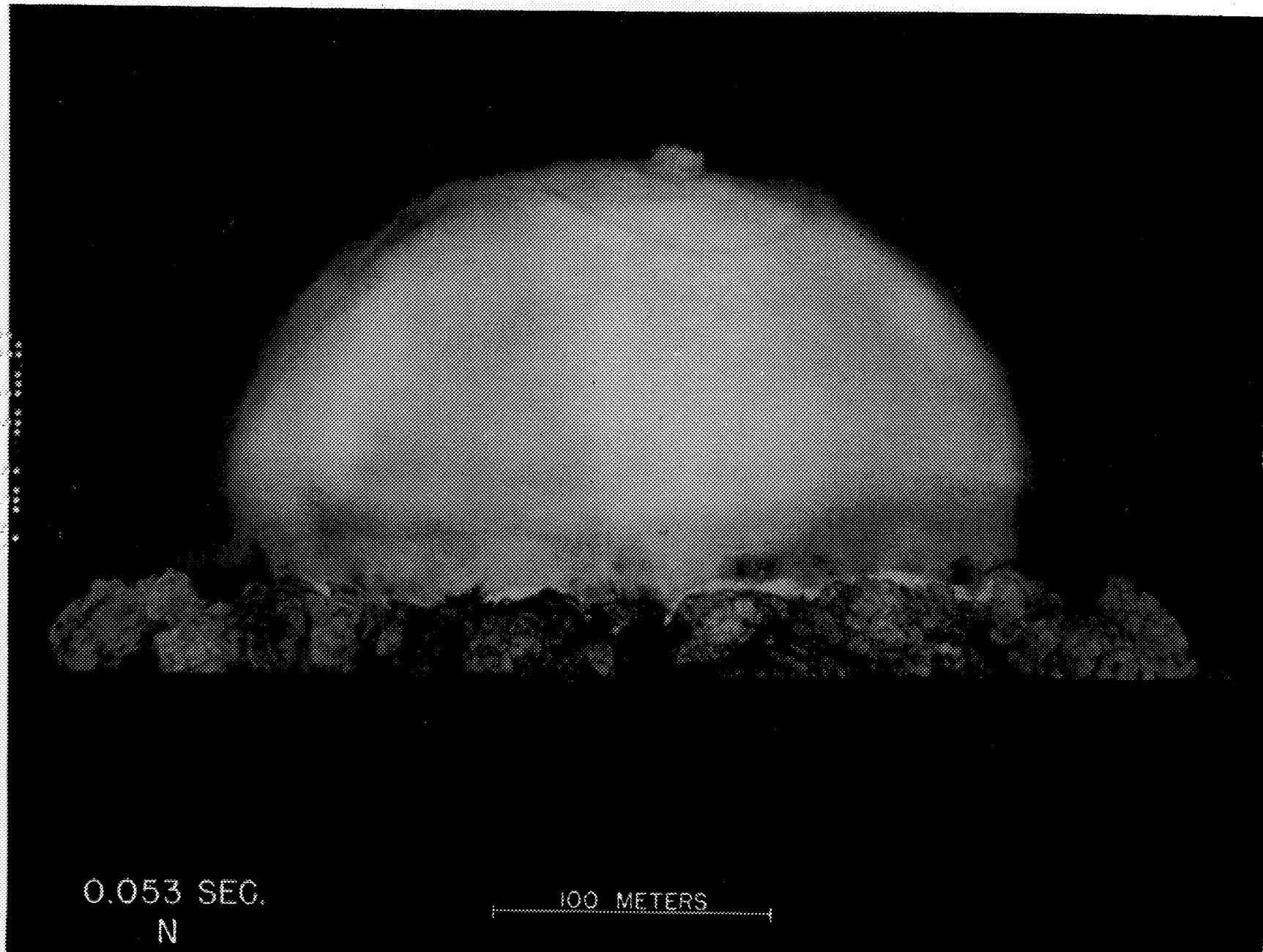
UNCLASSIFIED



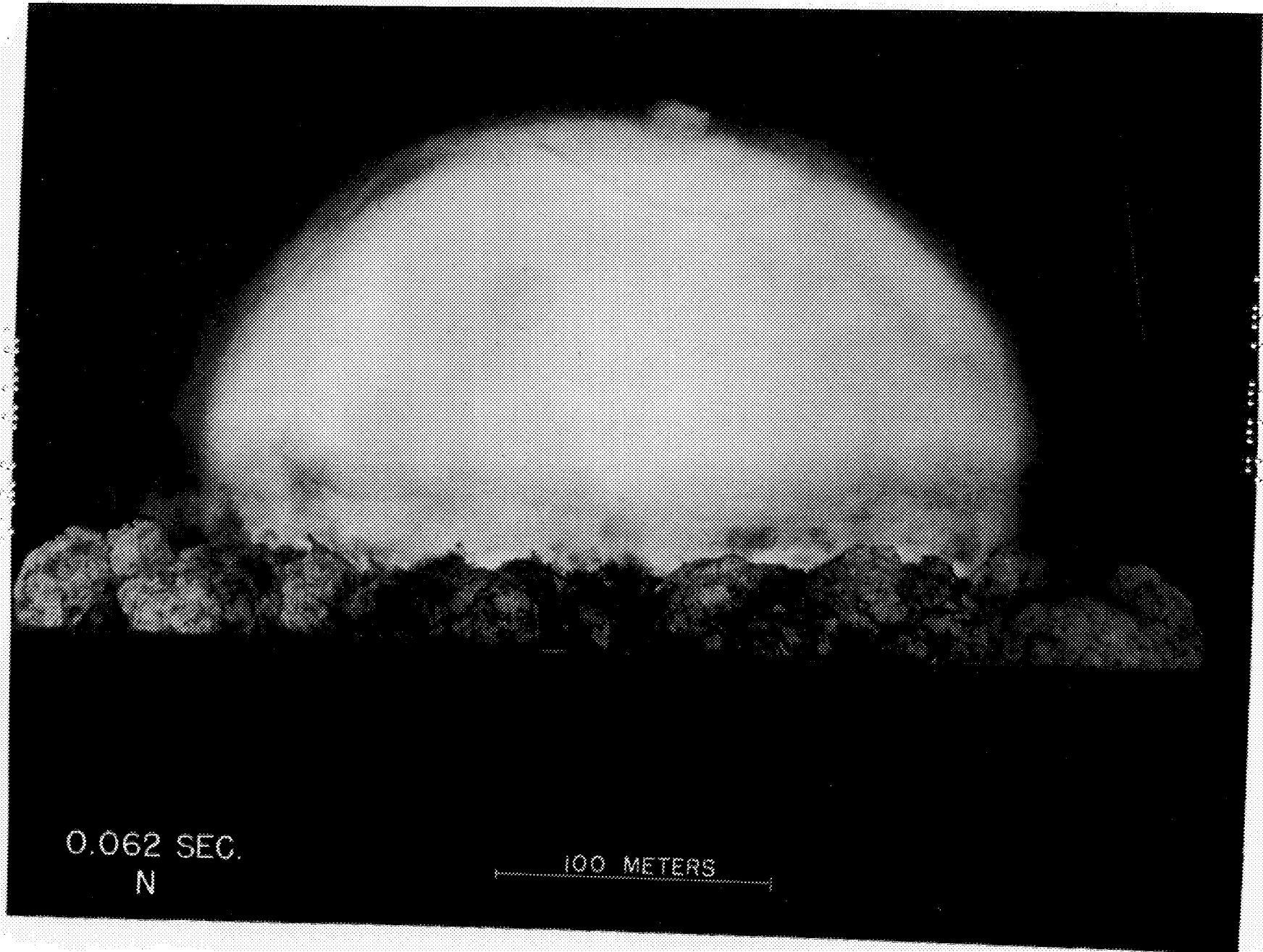
0.044 SEC.  
N

100 METERS

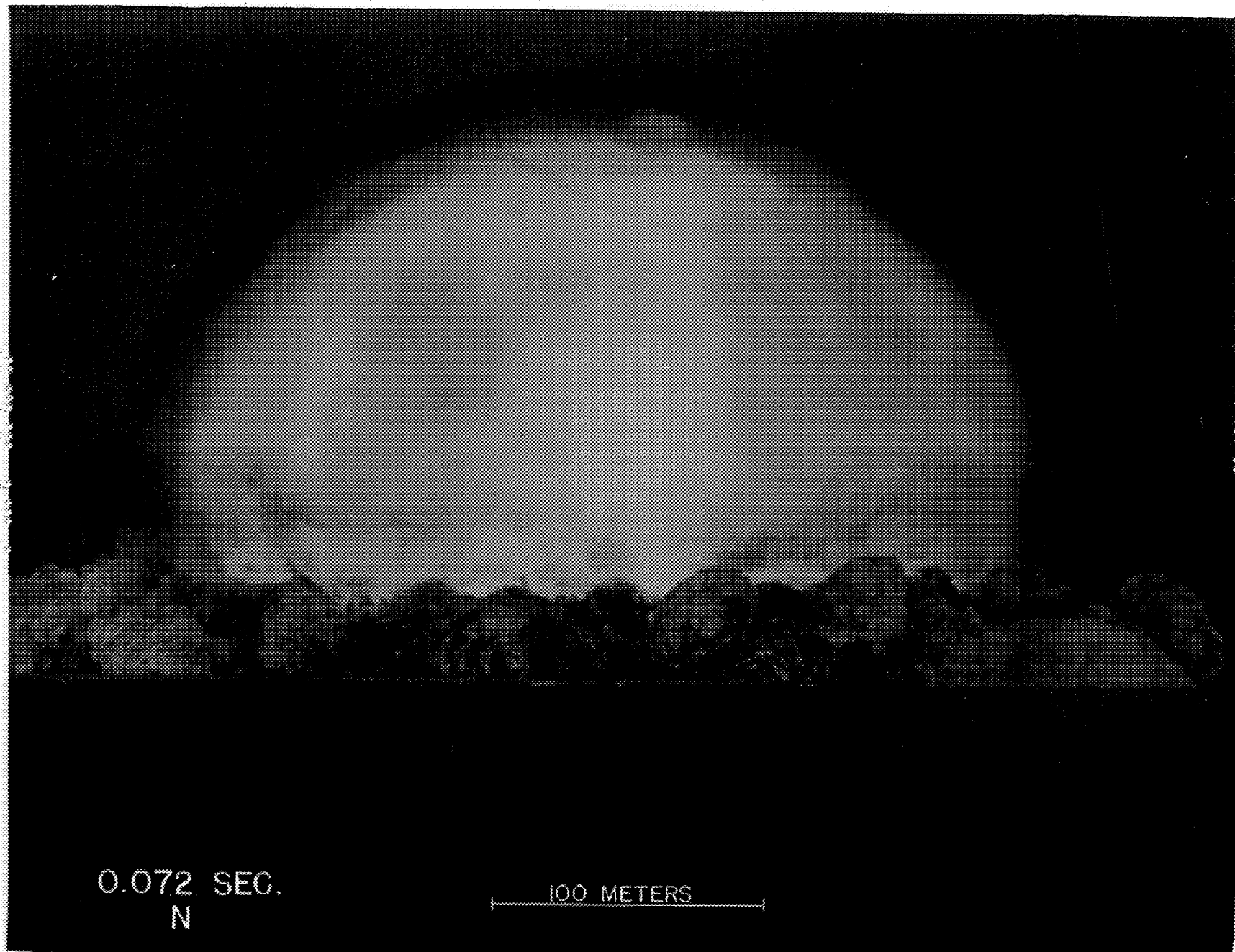


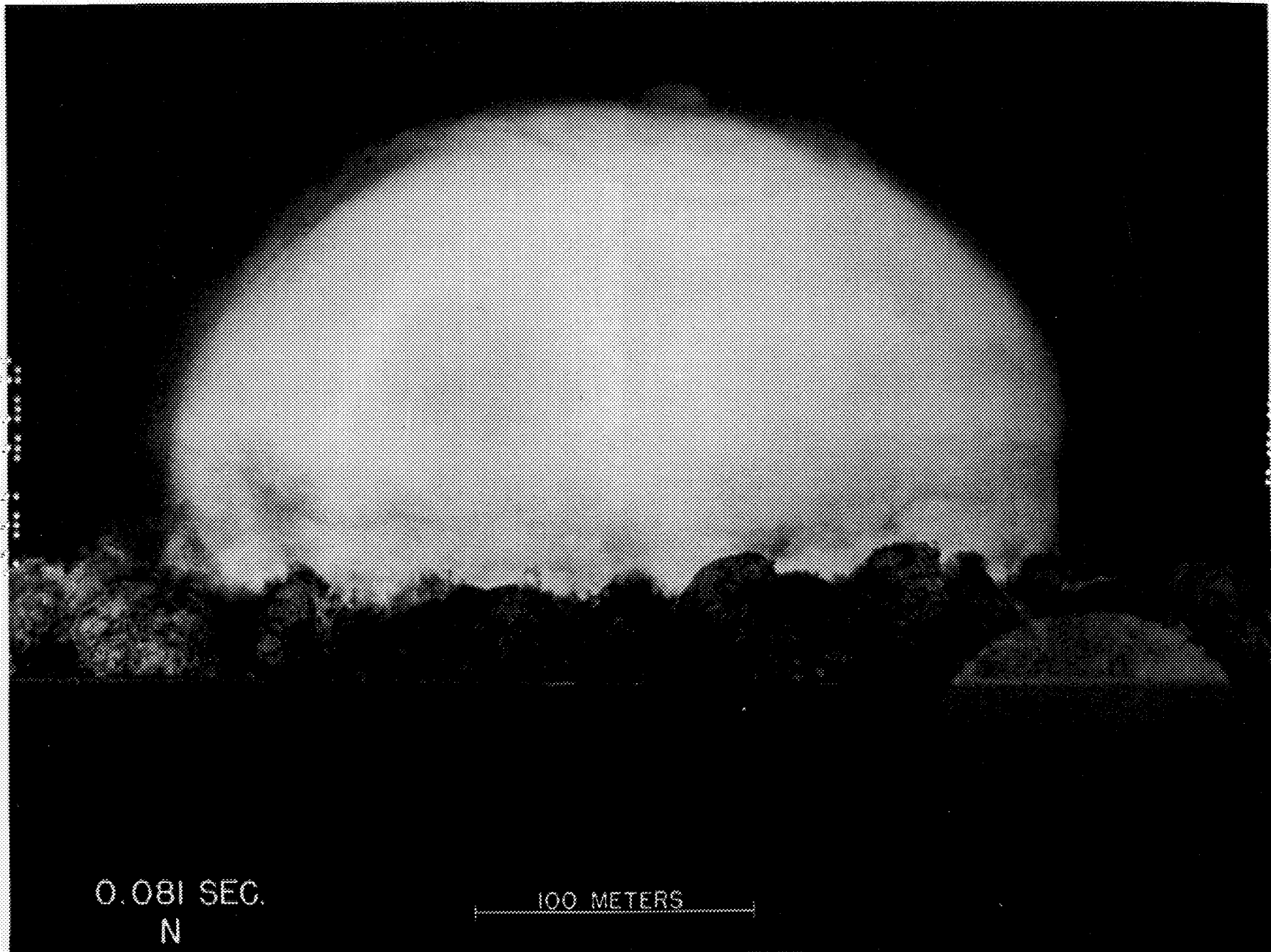


UNCLASSIFIED

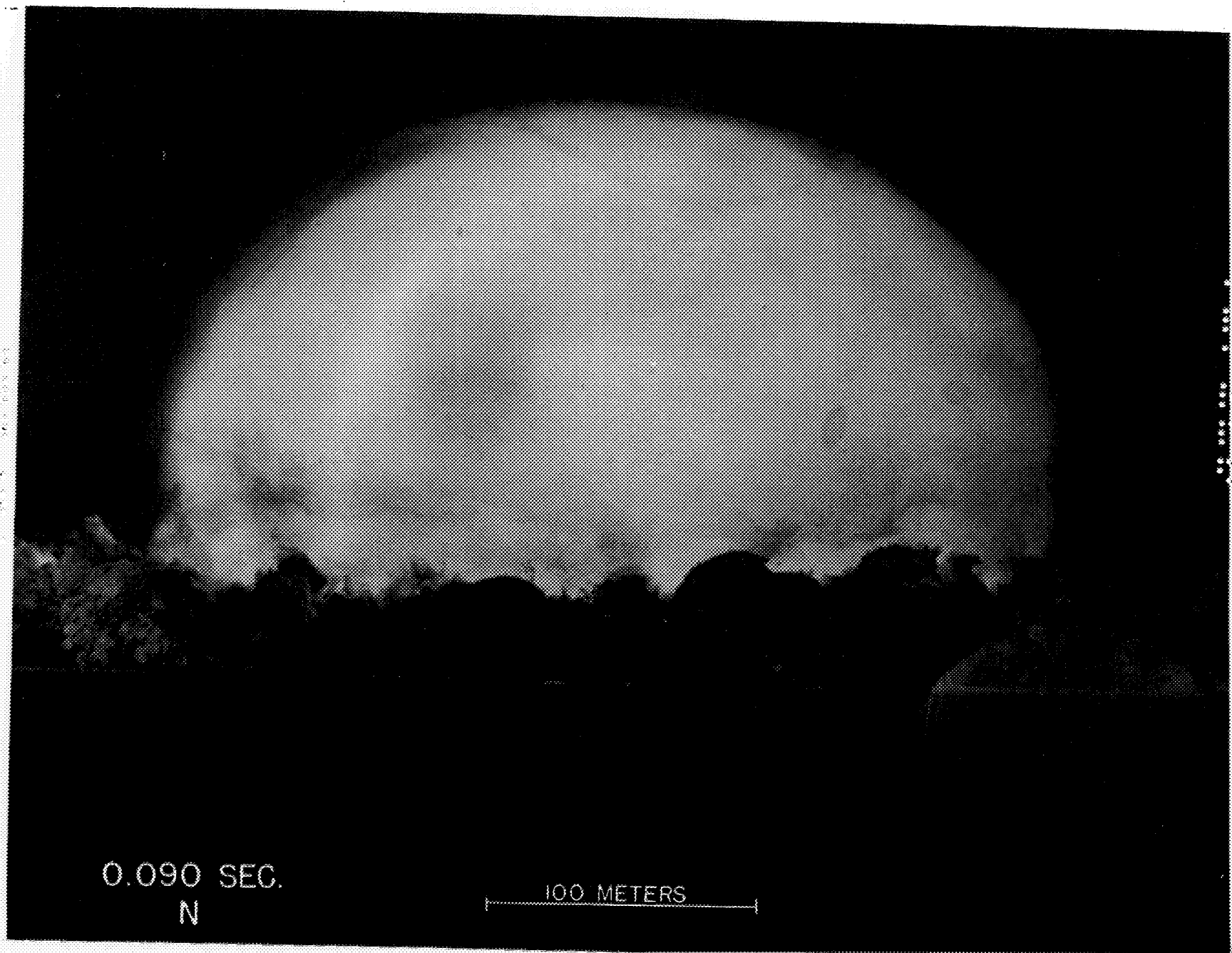






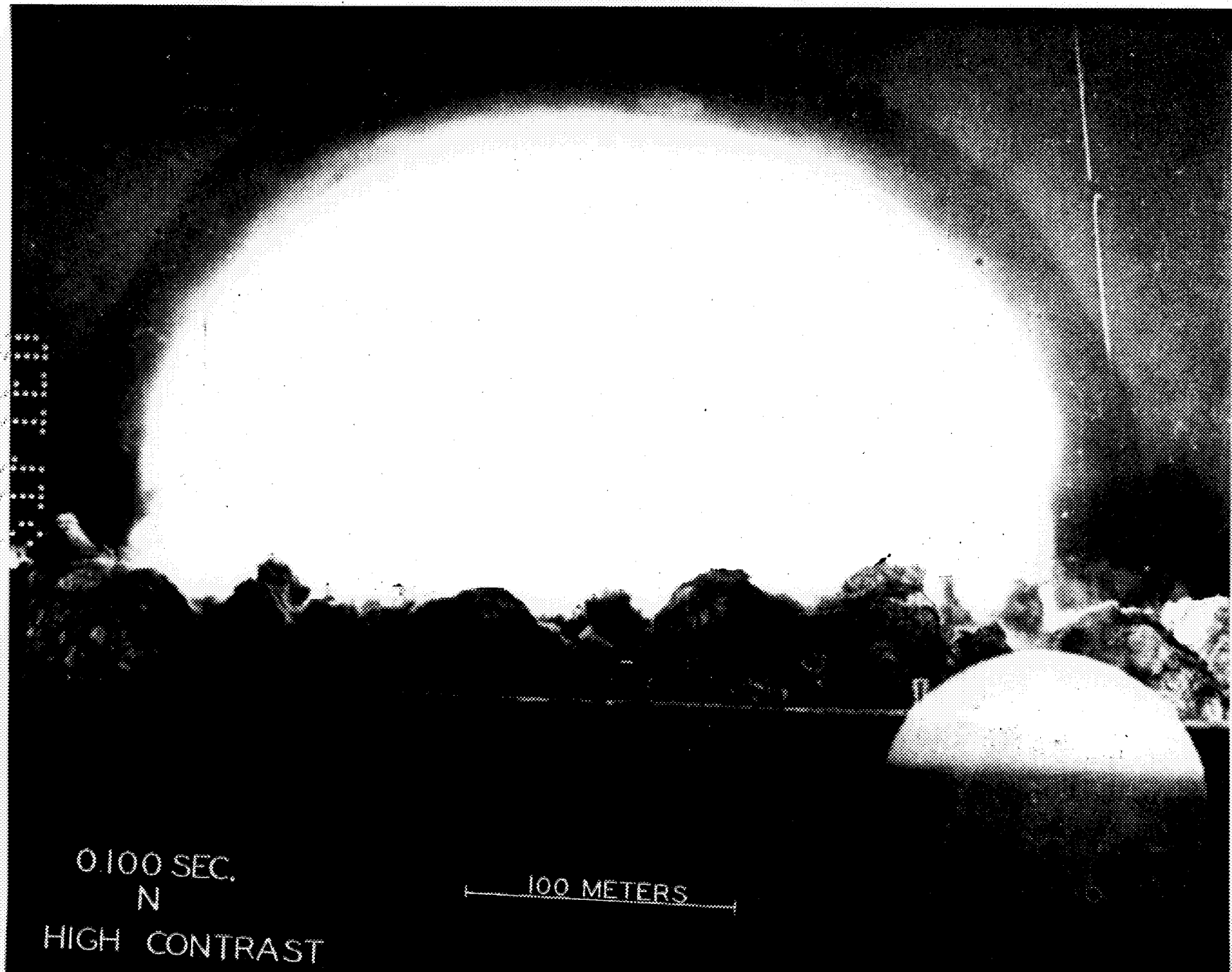


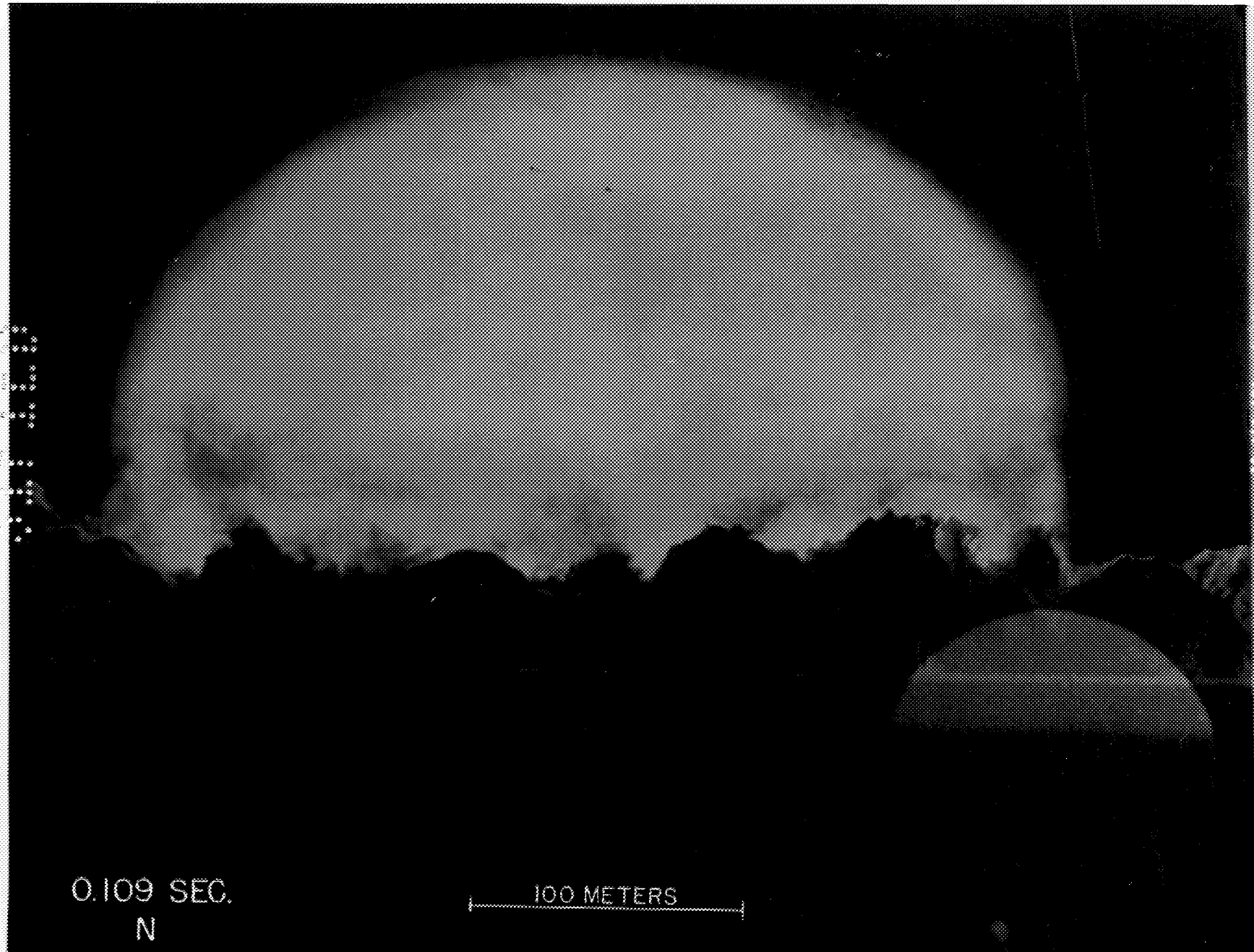
UNCLASSIFIED



UNCLASSIFIED

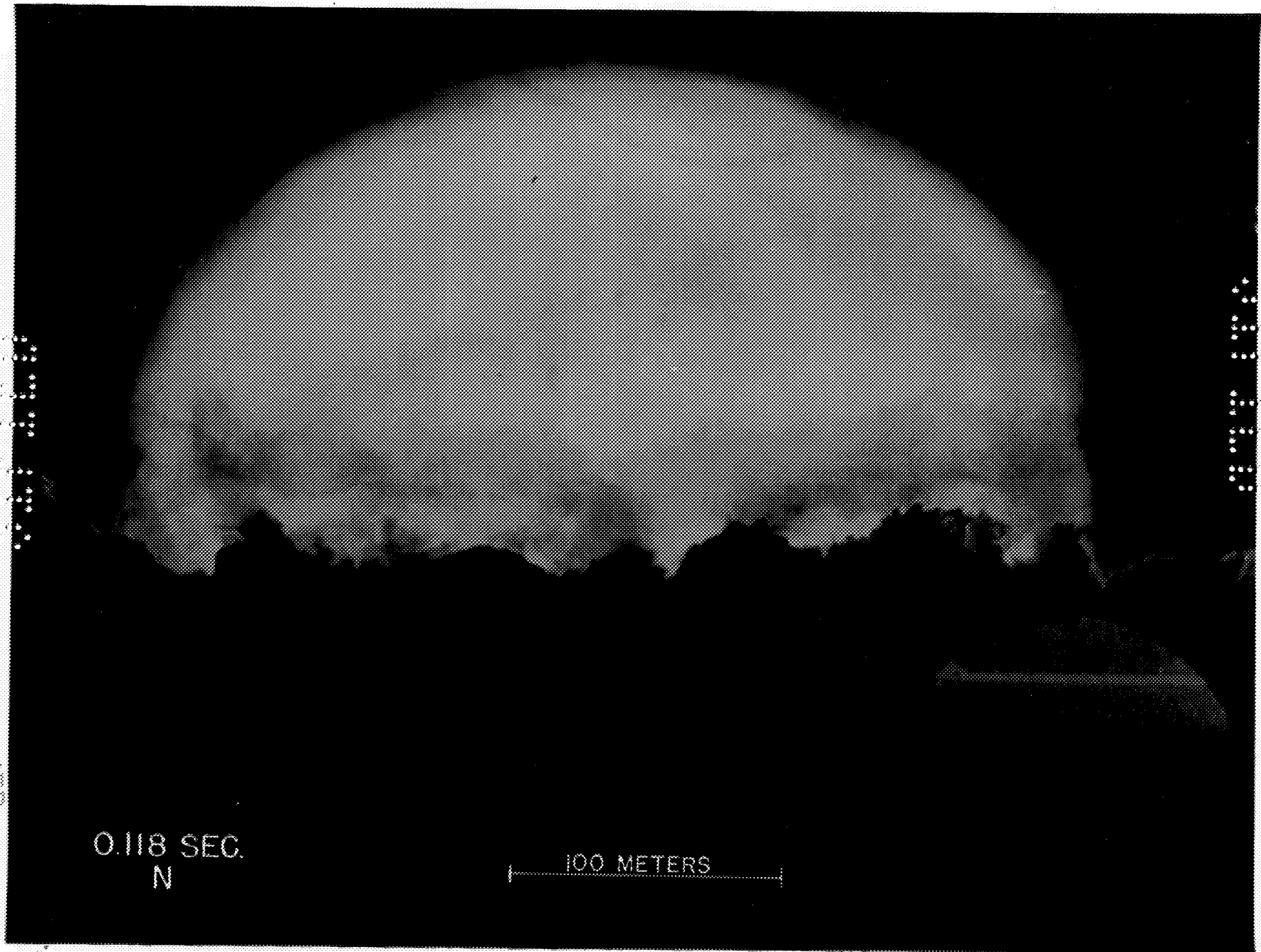


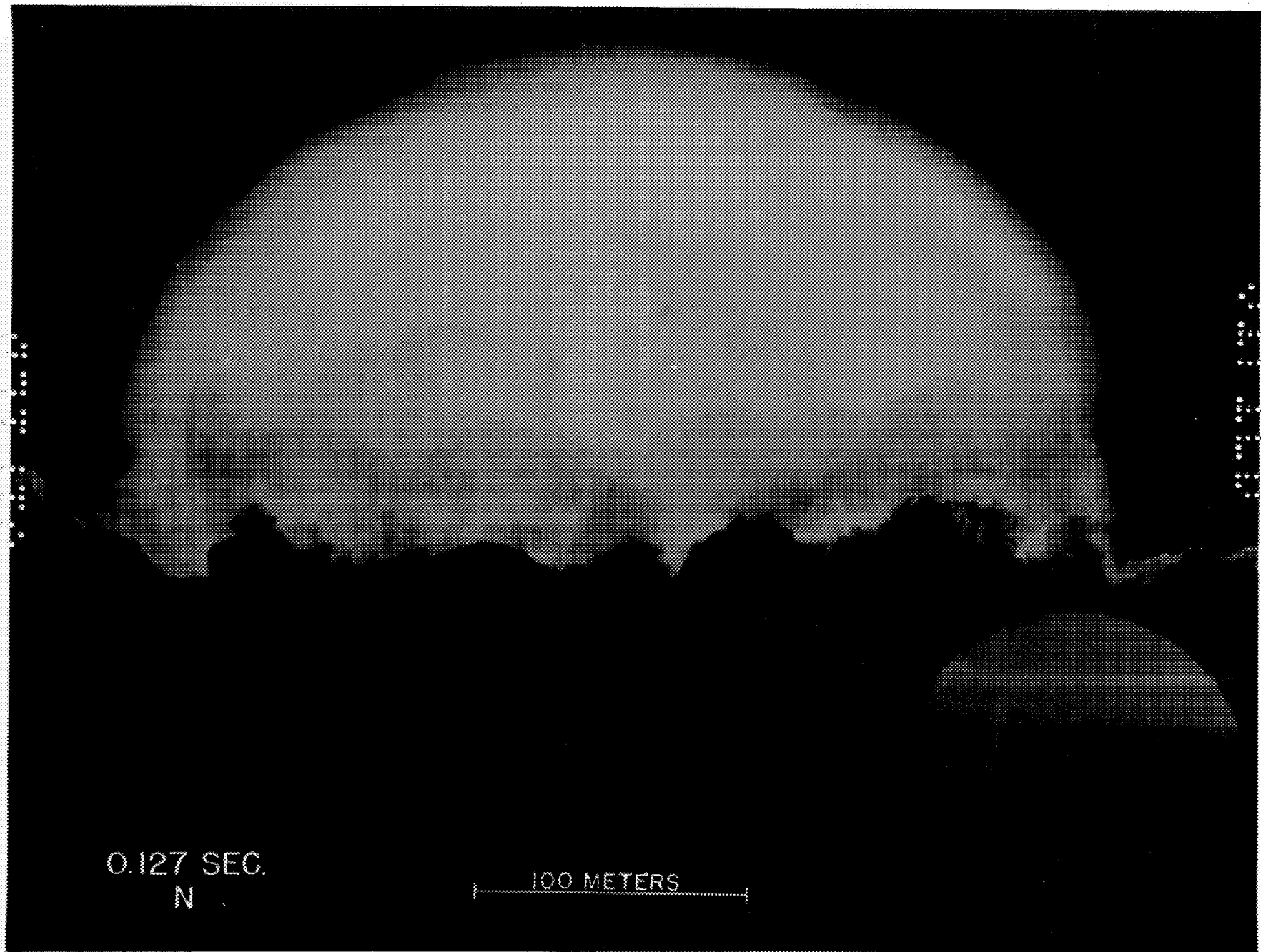




UNCLASSIFIED



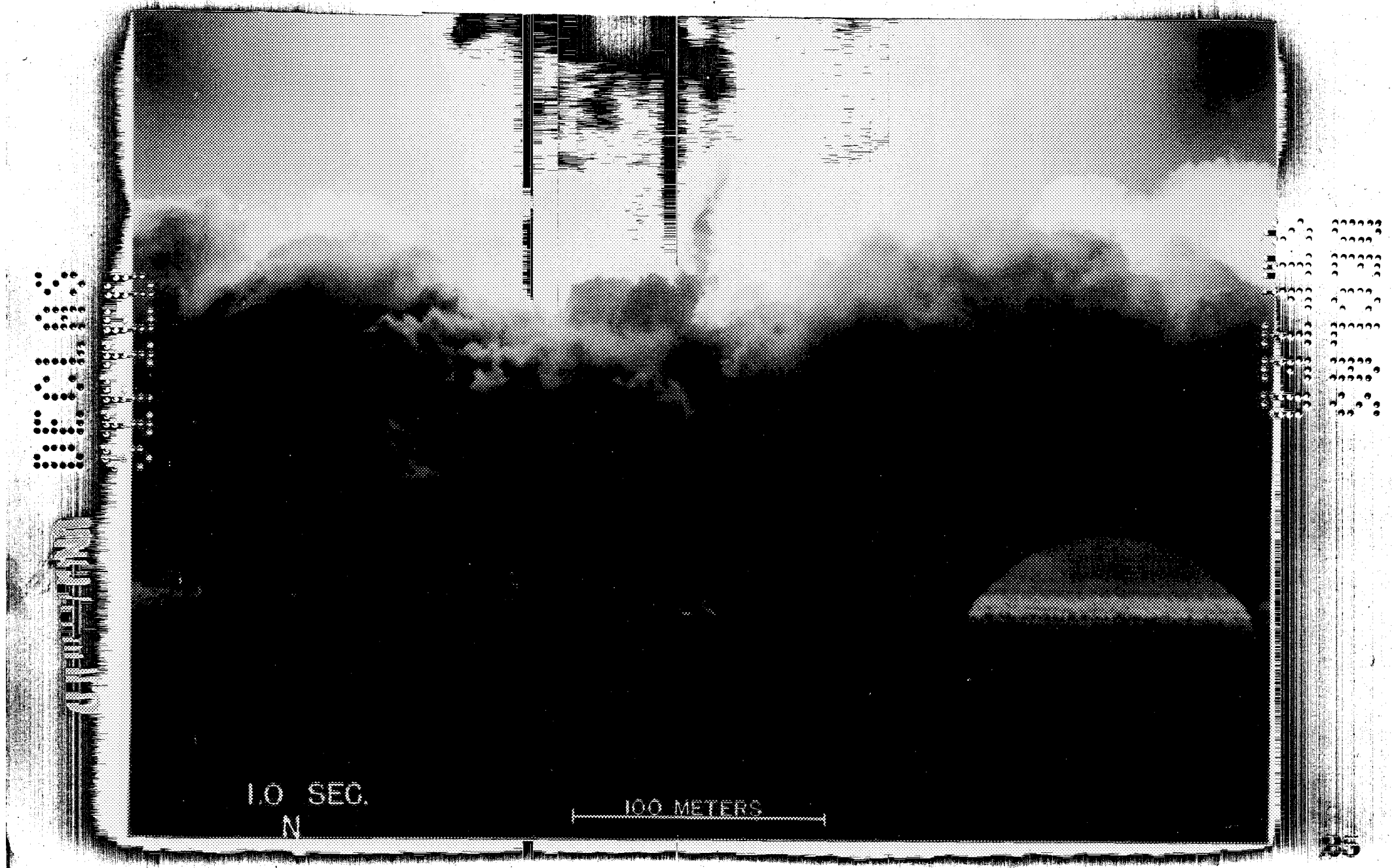


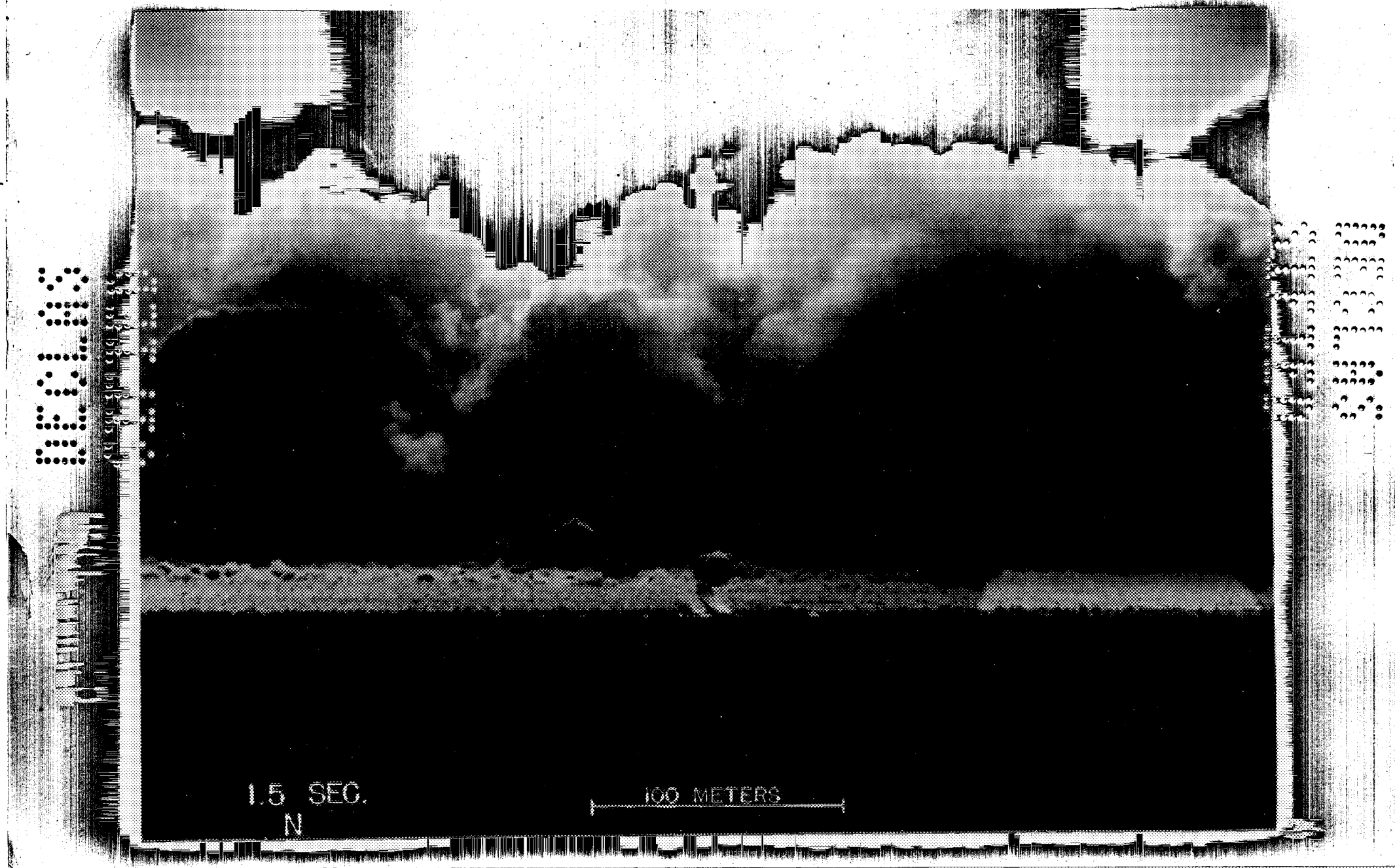




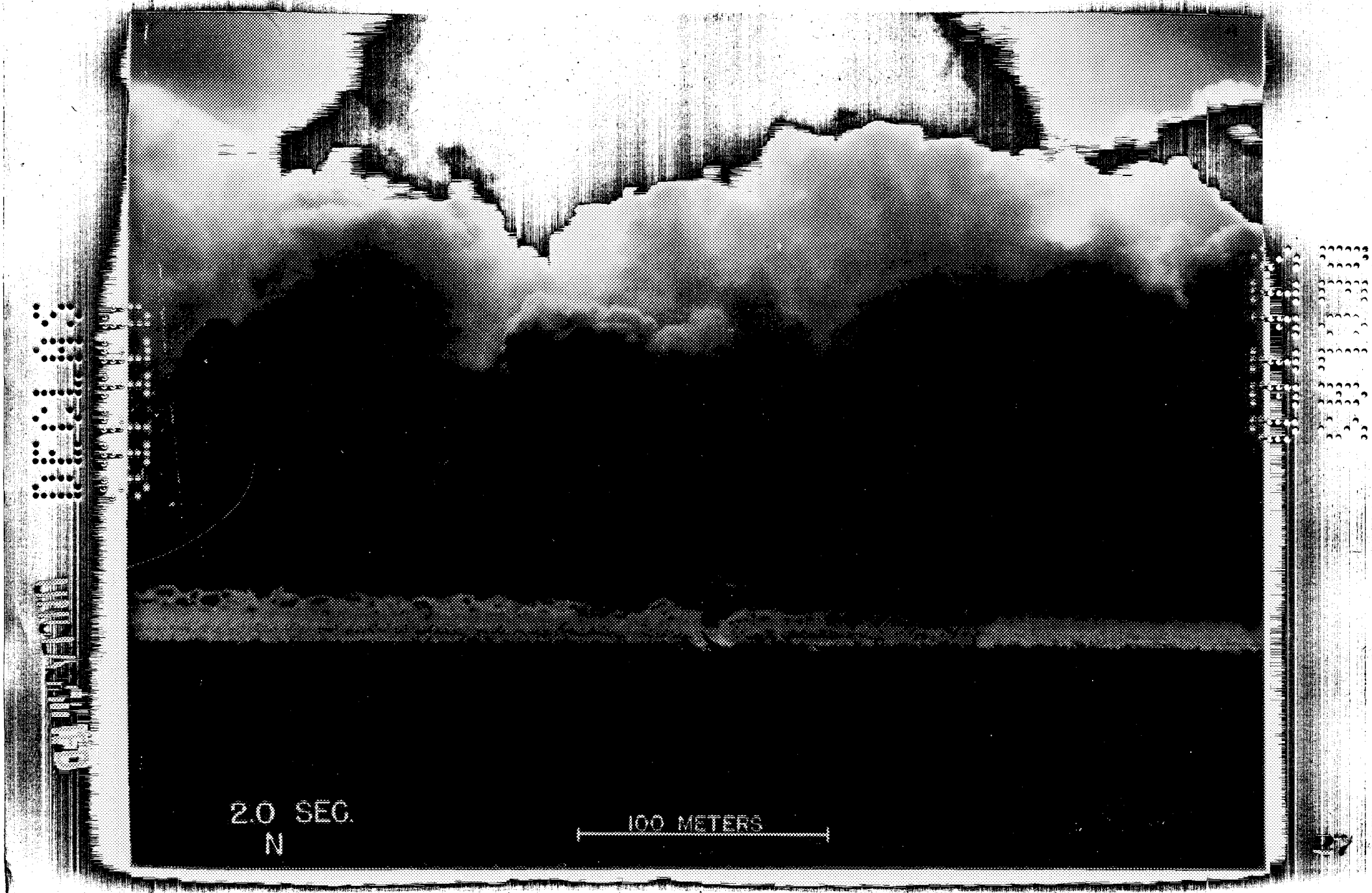




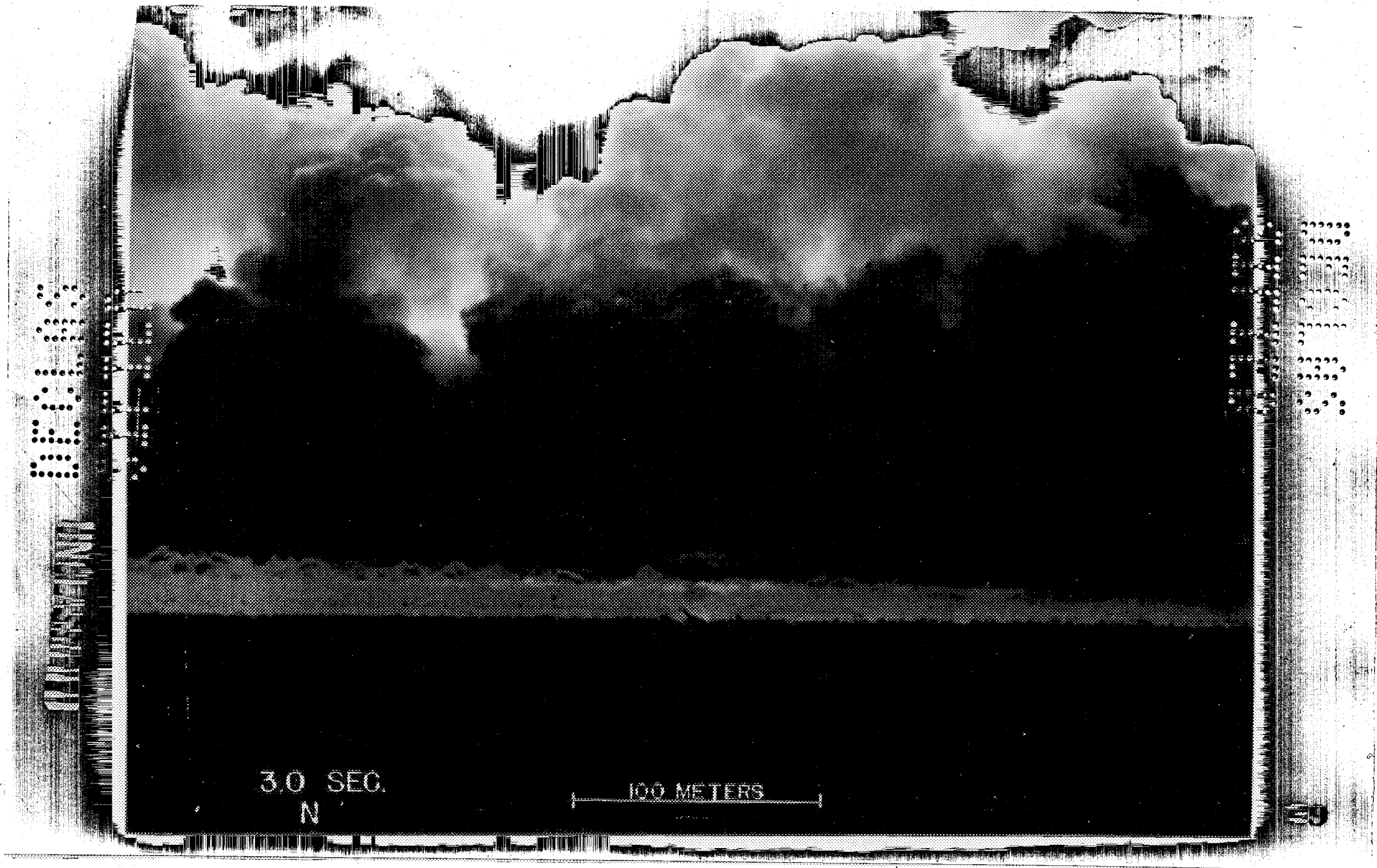








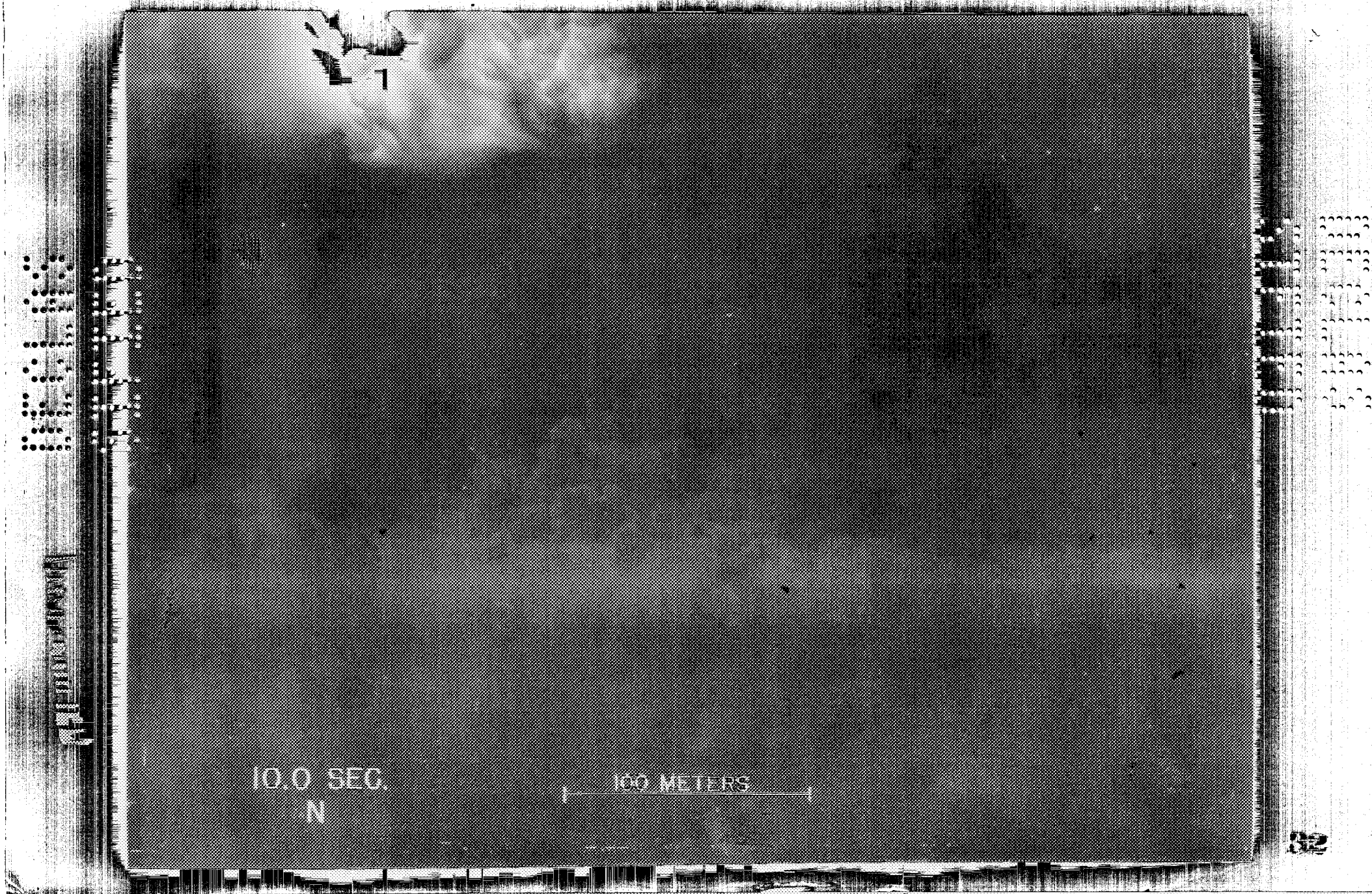




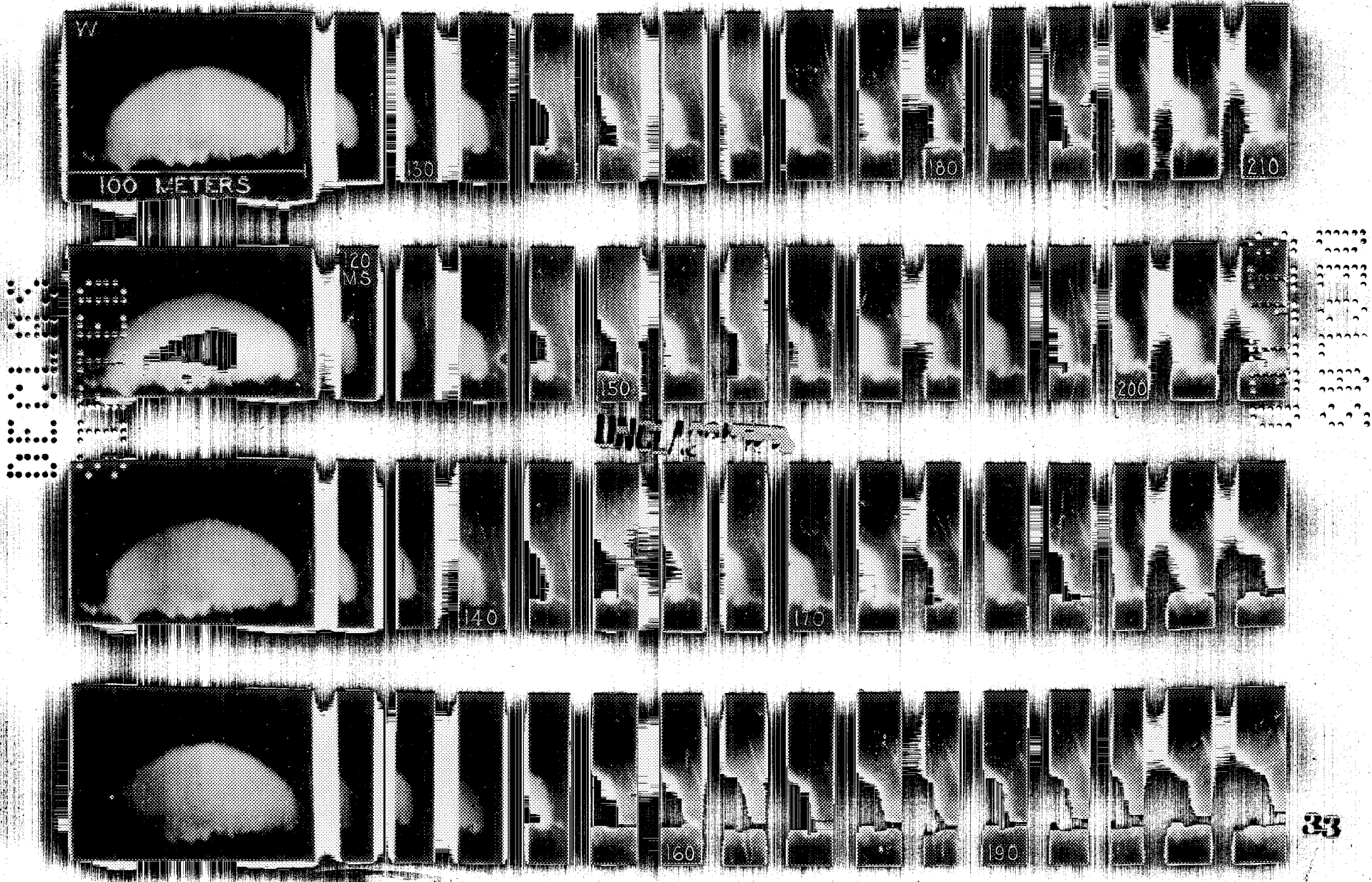


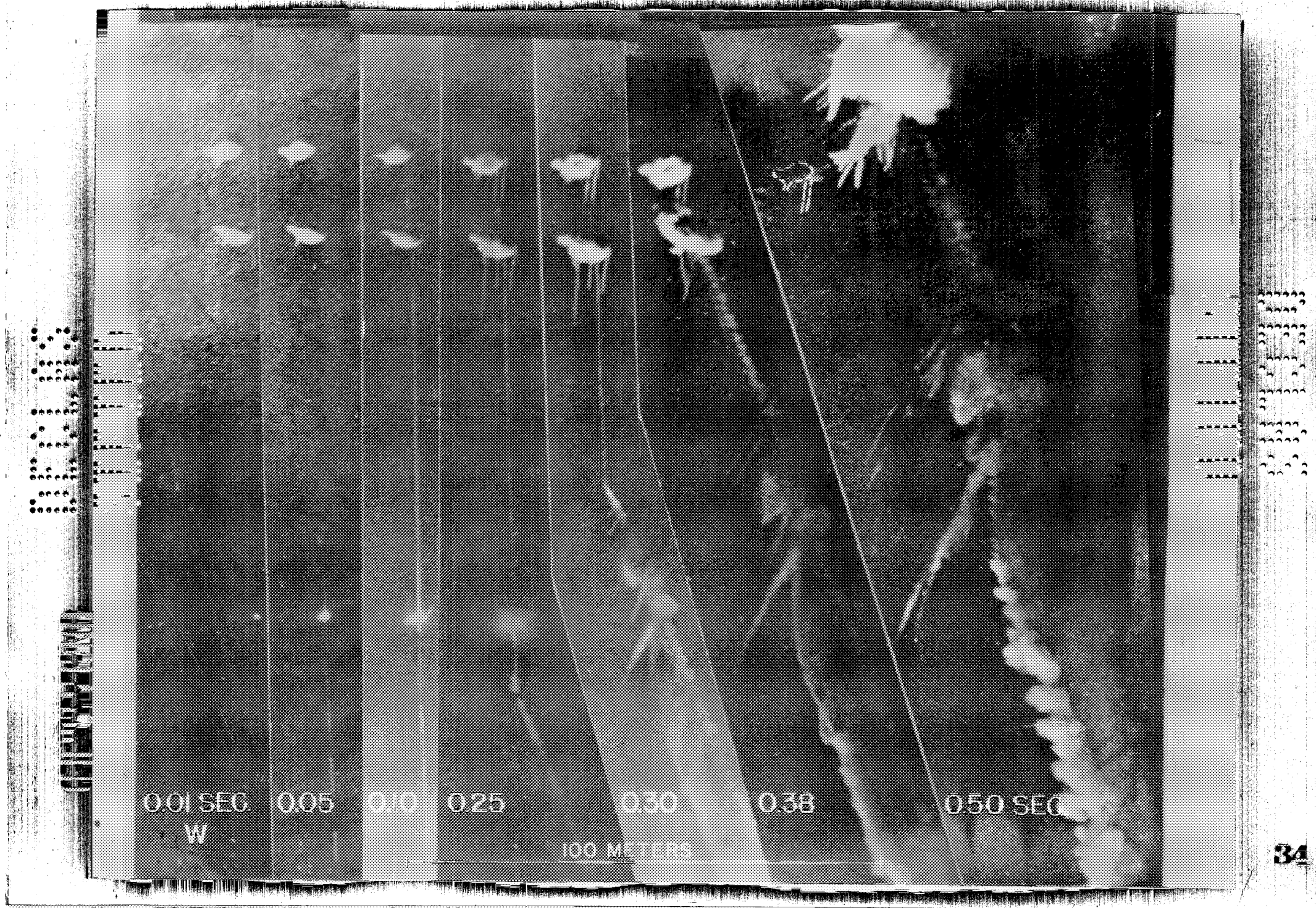






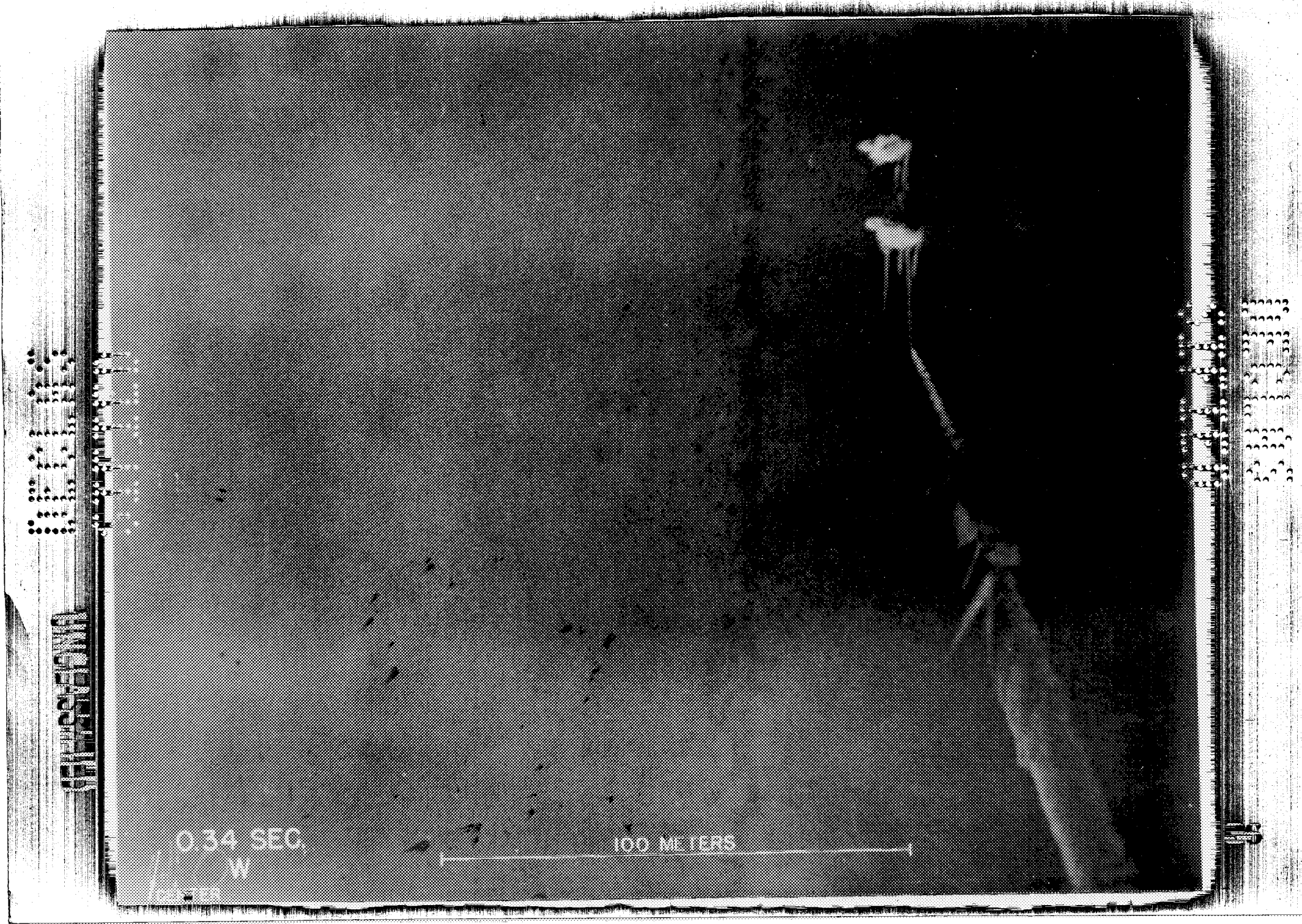


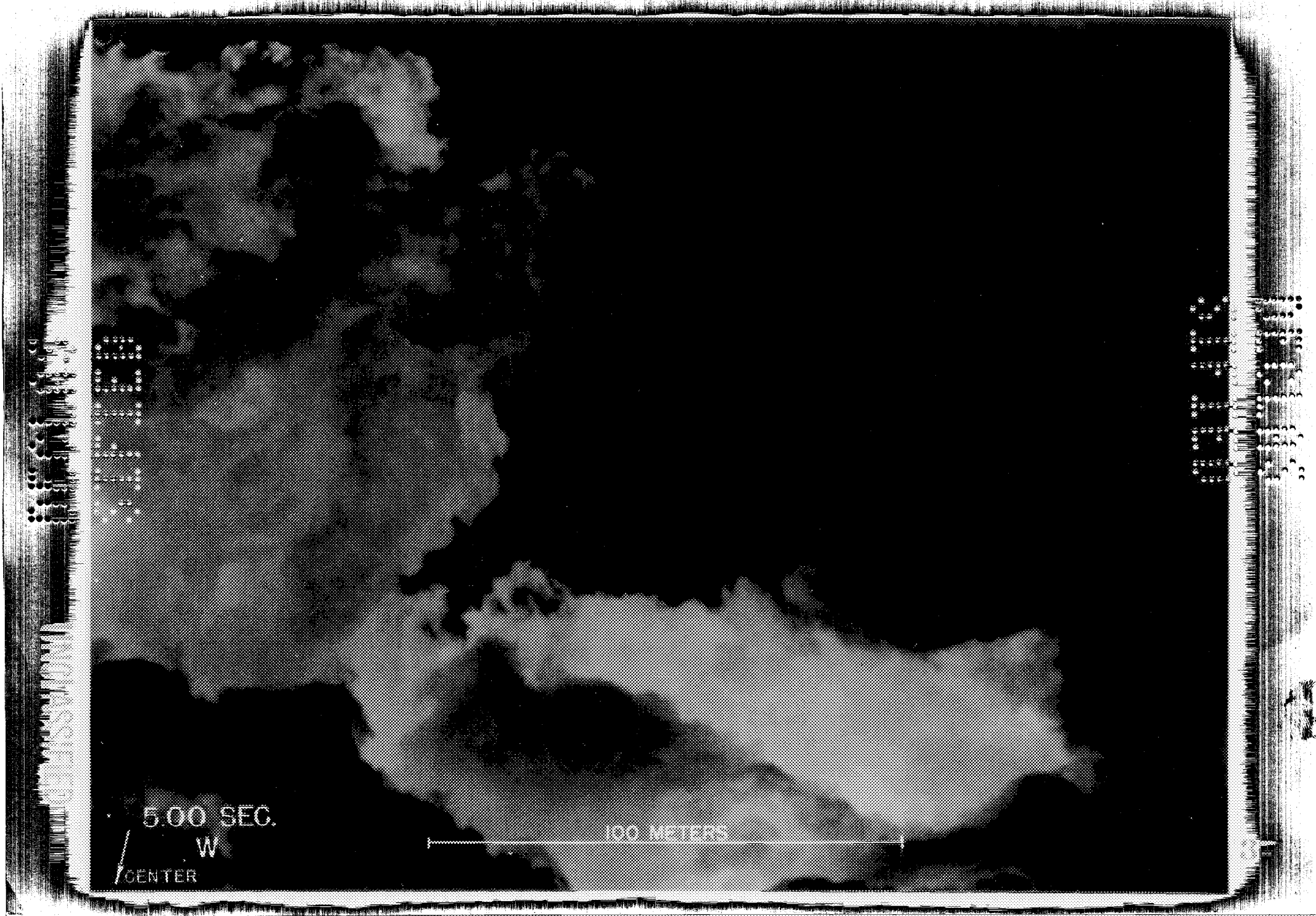












SECRET

UNCLASSIFIED

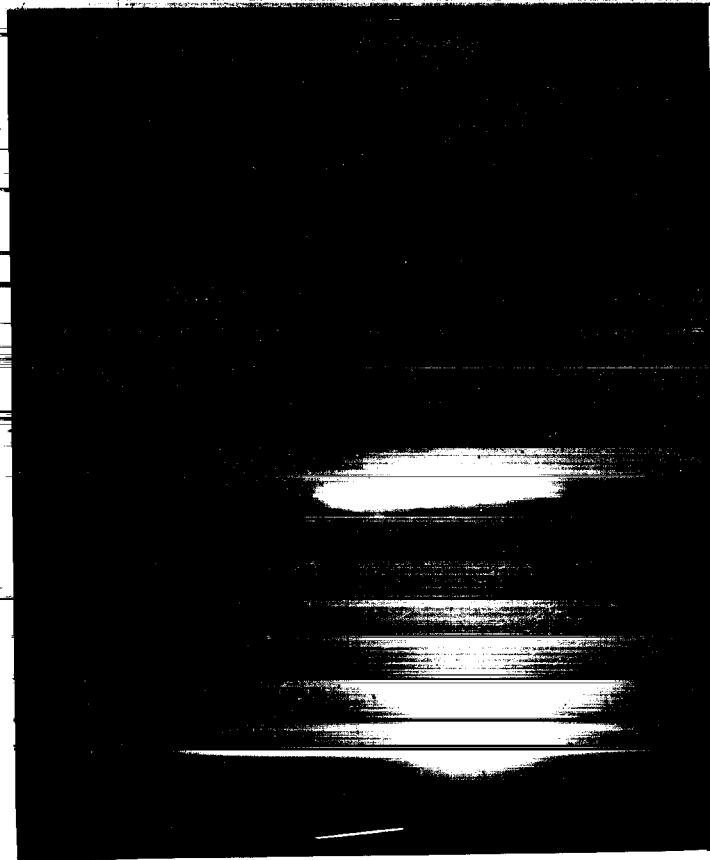


Fig. 36  
11.5 seconds NW

Note: For this and succeeding two vectographs use viewers in packet.

100 Meters



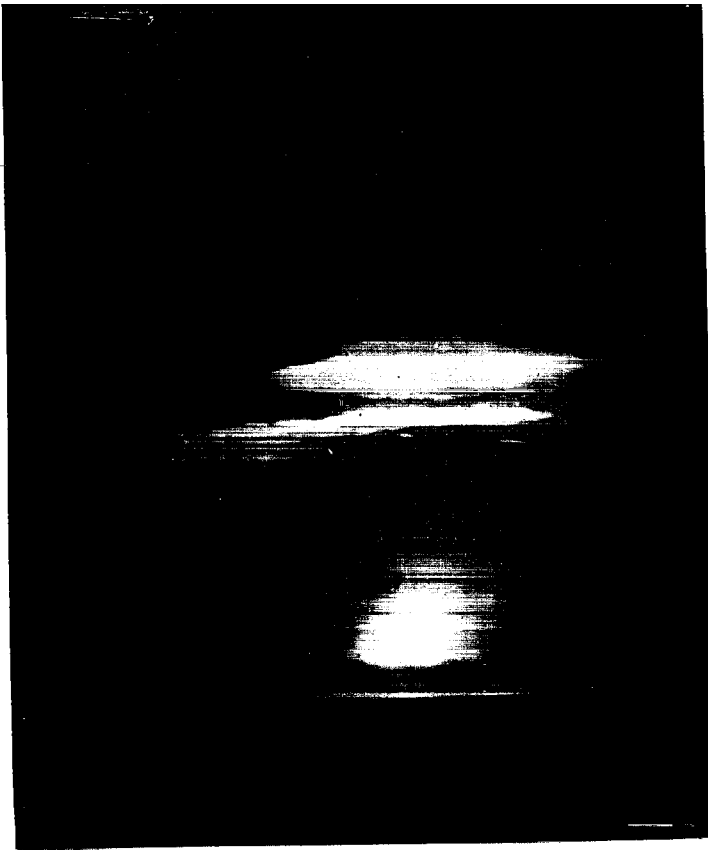


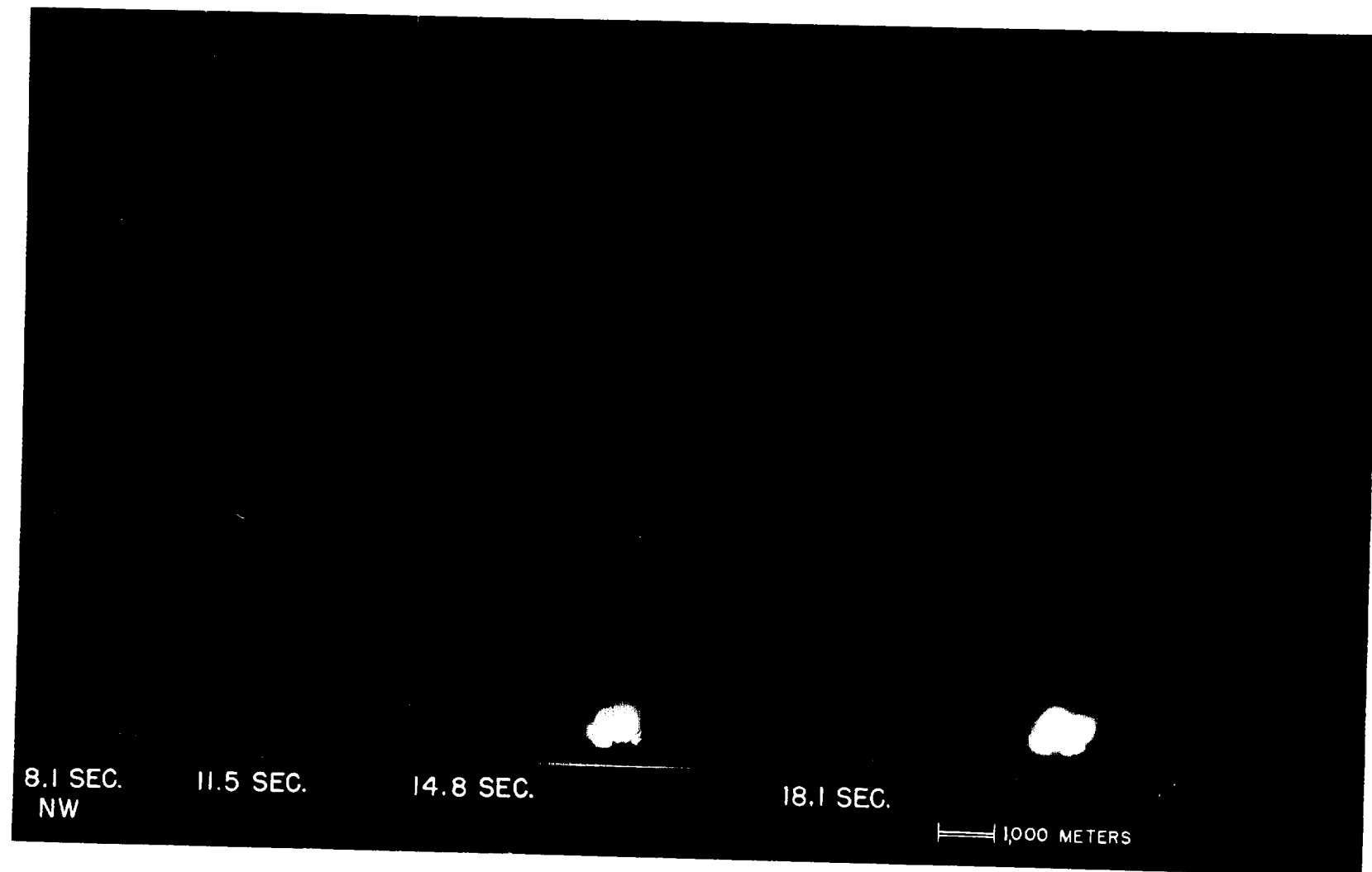
Fig. 59  
14.8 seconds NW

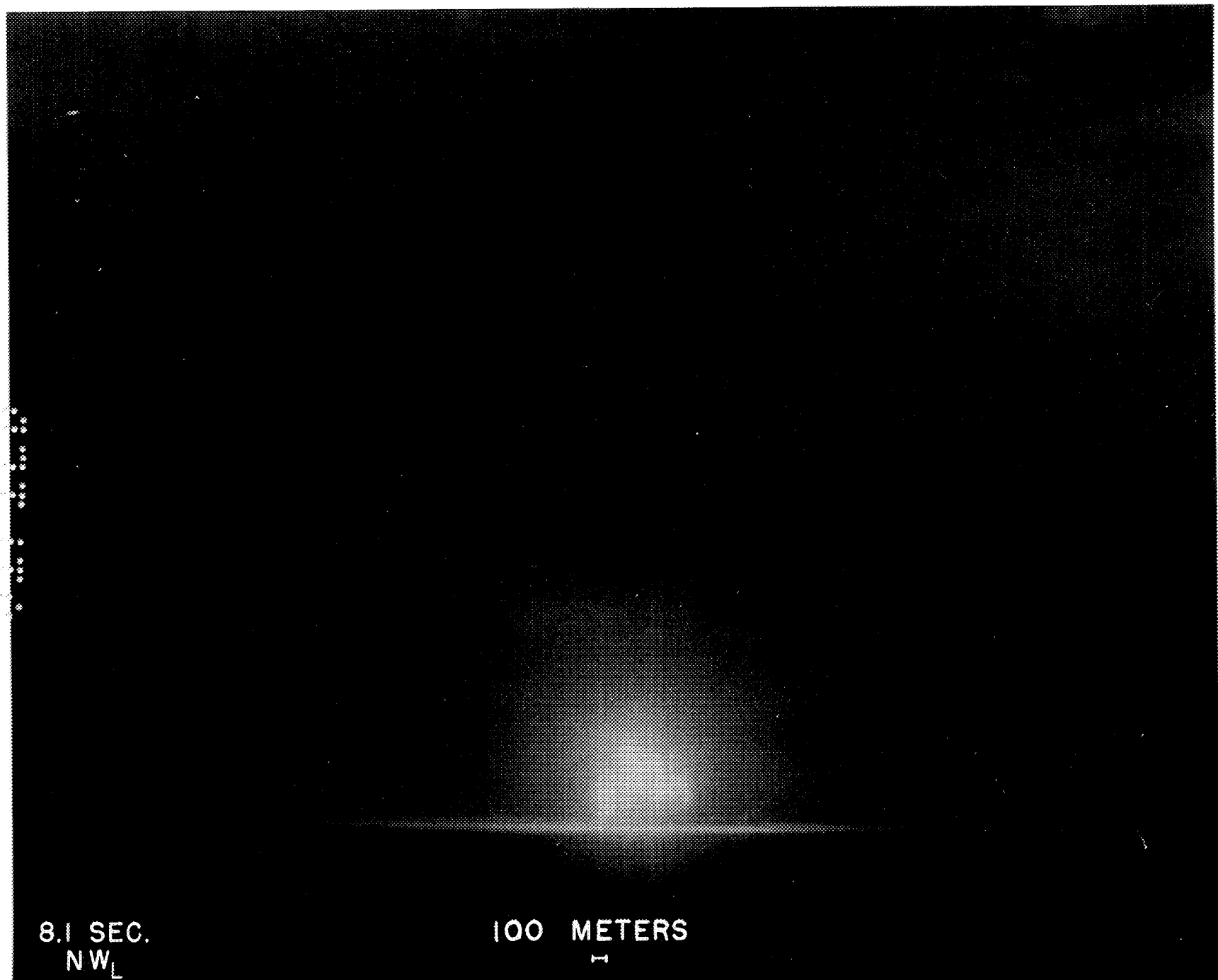


Fig. 60  
18.7 seconds NW

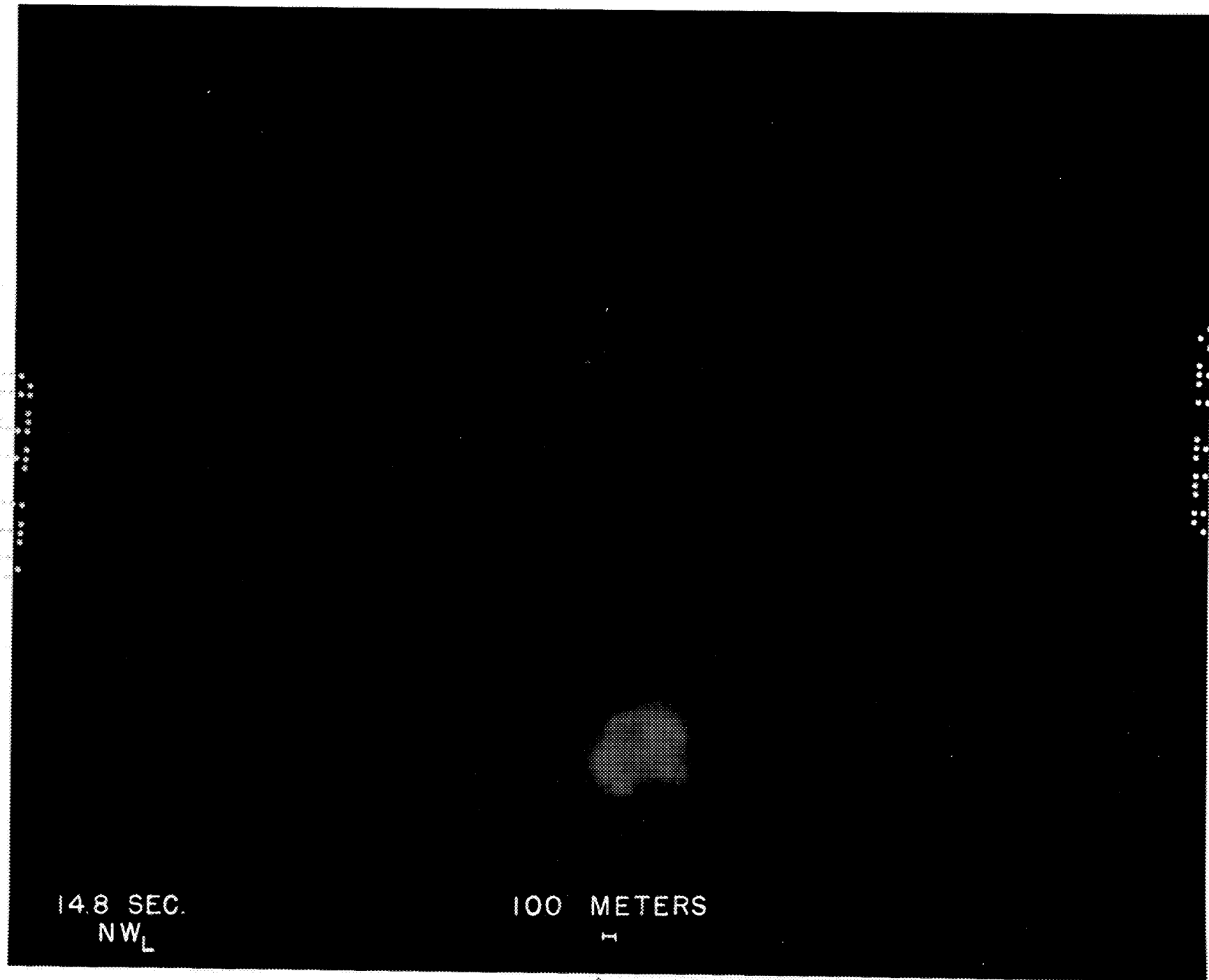
UNCLASSIFIED

100 Meters





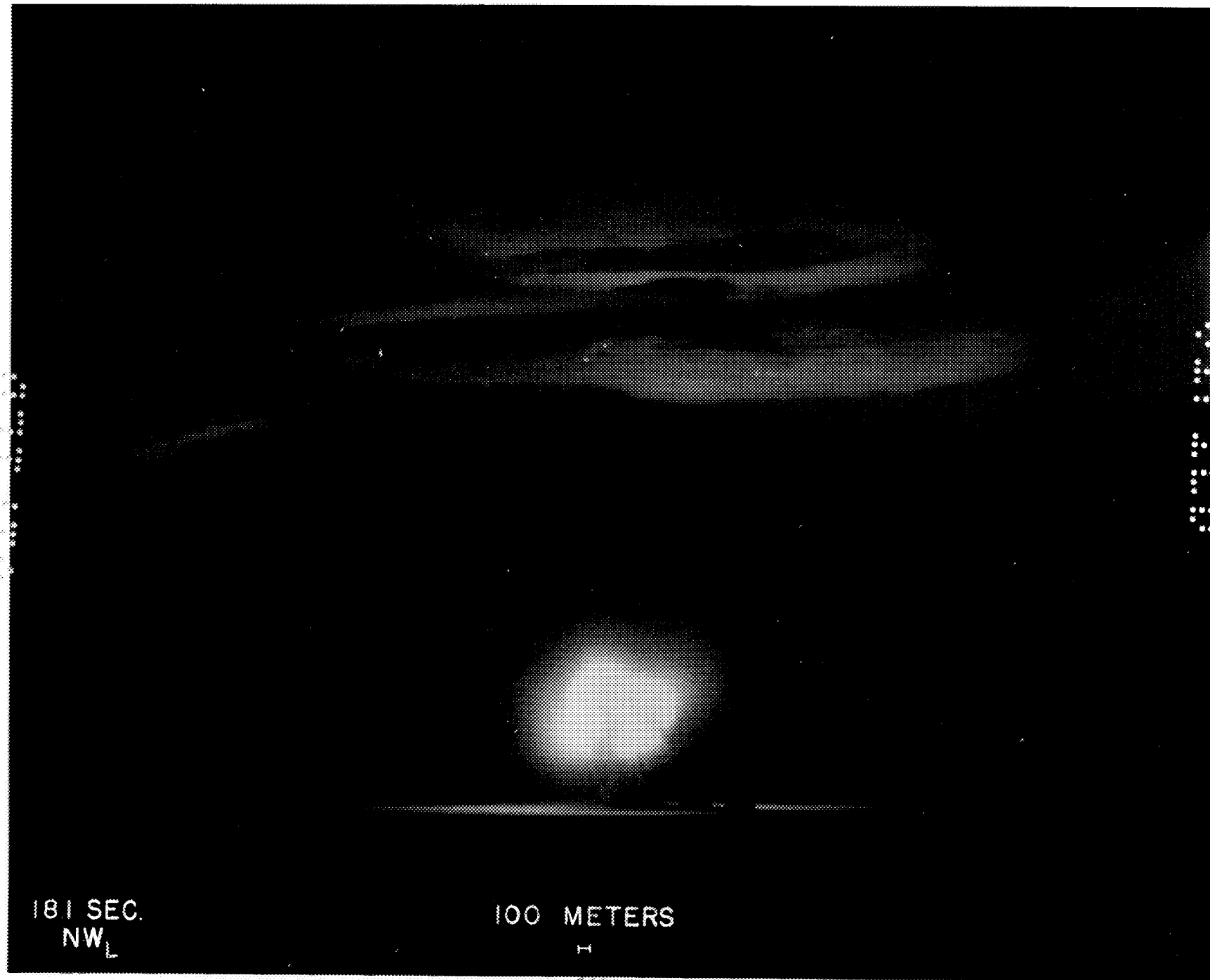


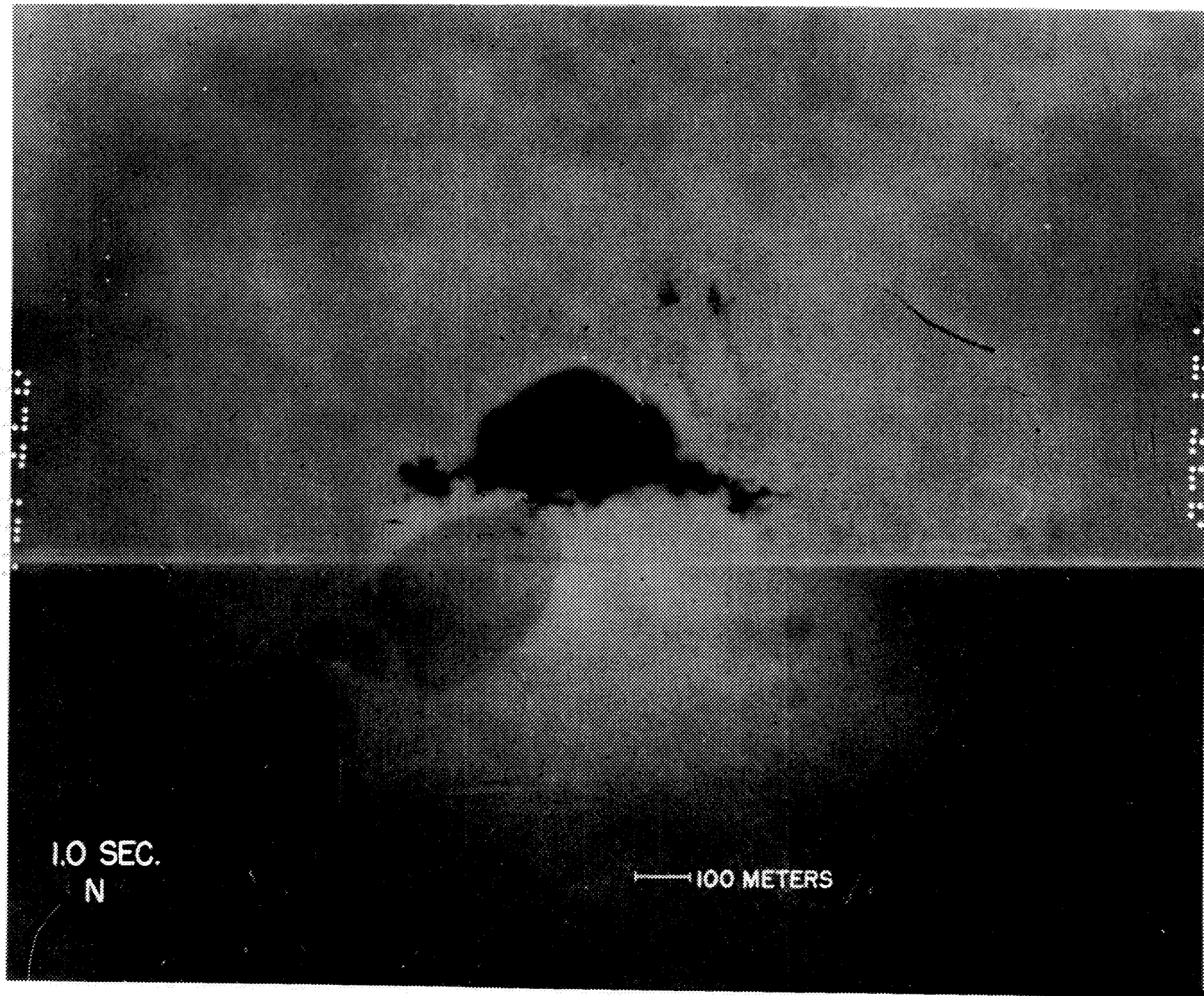


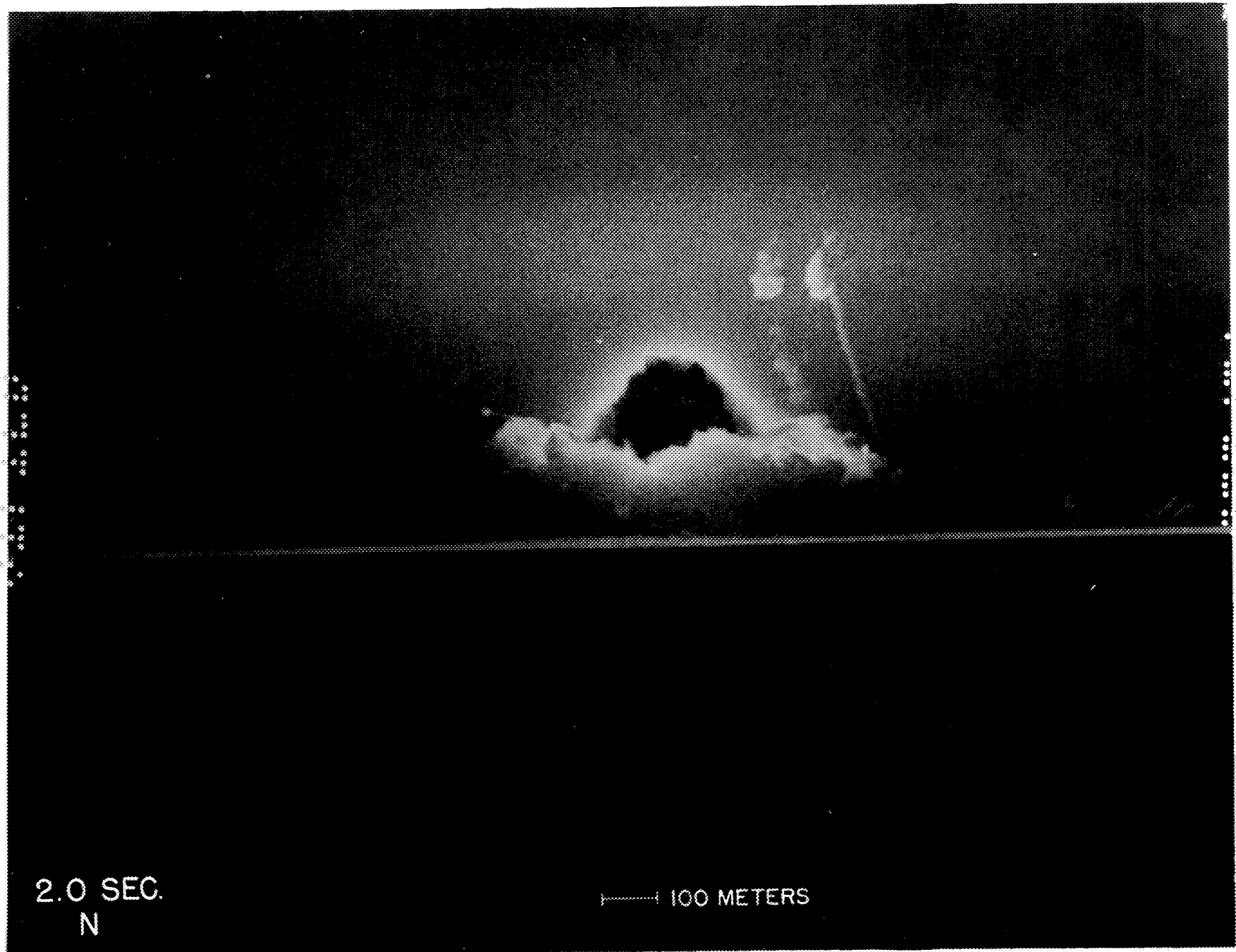
14.8 SEC.  
NW<sub>L</sub>

100 METERS  
—

UNCLASSIFIED







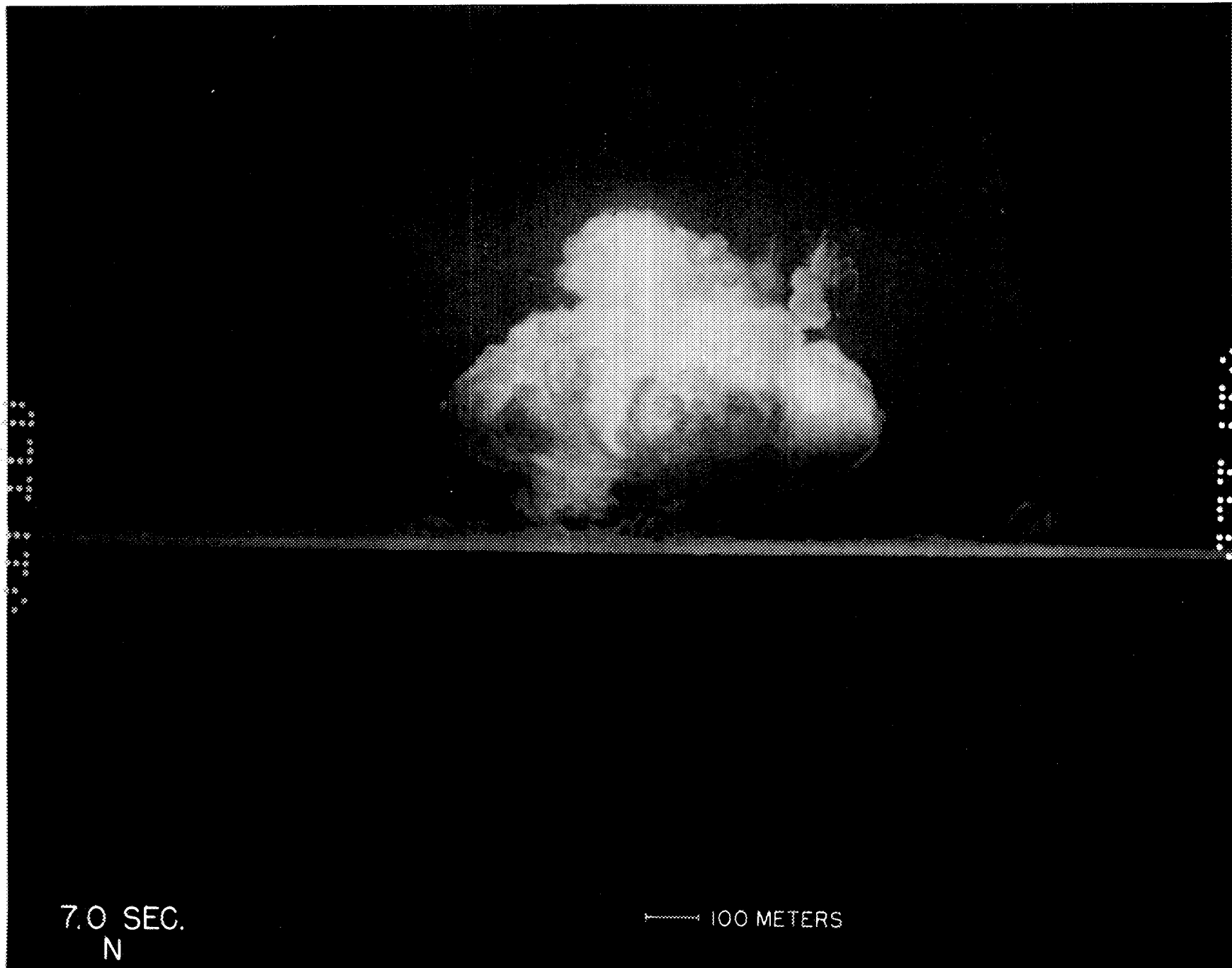


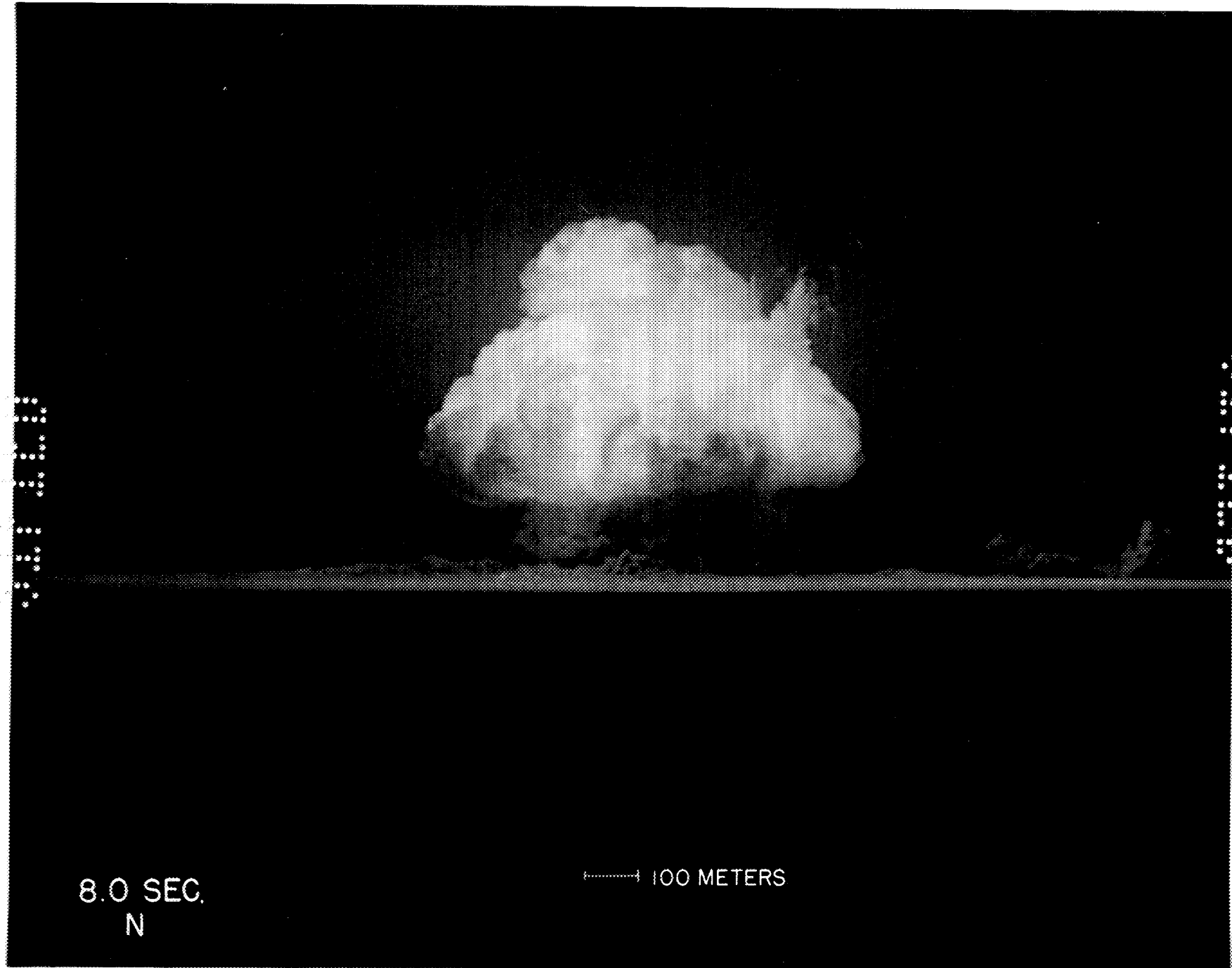


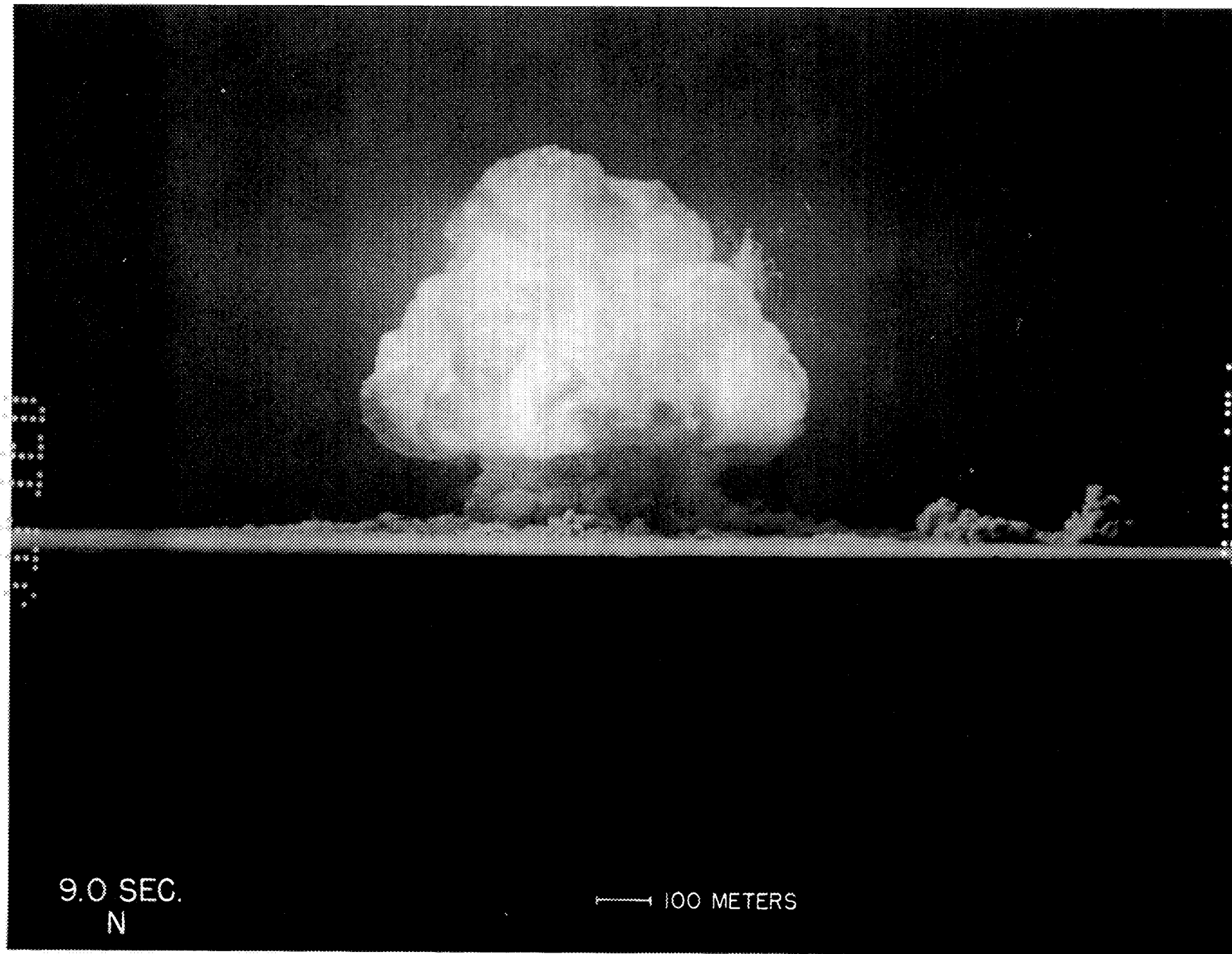






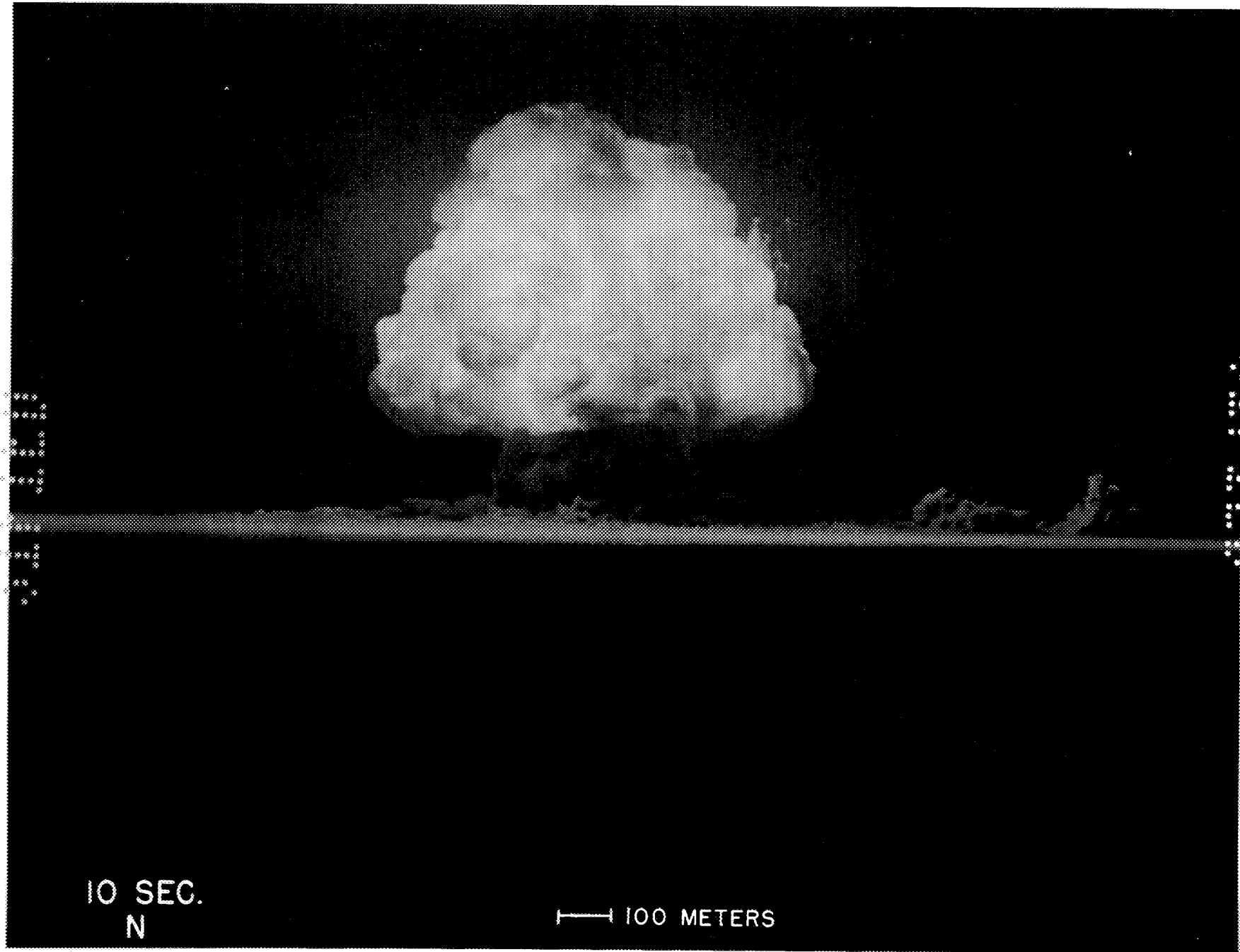




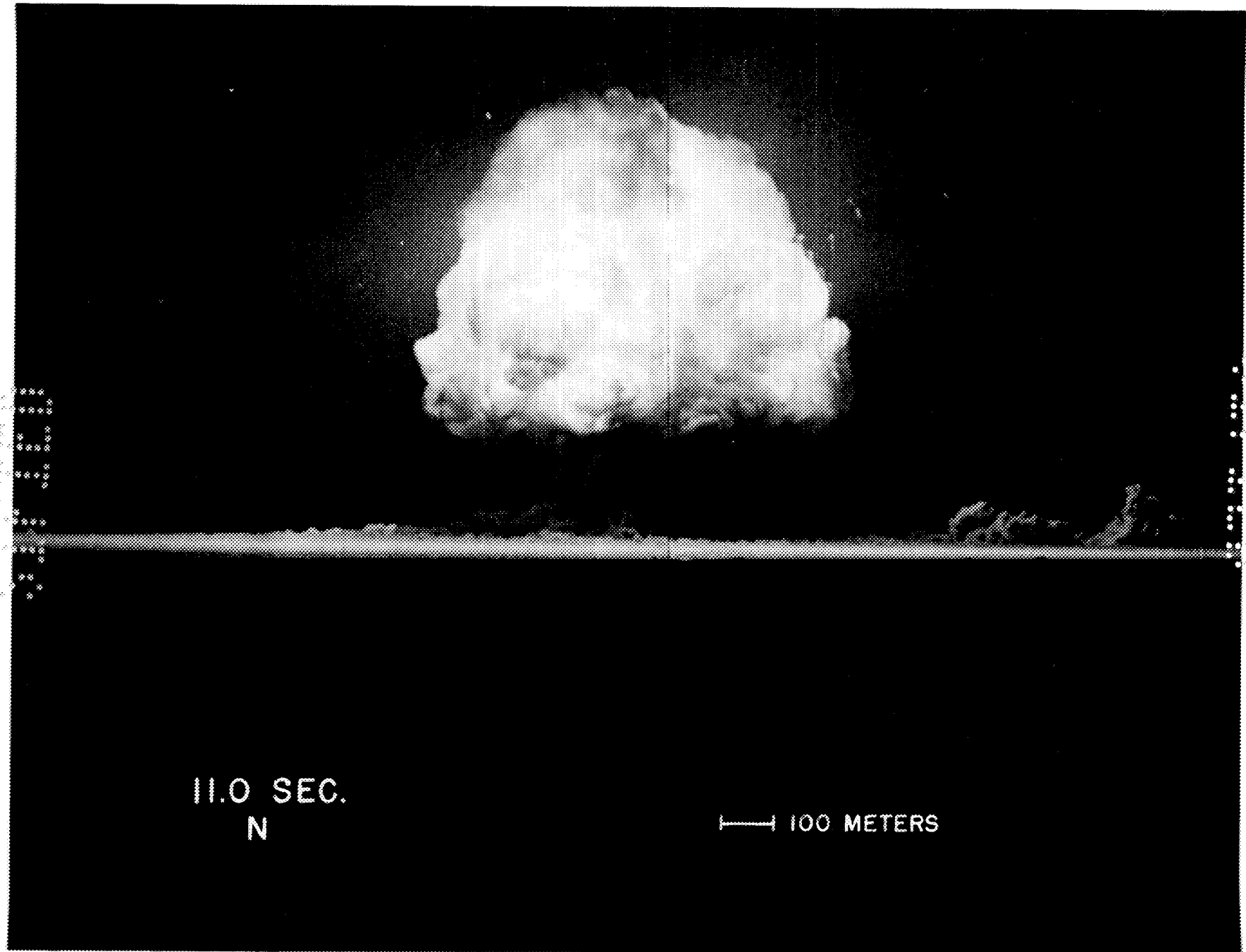


9.0 SEC.  
N

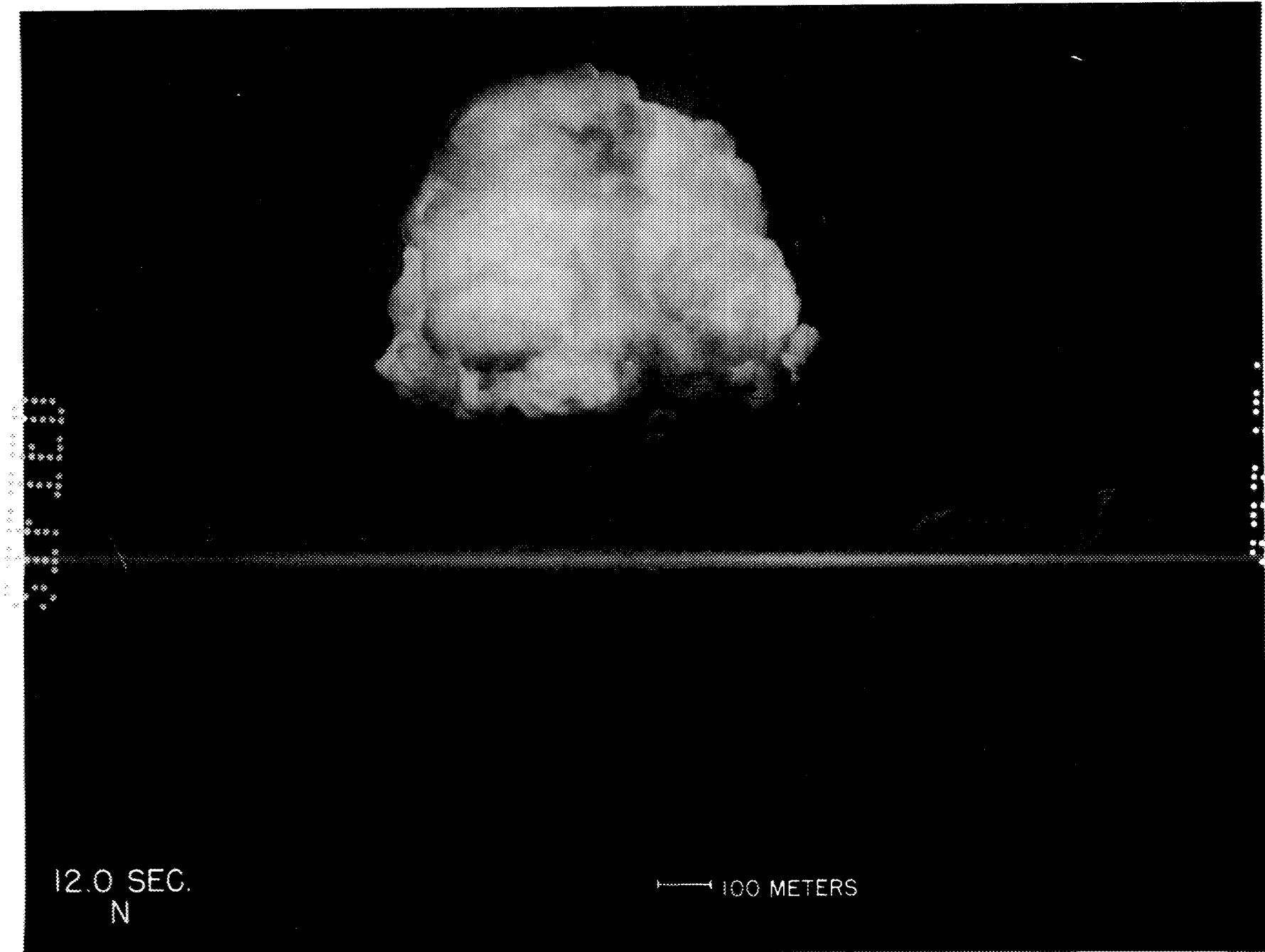
— 100 METERS

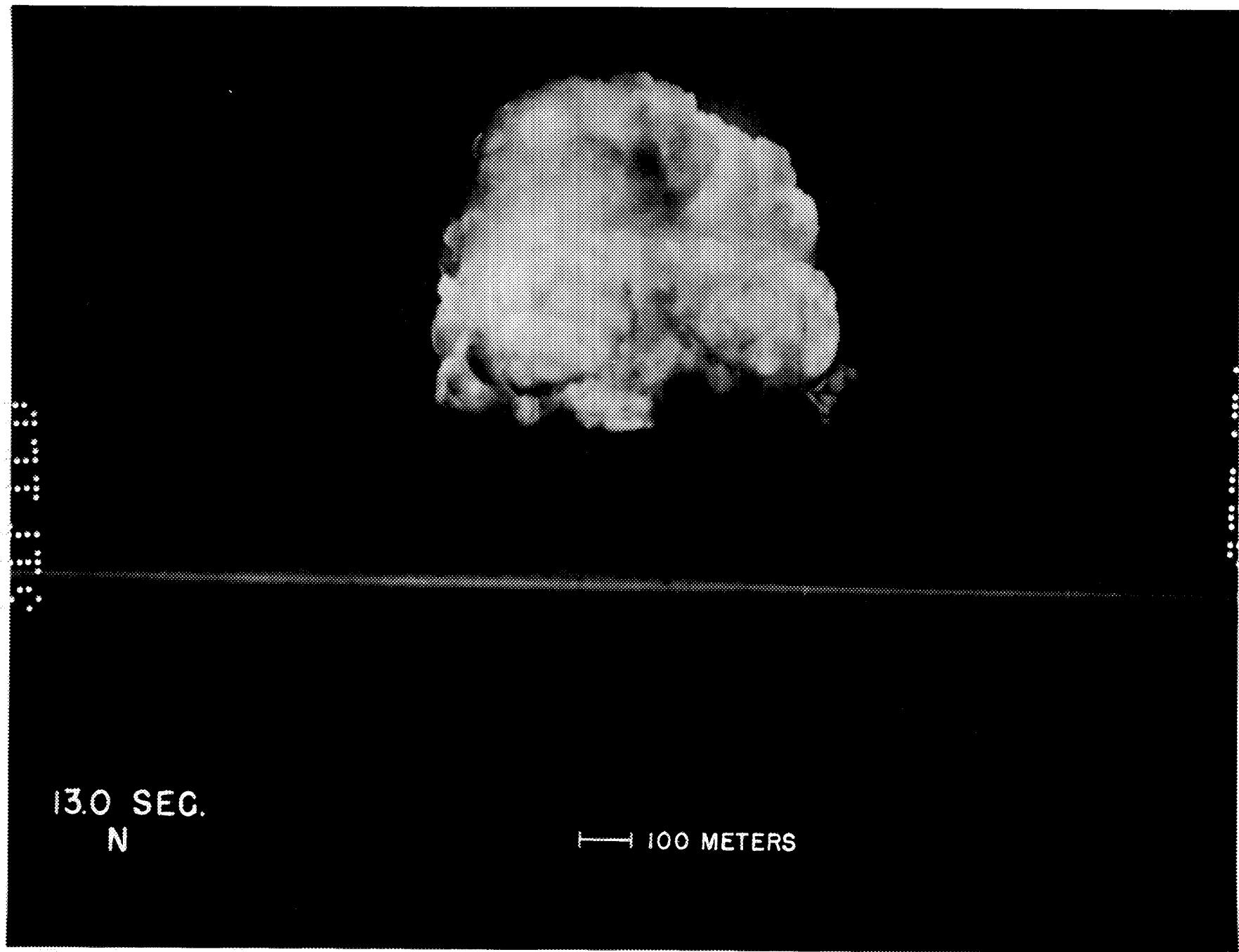






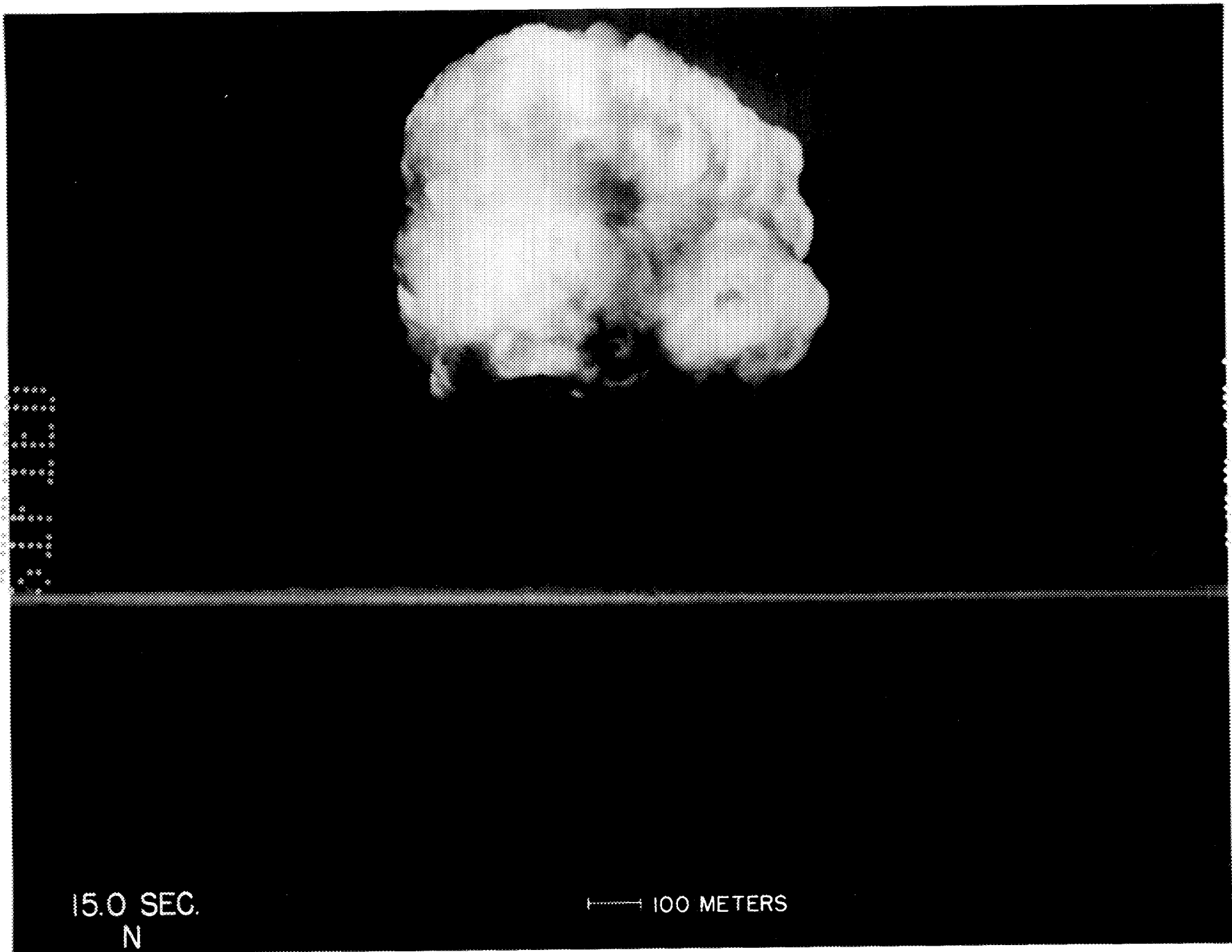
UNCLASSIFIED





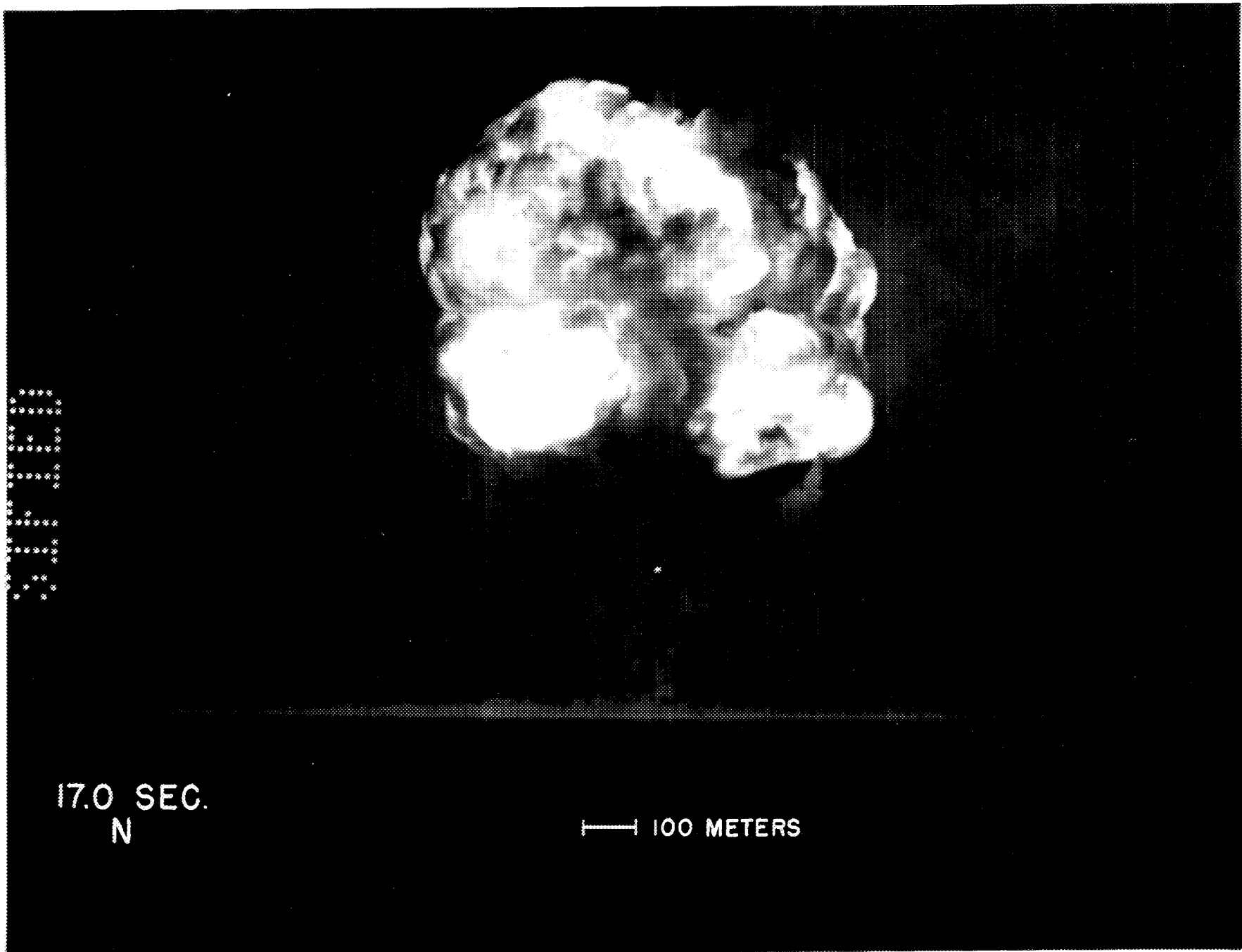
UNCLASSIFIED

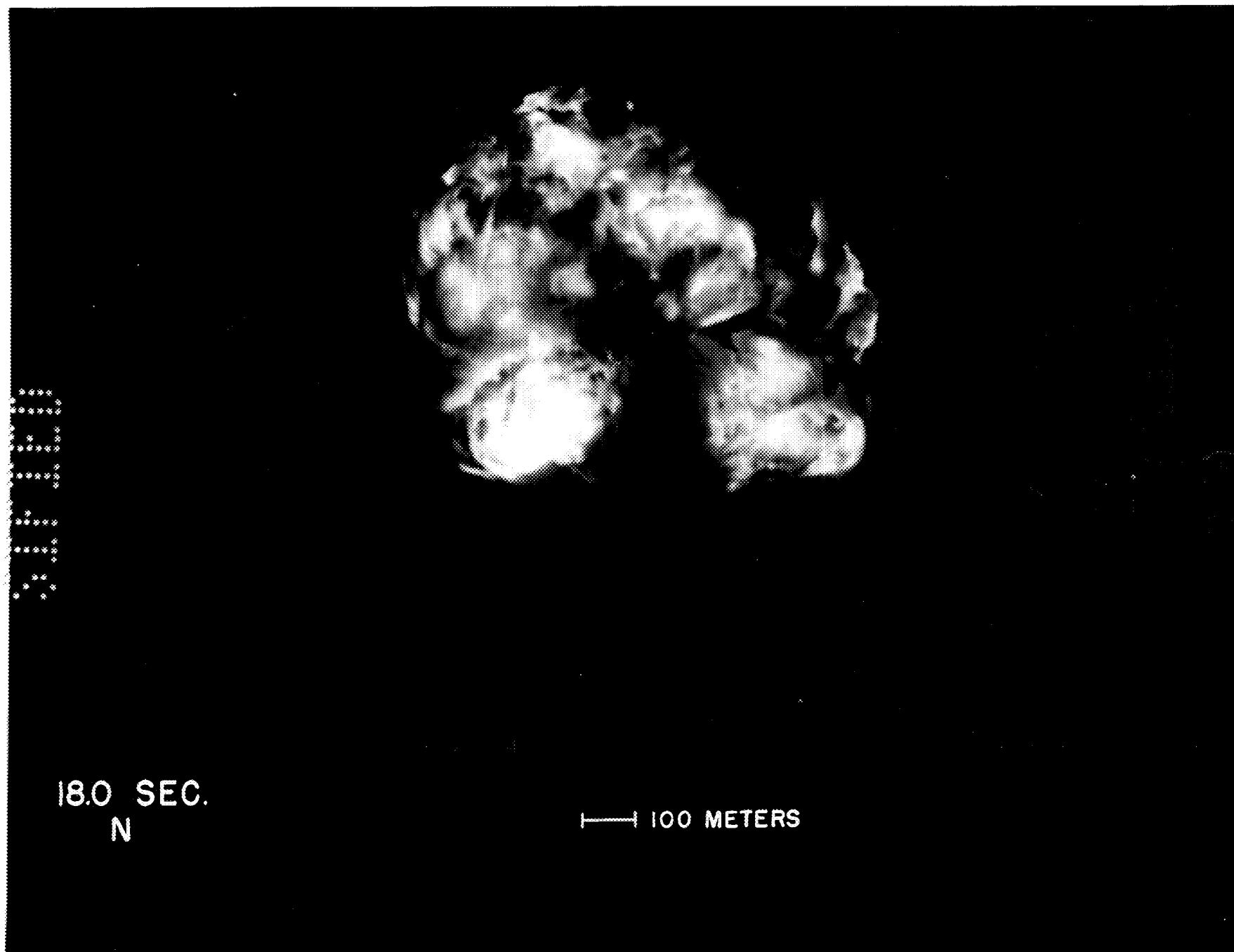




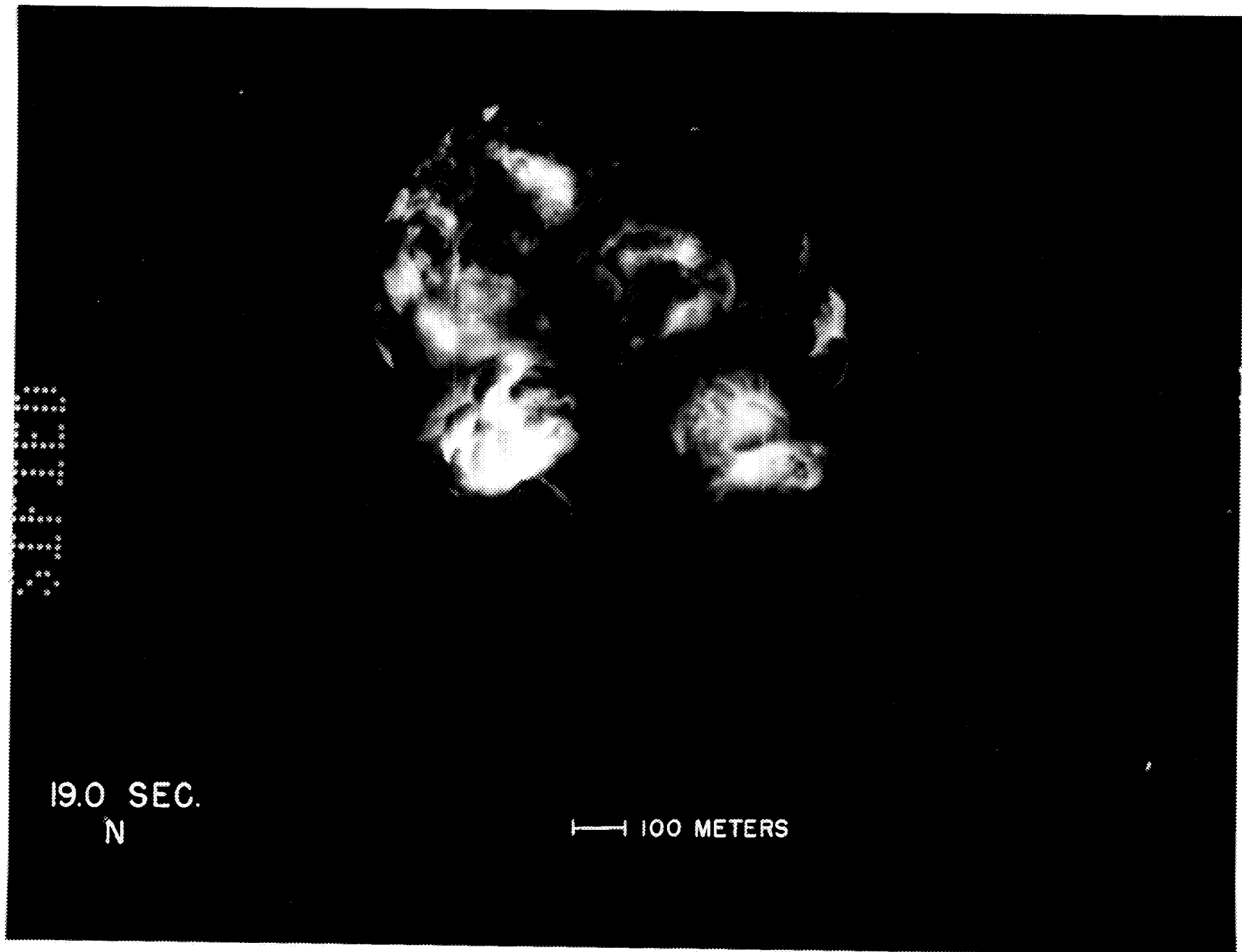
100' 100' 100' 100'



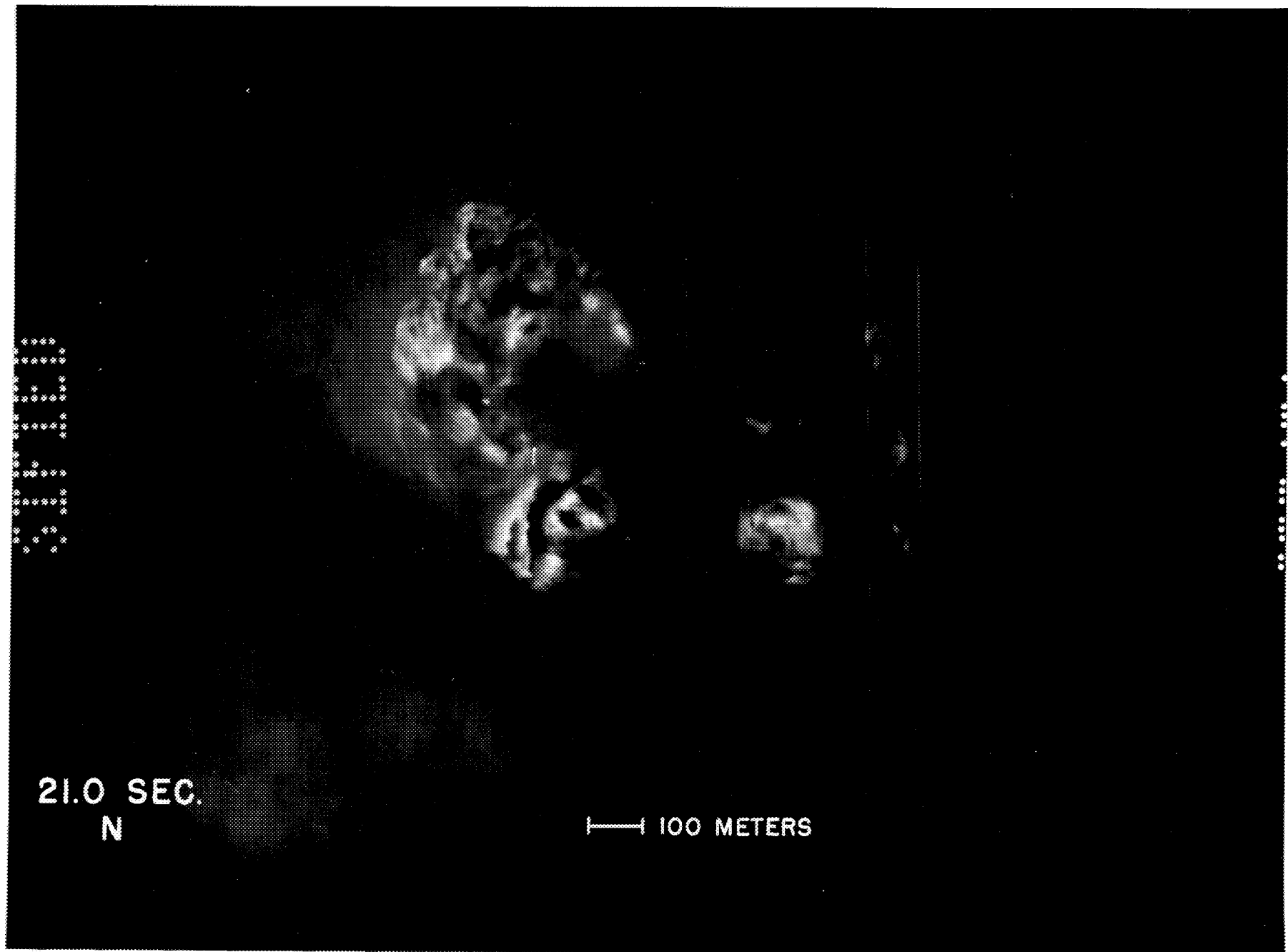




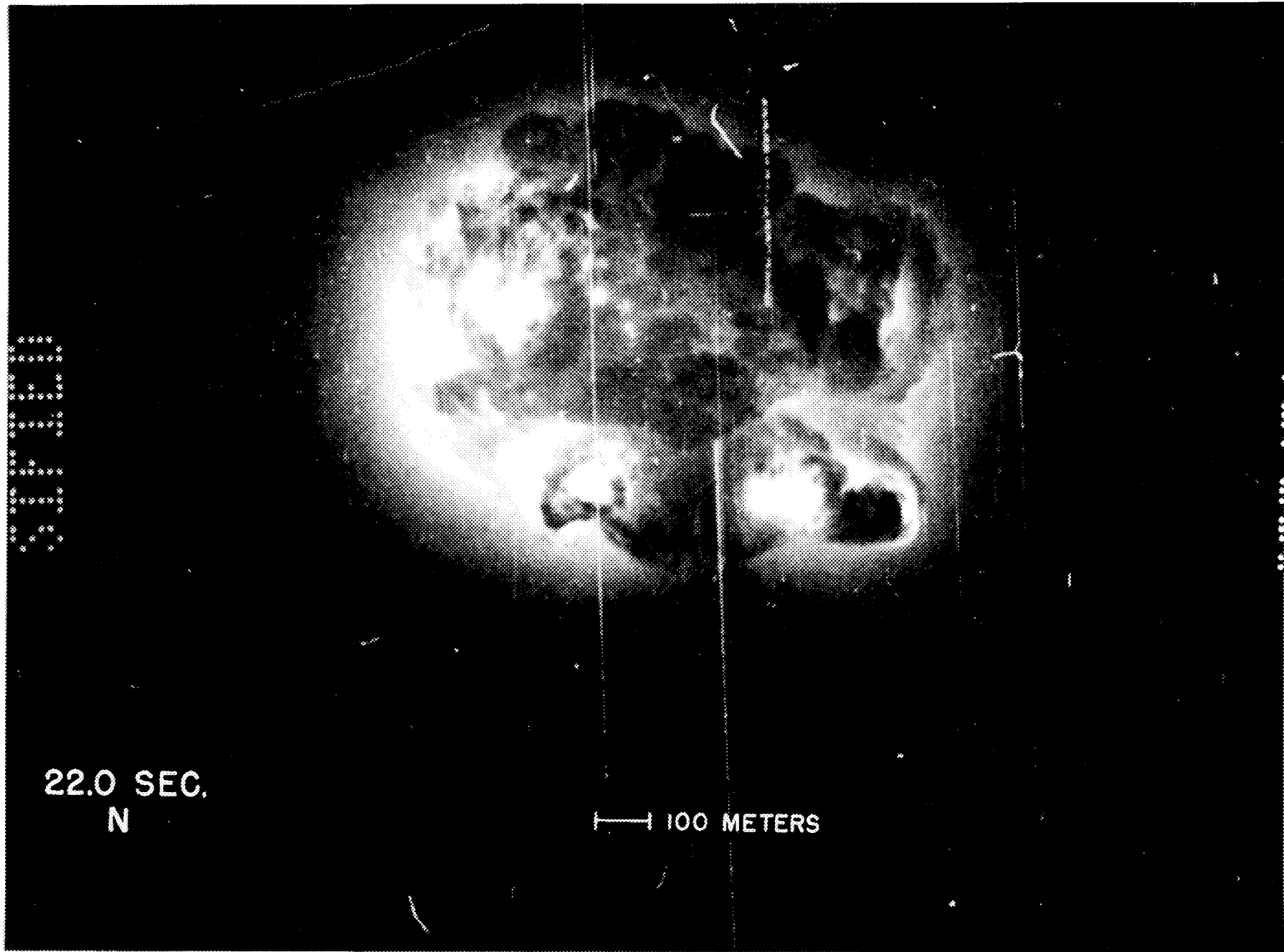


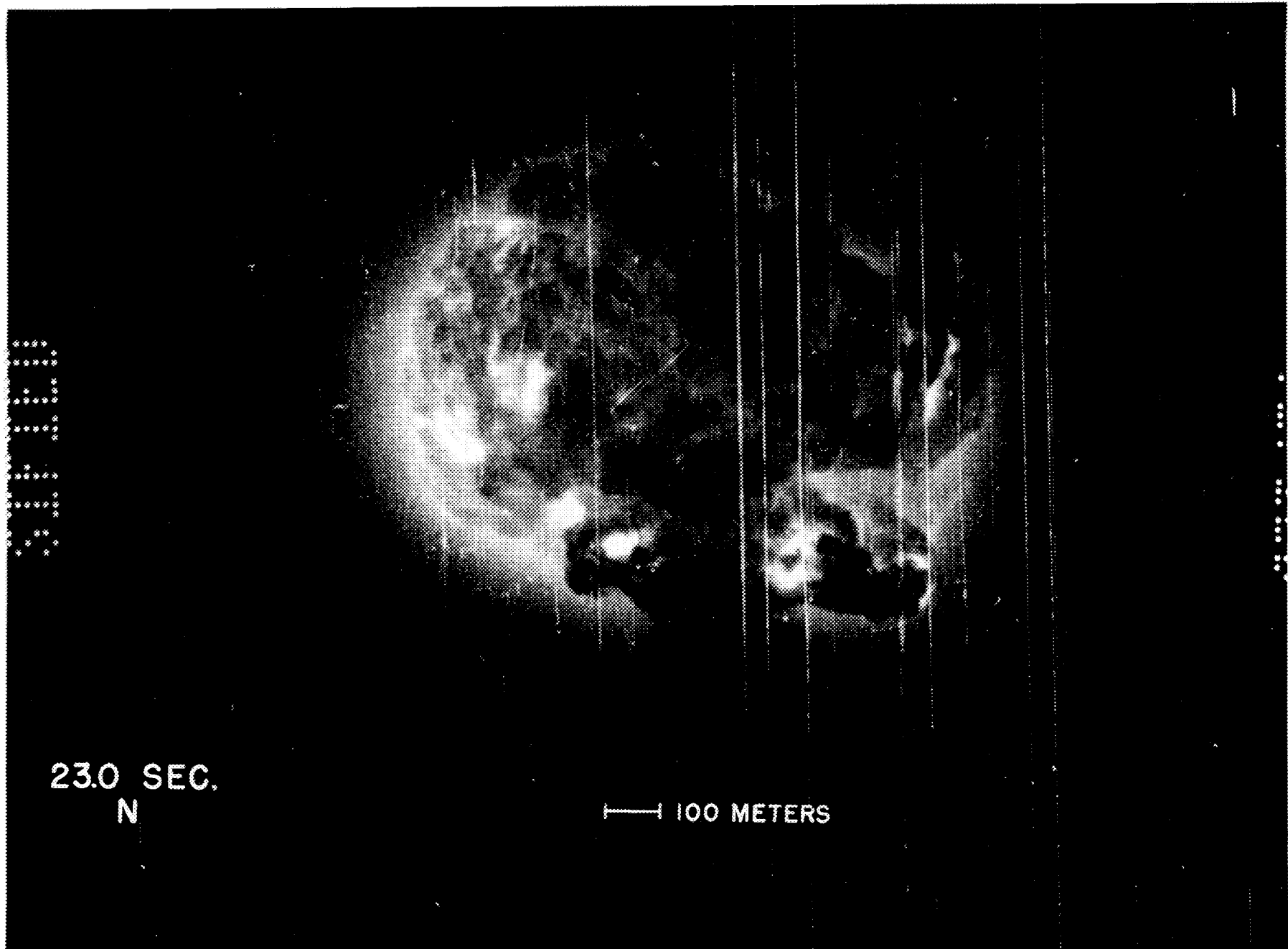




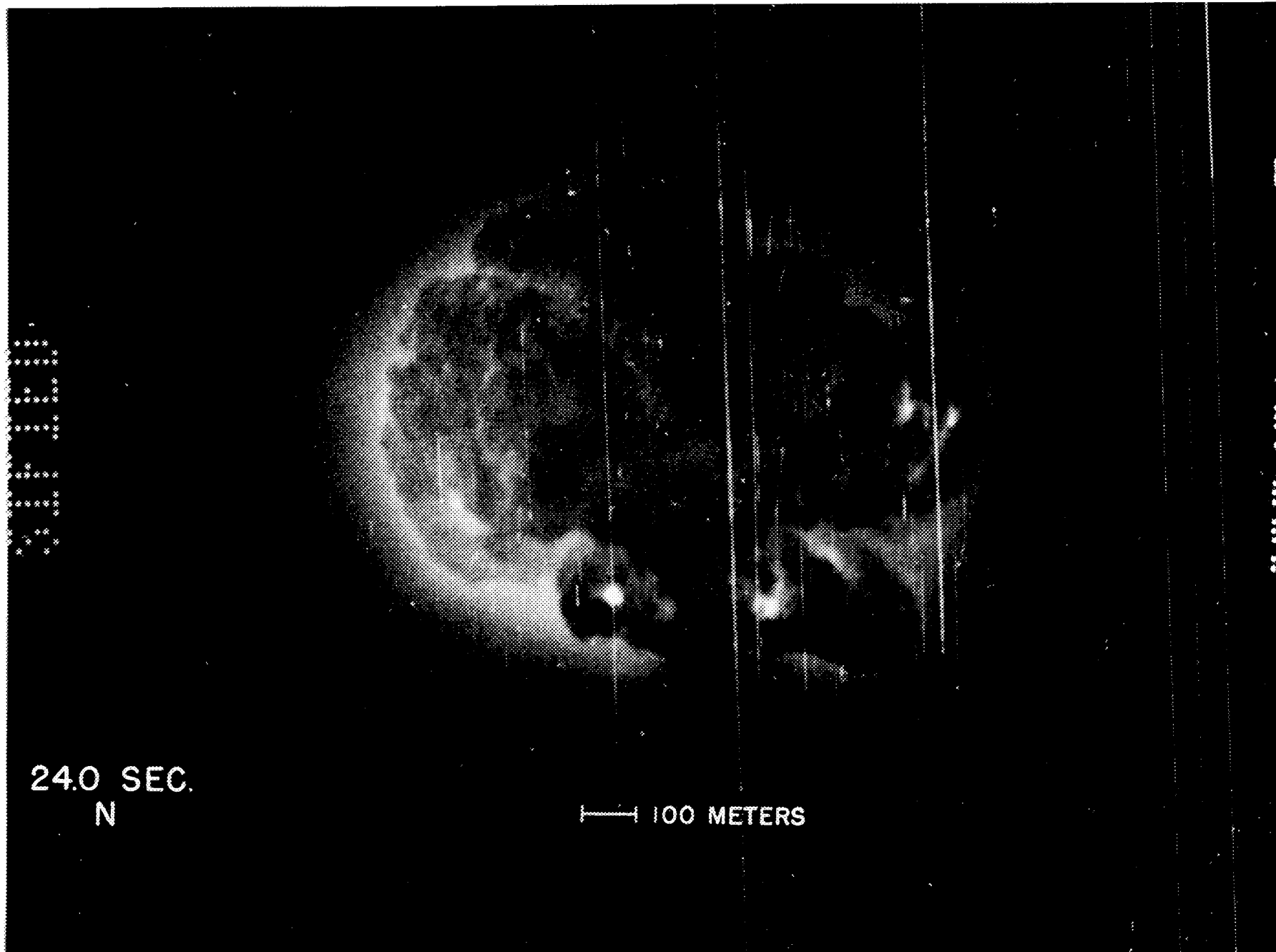


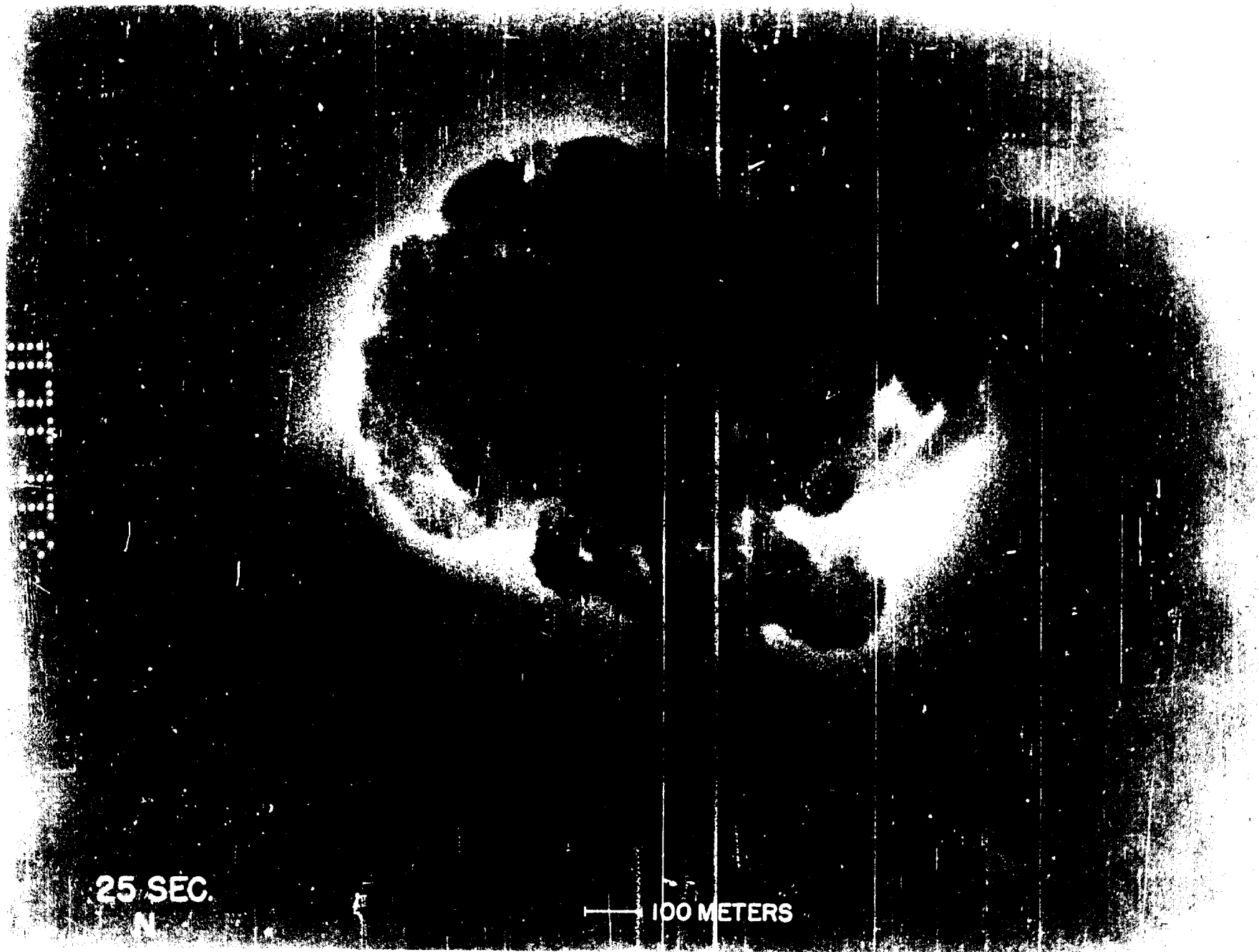
UNCLASSIFIED



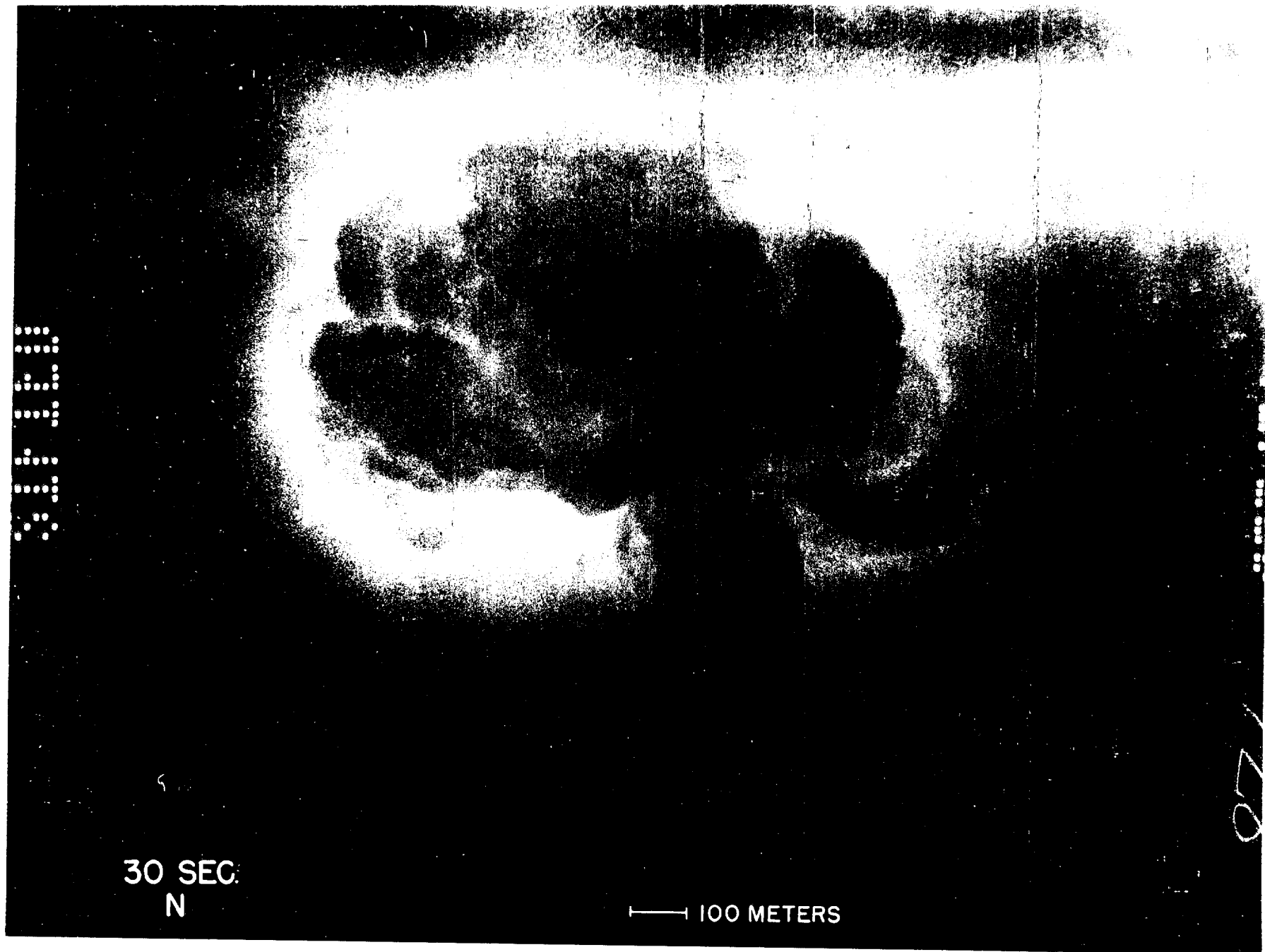


UNCLASSIFIED





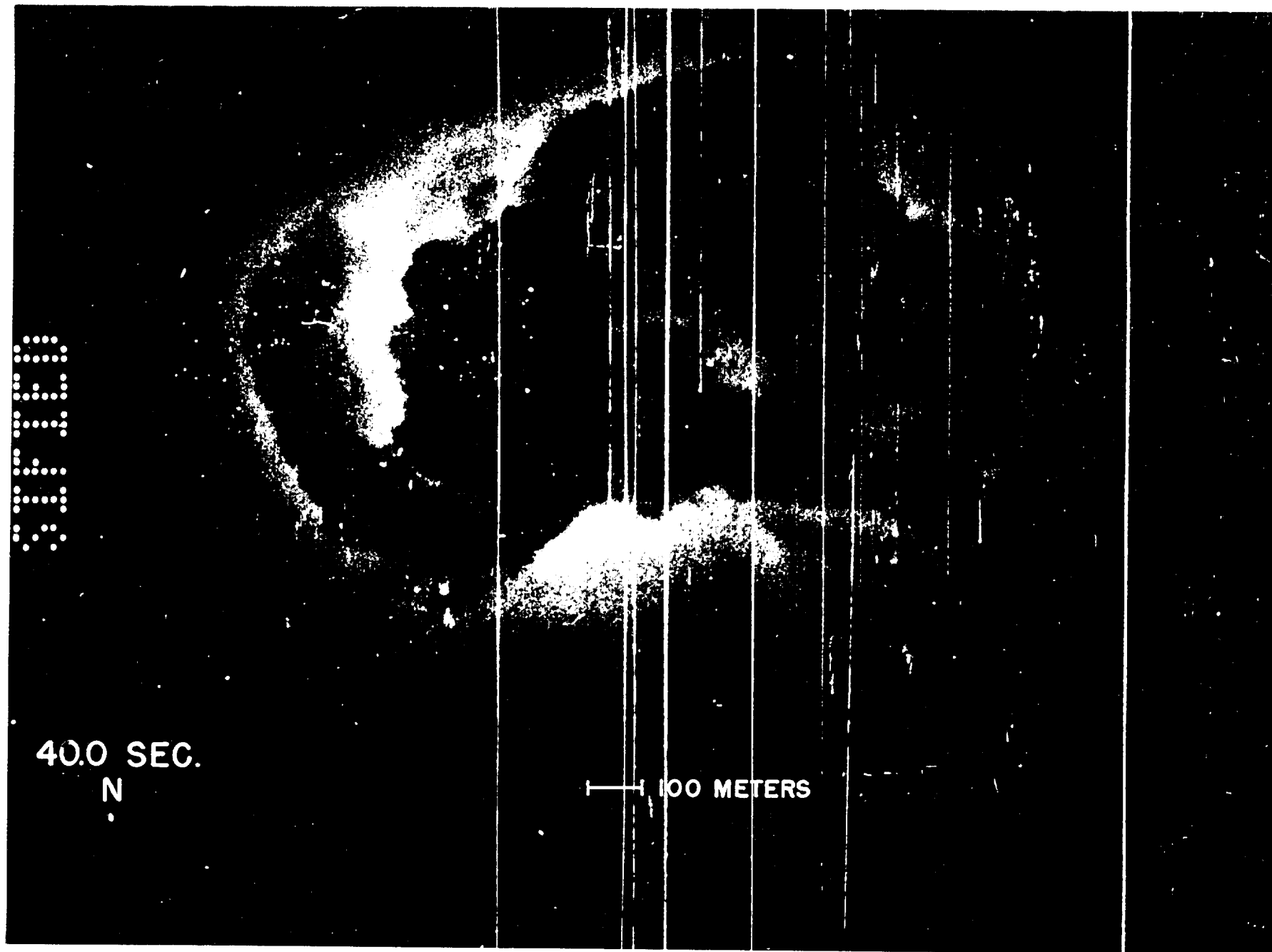




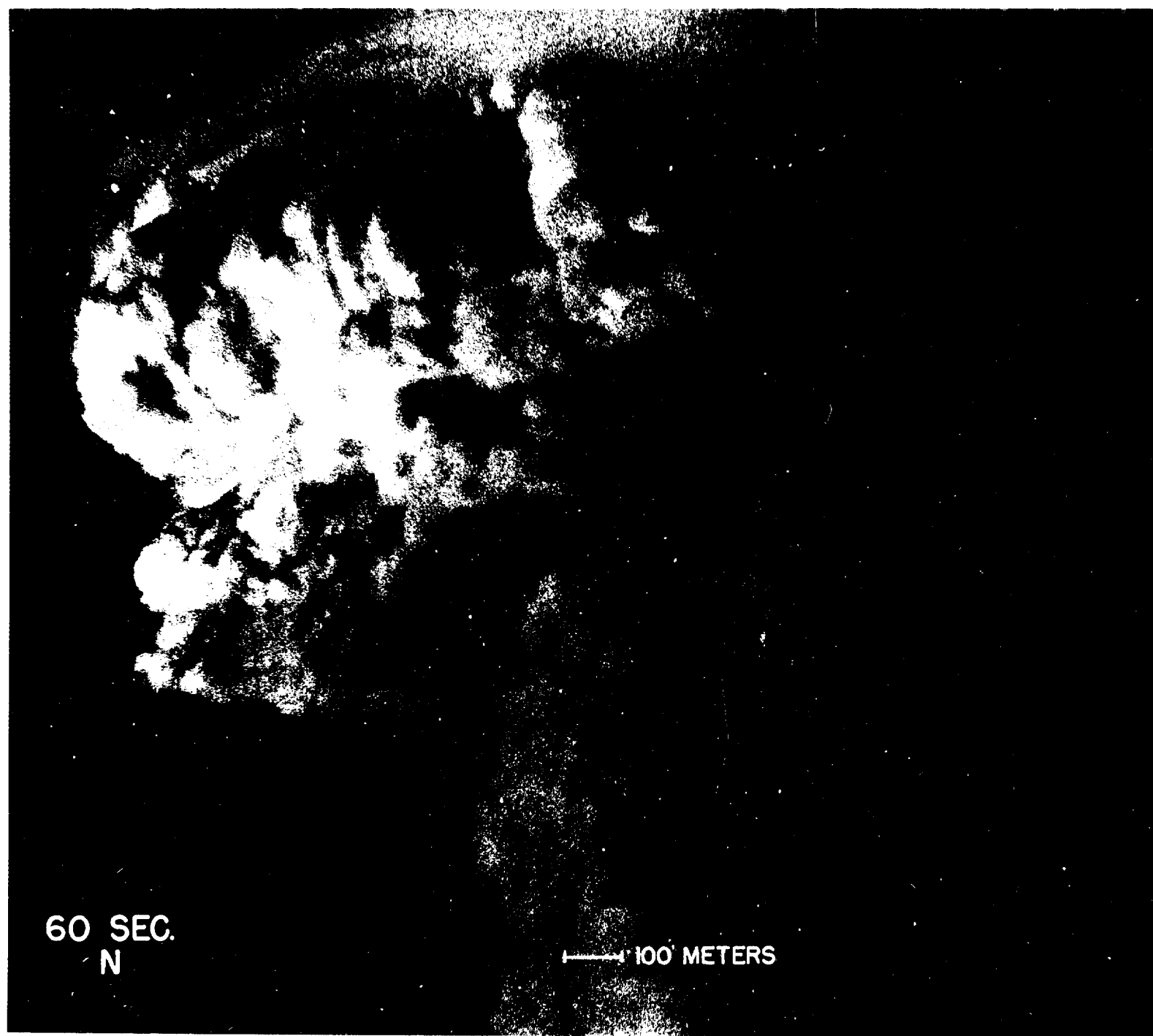
APPROVED FOR PUBLIC RELEASE



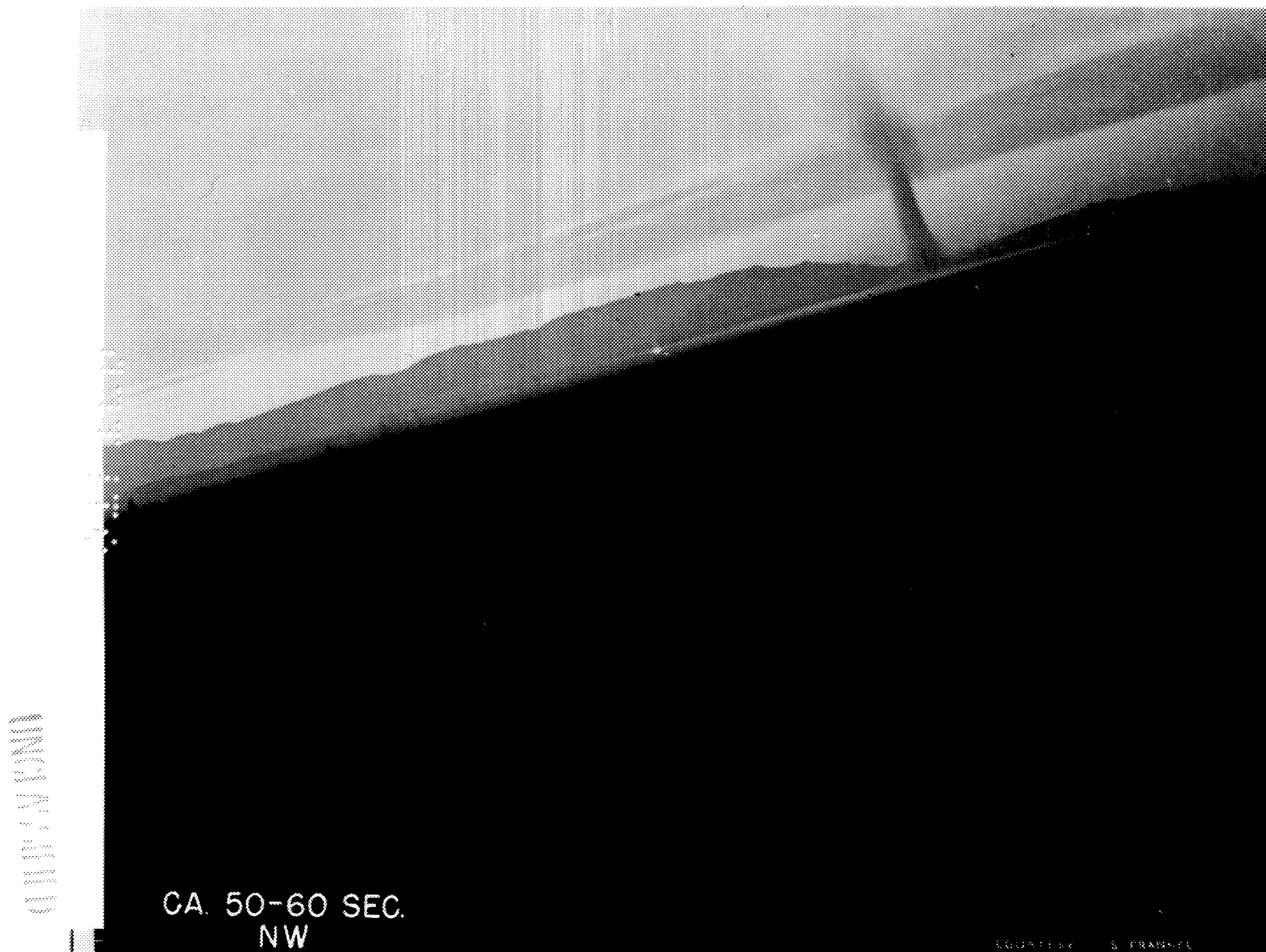
APPROVED FOR PUBLIC RELEASE



















80





Fig. 88  
40 p. 100 m. W

100 Meters

100 Meters

